ABSTRACT

Title of Dissertation:	FREEWAYS AND ARTERIALS TURNING MOVEMENT COUNTS ESTIMATION AND PREDICTION
	Amir Nohekhan, Doctor of Philosophy, 2022
Dissertation directed by:	Professor Ali Haghani, Department of Civil and Environmental Engineering

Accurate turning movement counts in interchanges and intersections are priceless information in traffic management and traffic signal design. The time-varying nature of traffic conditions can be captured with the massive deployment of traffic sensors, no longer a viable option considering the limited budget of transportation authorities. The present study proposes a framework to employ the available traffic data to estimate the turning movement counts in freeway interchanges and arterial intersections. The proposed framework for interchange turning movement count estimation illustrates that obtaining acceptable estimates of off-ramp hourly traffic volume is possible using only two days of data collection on each interchange. Next, this study investigates the intersection turning movement count estimation. The study explores this estimation from three aspects using the turning movement count data in Austin, TX. First is the

model structure, for which four different machine learning models are examined. The results indicated that the multi-layer perceptron trained on all intersections and fine-tuned over each target intersection yields the best results. Second, since the traffic volume of each leg of an intersection is not always available, a two-step framework is proposed to estimate the approach volumes in the first step and then input them into the turning movement estimation model in the second step. The third aspect is the sensitivity analysis of turning movement and approach traffic counts ground-truth data sizes on the accuracy of the proposed two-step framework. These analyses indicated that collecting only five days of turning movement counts and deploying continuous traffic count sensors on a quarter of intersection approaches generate acceptable results with a median absolute error of approximately eight vehicles per 15 minutes. The application of the proposed framework in the prediction of turning movement counts reveals that accurate counts can be generated up to 30 minutes in advance. Additionally, the framework's application in traffic signal design illustrates that a single intersection's annual user delay cost can be reduced from 8 to 2.5 million dollars.

FREEWAYS AND ARTERIALS TURNING MOVEMENT COUNTS ESTIMATION AND PREDICTION

by

Amir Nohekhan

Dissertation submitted to the Faculty of the Graduate School of the
University of Maryland, College Park, in partial fulfillment
of the requirements for the degree of
Doctor of Philosophy
2022

Advisory Committee:

Professor Ali Haghani, Chair

Dean's Representative Professor Vanessa Frias-Martinez

Professor Gang-Len Chang

Professor Paul Schonfeld

Kaveh Farokhi Sadabadi, Ph.D.

# Acknowledgments

I would like to express my most profound appreciation to my advisor, Professor Ali Haghani, for his unparalleled support, unwavering guidance, and patience that cannot be underestimated.

My special thanks also go to my doctoral examination committee members, Professor Gang Len-Chang, Professor Paul Schonfeld, Professor Vanessa Frias-Martinez, and Dr. Kaveh Farokhi Sadababi, for their constructive comments and suggestions on this work.

I want to acknowledge my colleagues from my research lab, The Center for Advanced Transportation Technology at the University of Maryland, Dr. Przemysław Sekuła and Zachary Vander Laan, and thank them for their technical and emotional support.

I want to extend my sincere thanks to my friends who were helpful to me during this time, especially: Sara Zahedian, Amirhossein (Sina) Yazdkhasti, and Mohammadamir (Amir) Zeighami, to whom I feel most indebted.

Finally, special thanks go to my father, mother, brother, and sister-in-law for their unconditional support and understanding during my years of doctoral study. Without their persistent encouragement, I would not have been able to make it through those difficult times.

Table of Contents

List of Tables

List of Figures

Chapter 1: Introduction

1.1 Motivation

The primary motivation of the present study is to propose a framework that can be used to predict the turning movement counts at intersections in real-time and modify the traffic signal timing per the expected demand. Modifying traffic signal timing in response to changes in turning movement counts can remarkably reduce the user delay due to reducing traffic congestion and lost time (Foy et al., 1992).

The purpose of a significant proportion of urban travel is participation in spatially separated activities (Ory and Mokhtarian, 2005). The space-time distribution of activities induces traffic congestion on the transportation network, resulting in extensive loss of time and resources for the users (Downs, 1962). According to the latest mobility report, adverse effects of traffic congestion are not reduced and are becoming worse year by year (Schrank et al., 2019). Table 1 illustrates the growing congestion problem in the US urban areas during the past decades. For instance, each US auto commuter spent 54 hours in 2017 in traffic congestion delays compared to 20 hours in 1982. Also, the total congestion cost has increased by more than tenfold during the same period - from 15 to 179 billion in 2017 US dollars. To elaborate on the trend of increase in the nation's cost, Figure 1 illustrates the constant increase in monetary and time losses of traffic congestion during the 35 years from 1982 to 2017. As shown in this figure, the total congestion cost is projected to exceed 200 billion dollars by 2020 and reach 250 billion dollars by 2025.

The traditional solution for the traffic congestion is expanding the road network infrastructure; however, scarcity of land, limited budget, environmental concerns, neighborhood residents' objections, etc., are increasingly restricting this solution (Ferguson, 2018). Traffic congestion is mainly experienced during rush hours in urban areas, a well-known phenomenon in transportation literature called the bottleneck

Table 1. Major findings of the 2019 Urban Mobility Report (Schrank et al., 2019)

		1982	2000	2012	2017	5-Yr Change
Individual Congestion	Yearly delay per auto commuter (hours)	20	38	47	54	+15%
	Travel Time Index	1.10	1.19	1.22	1.23	1 Point
	Wasted fuel per auto commuter (gallons)	5	16	20	21	+5%
	Congestion cost per auto commuter (2017 $)	$610	$920	$970	$1,080	+11%
National Congestion	Travel delay (billion hours)	1.8	5.3	7.7	8.8	+14%
	Wasted fuel (billion gallons)	0.8	2.5	3.2	3.3	+3%
	Truck congestion cost (billions of 2017 $)	$1.8	$7.0	$14.5	$19.5	+35%
	Congestion cost (billions of 2017 $)	$15	$75	$150	$179	+19%

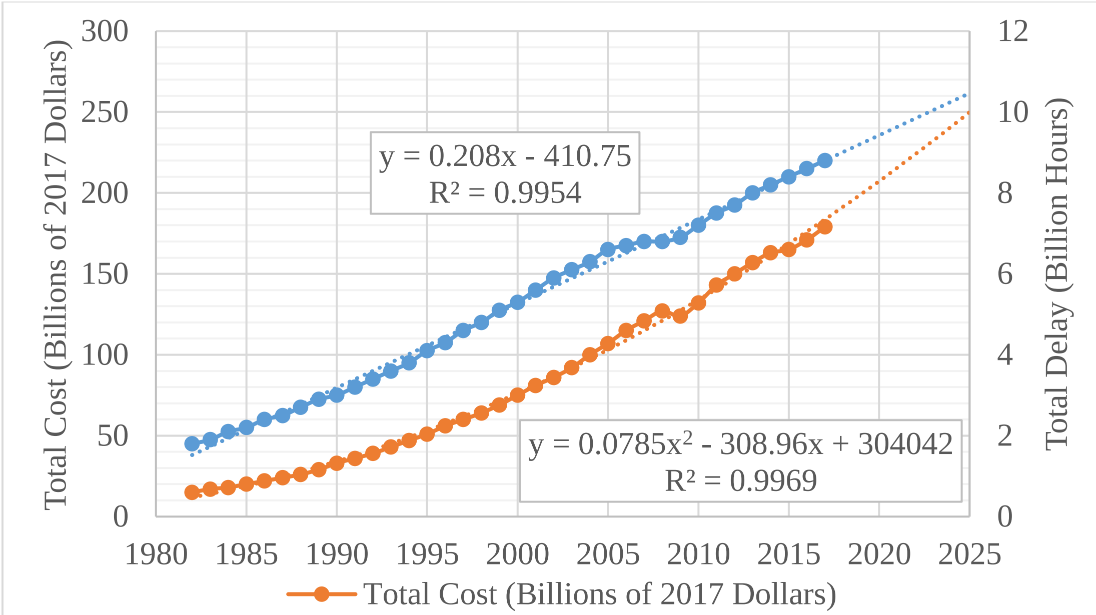

Figure 1. Total national cost and delay of congestion in the US

effect (Xiao et al., 2013). Bottlenecks emerge in the presence of merging or diverging, lane drops, etc. (Chen et al., 2004). Thus, intersections are usually a bottleneck in the road network as they are a point where different approaches converge and diverge (Katriniok et al., 2017). However, this is not limited to arterials and intersections. In a freeway system, the same issue arises at the location of interchanges. Reducing the congestion on intersections and interchanges requires information on turning movements and through movement traffic volumes. This information is essential for designing and improving intersections and interchanges and optimally setting traffic signal timings (Nihan and Davis, 1989).

Turning movement counts in a road network are critical for analyzing high-level traffic conditions such as origin-destination (OD) patterns. Besides, this data can provide vital information for micro traffic operations. For instance, turning movements can be feedback to the traffic controller to dynamically set the traffic signal timings or change the traffic signal phasing in real-time.

Since traditional traffic data collection methods are cost- and/or labor-intensive, available data for this purpose is limited both temporally and spatially. In fact, due to the budget constraints of the transportation agencies, the turning movement count at intersections is not available for most, and for those with a data collection record, the duration of data collection is at best once or twice a year to set the signal timing until the following data collection. Therefore, relying on such sparsely collected data to predict the turning movement traffic counts, which is a complicated behavior, cannot provide enough accuracy levels (Hu and Liou, 2012). However, the recent growth in the amount of available heterogeneous traffic information besides the advanced modeling methods has provided transportation planners the opportunity to estimate the turning movement counts with accurate-enough precision (Mahmoud et al., 2021). Therefore, considering the described obstacles in continuous data collections, especially for turning movement counts, investigating the methods that can be used to predict this traffic behavior is of particular importance to the transportation authorities.

1.2 Scope of the dissertation

This study aims to estimate the turning movement traffic counts at junctions of the road network. The underlying theory behind this research is that traffic volumes can be estimated using the recently adopted data sources such as probe vehicle data, which are used to estimate traffic speed. Many studies in the literature have shown a high degree of correlation between traffic speed and traffic volumes. Additionally, temporal features significantly impact the magnitude of turning movement counts as the travel patterns change with changes in months, days, and time of the day.

In the first step of this study, an artificial neural network model is trained using volume count data, speed data, and road characteristics for several interchanges on the US national highway system (NHS) in California. This step is designed as the proof of concept of estimation feasibility of the turning movements based on temporal and spatial correlations between traffic volumes and the applicability of emerging large-scale datasets. The model confirms the estimation feasibility of turning movement proportions. The results of the models illustrate that turning movement proportions can be predicted by having data of a set of locations or a short time duration. Besides, the results demonstrate the impacts of issues in the input data, such as missing data or faulty detectors installed on the road.

Further, building upon the findings of the first step, the estimation of turning movement counts at intersections is explored. This investigation aims to estimate and predict each allowed movement's counts of intersections during a specific time interval. In this investigation, several issues are addressed, ranging from the model structure for estimation of turning movement counts, the required input data for model development, and the duration of turning movement data collection. Addressing these issues makes the study applicable to real-world problems and of interest to the transportation agencies.

Finally, using the investigation findings mentioned above, the proposed framework is used in one of its applications to design the traffic signal timing of an intersection as an example and compute the costs and benefits of such an application. The cost-benefit analysis presented in the final step provides a clear understanding of the benefits of the study's proposed framework.

1.3 Contributions

This study aims to address several gaps in the turning movement estimation literature. The contributions of this research are as follows:

1) Estimate interchange turning movement counts using the traffic conditions at the main section, therefore solely relying on sensors on the main section of the highway or freeway.

2) Illustrate the developed model's capability to capture the temporal variations on the same ramp used in model training.

3) Comparison between the actual intersection turning movement proportions and a commercialized probe vehicle dataset turning movement proportions

4) Illustrate the performance of three well-established machine learning models in intersection turning movement count estimation

5) Developing an estimation framework for intersection turning movement counts using incomplete input features

6) Create a baseline for turning movement count data collection duration and the resulting turning movement count estimation model accuracy

7) Application of the proposed framework in real-time modification of traffic signal timing in response to the predicted turning movement counts

8) Provide a cost-benefit analysis employing the proposed framework and required data collection.

1.4 Dissertation structure

The rest of the dissertation is organized as follows:

Chapter 2 summarizes the turning movement estimation literature and elaborates on the strengths and shortcomings of the existing methodologies to illustrate the gaps in this field.

Chapter 3 describes the machine learning models used in this study, along with the performance measures for evaluations and comparisons of these models.

Chapter 4 investigates the estimation of off-ramp hourly traffic volumes to illustrate the capabilities of machine learning models in providing accurate estimates of traffic volumes using the traffic conditions of the freeway's main section. This chapter begins with introducing the data sources used for the investigations, followed by presenting the considered traffic sensor deployment scenarios, training and testing configurations of the models, and finally, the results of applying the trained models in estimating off-ramp traffic volumes.

Chapter 5 introduces the data sources used to investigate intersections' turning movement estimation. Additionally, a detailed comparison of the ground-truth turning movement counts and proportions are compared against the turning movement proportions obtained from a commercialized probe vehicle dataset. This chapter concludes with figures and tables illustrating the distribution of key attributes in the dataset to clear the path for further analysis.

Chapter 6 designs several experiments in training and testing the intersection turning movement count estimation to evaluate different machine learning model structures, input features for the model, and duration of turning movement count data collection.

Chapter 7 applies the findings of the previous chapter in predicting the turning movement counts in advance in different time horizons as the first application of the proposed framework. Further, the prediction results are used to design the traffic signal timing in one of the study intersections to illustrate another application of the framework introduced in this study. Finally, based on the traffic signal timings obtained using the predictions of turning movement counts, the user delay costs in terms of time and money are computed and compared against the costs of developing the proposed prediction model.

Chapter 8 summarizes the findings, draws conclusions from the study's experiments, and makes suggestions for the real-world application of the proposed framework. The chapter concludes by describing the study's limitations and recommendations for future studies.

Chapter 2: Literature Review

2.1 Overview

The matrix of OD flows at intersections, also named turning movement (TM) counts, is an essential input in urban traffic networks' design, planning, management, and operations (Chen et al., 2012). There are applications, adaptive traffic signal controls, for example, in which turning movement counts are needed in real-time to maximize the performance of the control algorithm (Lan and Davis, 1999). The conventional methods of directly acquiring the turning movement counts are expensive and time-consuming (Shoup et al., 2013). The infeasibility of direct turning movement count collection led researchers to develop indirect approaches (Ghods and Fu, 2014). Indirect methods tend to estimate turning movement counts from readily available traffic volume data.

The application of turning movement counts is not limited to intersection signal control. Turning movement counts can be a rich data source in origin-destination demand estimation. By far, the most common resource of data for OD demand estimation is individual link volumes. However, several studies have shown that incorporating turning movement counts into the models improves the estimation quality (Hurdle et al., 1983; Alibabai and Mahmassani, 2008).

The studies on turning movement estimation started in the late 70s (Michalopoulos et al., 1978; Van Zuylen, 1979) and early 80s (Hauer et al., 1980; Mountain and Westwell, 1983). With the advances in rich data sources and powerful machine learning algorithms, the interest in estimating turning movement counts is growing fast, considering the huge benefits of the product in traffic operations and management.

The proposed framework in this study requires the extraction of ground truth data of turning vehicles at intersections from the installed cameras on those intersections for the turning movement estimation model. In line with the steps of the framework, the literature review is divided into multiple subsections. In what follows, a brief overview of the volume estimation literature and a comprehensive review of turning movement estimation methodologies are provided, describing each method's strengths and shortcomings.

2.2 Deep learning models for traffic flow estimation

Traffic flow in links of a road network has temporal dynamics and a unique spatial dependency (Li et al., 2017). Recurring incidents such as peak hour travel behavior and demand or non-recurring incidents such as accidents and road maintenance can drastically change the traffic flow characteristics. Additionally, in a transportation network, adjacent links in terms of Euclidean distance are not necessarily correlated and vice versa, such as in the case of segments along a freeway.

As an essential topic of traffic flow, turning movement proportions also illustrate such dynamics and dependencies. For instance, a change in traffic flow volume between an

OD pair can alter the turning movement proportions at intersections belonging to the competing paths connecting that OD pair. Therefore the data-driven approaches for modeling traffic characteristics should be able to capture such complex relations to generate accurate and reliable estimates (Cheng et al., 2018).

Recently, deep learning models are attracting the attention of researchers for modeling problems such as traffic flow in the road network primarily due to improved processing power, efficient algorithms, and their capability in capturing dependencies between instances in the dataset. Wu and Tan (2016) and Ma et al. (2017) modeled link traffic flow and link speed, respectively, in a road segment as a 2D image. They use a convolutional neural network (CNN) with spatial and temporal correlation though the spatial relationship exists in Euclidean space.

Li et al. (2017) propose modeling the traffic flow as a diffusion process on a directed graph with a diffusion convolution recurrent neural network (DCRNN). Their proposed model captures spatial dependency through bidirectional random walks on the graph and temporal dynamics using the encoder-decoder architecture.

In another study, DeepTransport, a deep learning model, is proposed to learn spatial-temporal dependencies for modeling traffic conditions (Cheng et al., 2018). For each road segment, they collect upstream and downstream neighborhood roads to explicitly model the spatial dependency, followed by applying convolution operation to these neighborhoods. Through real-world data experiments, they illustrate the superiority of their model relative to baseline models. These models are Auto-Regressive Integrated Moving Average (ARIMA) with Kalman filtering, Vector Auto-Regression (VAR), Support Vector Regression (SVR), Feedforward Neural Network (FNN), and Recurrent Neural Network with fully connected Long Short-Term Memory (LSTM) hidden units (FC-LSTM). However, their convolution operators are not confined to the real structure of the traffic network.

Cui et al. (2019) present a traffic graph convolutional LSTM (TGC-LSTM) to model the traffic network based on the network links' interactions. A simple free-flow reachability matrix is used to find the influencing links for a particular link, and it is illustrated that their model is also capable of determining the most influential links in the network. Although GCN models can replicate the relation between link traffic flow, the graph is generally fixed, and constructing the graph requires expertise. Guo et al. (2020) present a method to optimally learn the graph from the observed traffic data called Optimized Graph Convolution Recurrent Neural Network (OGCRNN) for traffic prediction. Their introduced model reveals the latent relationship among road segments from the traffic data in the training phase.

2.3 Turning Movement Estimation

Estimating turning movements has been of interest due to its applications in OD demand estimation, adaptive traffic signal controls, advanced traffic management systems, regional traffic assignment, etc. The vast expanse of the use of turning movement information has led researchers from the 70s to propose more accurate methods for turning movement proportions or counts estimation.

One of the pioneering studies on turning movement count estimation is the research of Jeffreys and Norman (Jeffreys and Norman, 1970). This study proposes three approaches to estimate intersection turning movement proportions: linear programming method, straightforward algebraic means, and graphical approach (Hu and Liou, 2012). While turning movement is a naturally underdetermined problem, researchers have proposed strategies to solve the problem by making assumptions (Bell, 1984).

Reviewing the studies on turning movement estimation reveals that most studies can be classified into two categories of non-recursive and recursive approaches. Typically, these studies tend to minimize the difference between observed and estimated counts (minimize prediction error) or maximize the probability of calculating the observed counts.

In the category of non-recursive approaches, several studies investigated the least-squares-based methods to estimate turning proportions using traffic counts (Hurdle et al., 1983; Nihan and Davis, 1989; Kessaci et al., 1990; Bell, 1991a). In non-recursive approaches, the primary assumption is that turning movement counts remain constant over a time interval, which is split into shorter periods. This assumption reshapes the underdetermined problem into an overdetermined one (Jiao et al., 2005).

In the category of recursive methods, the parameters of turning movement estimation are calibrated in a step-by-step process. The most well-known methods in recursive models have been recursive least square and Kalman filtering for decades (Okutani, 1987; Ashok and Ben-Akiva, 2000; Ashok and Ben-Akiva, 2002). Cremer and Keller (1987) and (Nihan and Davis, 1987) consider traffic flow in a road segment as a dynamic process dependent on time-variable parameters of entering traffic flow. In this regard, they take a dynamic approach to estimating OD flows in traffic networks and develop time-dependent models. Their proposed models are ordinary least squares estimators involving cross-correlation matrices, constrained optimization method, simple recursive estimation formula, estimation by Kalman filtering (Cremer and Keller; 1987), Recursive Least Squares (RLS), and discounted RLS (Nihan and Davis, 1987). Although their dynamic models have superior performance relative to static models, they have the assumption that the time of traversing the intersection is negligible relative to the chosen time interval or is equal to a fixed number of time intervals. Additionally, these models may result in turning movement proportions that violate equality or inequality conditions.

Bell (1991b) proposes two methods to relax the restrictive assumptions of the previous studies by considering junction travel time distribution that may take more than a single time interval. The first method assumes geometrically distributed travel time, while the second one does not assume any travel time distribution. In this study, a constrained, recursive least-squares estimation algorithm is used, and it is shown that this approach produces better turning movement estimates. With the existence of a complete set of detectors at an intersection, these studies can provide unbiased turning movement proportions estimates. These studies have shortcomings when such a dense installation of count sensors is not feasible or if a single detector at an intersection is malfunctioning (Lan and Davis, 1999). Besides, it has been shown that these studies cannot produce reliable estimates if there is a significant distance between the entering and existing count sensors (Davis, 1993).

Taking into account the possibility of malfunctioning of the count sensors, Davis and Lan (1995) developed a framework to assess the feasibility of solving the turning movements when only a partial set of link counts are available. Although this scheme can be solved offline, the configuration of detectors should satisfy an identifiability condition. Lan and Davis (1997) describe the advantages of Markovian compartment models in characterizing the traffic flow. In a subsequent paper, Lan and Davis (1999) propose real-time algorithms based on nonlinear least square (NLS) and quasi-maximum likelihood (QML) approaches to recursively estimate the turning movement proportions at an intersection when a partial set of detector counts are accessible. They implemented their method on simulated and real data in which the actual data comes from videotaping two closely located intersections near downtown Minneapolis from 4:15 to 5:45 pm. They found that while the NLS estimator has a lower bias, the QML estimator is superior to the NLS estimator in terms of total mean square error because of the lower variance in QML estimates. Chang and Tao (1998) propose a time-dependent turning movement estimation model to compute the time-varying turning fractions at signalized intersections. Enhanced estimation accuracy is achieved by incorporating the signal setting and pre-estimated OD flow from a longer time interval as an additional constraint. The incorporation of pre-estimated OD flow is based on more stable dynamic flow patterns with an increase in the time interval.

Considering the significant effects of outliers of detected flows on deteriorating the performance of the least square-based models, Jia et al. (2005) designed a least absolute deviation model and a genetic algorithm to solve the problem. It is shown that their approach outperforms the least square and Kalman filtering methods in accuracy and efficiency. Although this model is adequate for real-time turning flow estimation, like other parameter optimization methods, it falls short in predicting turning movements (Jiao et al., 2014).

In another study, instead of solely using the approaching volumes to an intersection, the information of turning movement proportions is used to estimate dynamic origin-destination demand (Alibabai and Mahmassani, 2008). This approach is applied to the US-29 in Maryland; however, due to inaccessibility to ground-truth turning movement counts, they simulated the network with a predetermined OD demand. It is shown that this approach has performance superiority over the models that do not explicitly consider the turning movement information.

The rapid development of intelligent transportation systems (ITS) has made sensor technologies more accurate and less costly. Considering the benefits of ITS in improving the network operations, such as traffic signal timing, ramp metering, and various other applications, numerous urban regions have installed sensors on their roads to obtain information about the network conditions. Hu and Liou (2012) use the data of vehicle detectors and video sensors to estimate the time-dependent turning proportions at intersections. They develop a nonlinear least-squares model based on minimizing the difference between the observed and estimated traffic flow and turning movement proportions. The model is evaluated on two simplified networks using DYNASMART-P for traffic simulation. They consider two distinct scenarios of the installation of turning movement detector sensors. The first scenario, full deployment, is installing sensors on a few selected intersections counting vehicles at all possible turning movements in each of these intersections. The other one, partial implementation, is the installation of sensors on several intersections and recording a subset of possible turning movements at each intersection. Interestingly, they found that partial deployment of turning movement detection sensors results in more accurate model performance than full deployment strategy, which signifies the importance of strategically deploying sensors in the network, also called the network sensor location problem (Gentili and Mirchandani, 2011).

Several studies proposed frameworks to detect and count the number of turning movements at a specific time in an intersection with varying levels of success (Xu et al., 2013; Santiago-Chaparro et al., 2016; Gholami et al., 2016; Shatnawi and Khliefat, 2018). These frameworks use a vast number of detectors on approaches that limit their applicability in a network consisting of numerous intersections.

In a study in 2014, Jiao et al. proposed a Bayesian combined model to predict the entering and exiting flows at an intersection and later a backpropagation neural network model and a Kalman filtering model to predict the dynamic turning movement proportions. For the entering and exiting flow estimation, they adopt a weighted average between volumes predicted by the nonlinear regression, moving average, and autoregressive methods. In the neural network model, they consider the counts at the entering approaches as the input layer. The framework was applied to an intersection in Beijing, China, and achieved mean absolute prediction errors in order of 30 percent (Jiao et al., 2014). The movement of the vehicles in this study is assumed to be completed in a single time interval, which can be restrictive where there is congestion in the intersection, which is highly likely in the urban intersections at peak hours. Additionally, while the long-term prediction of turning movements is crucial for traffic congestion mitigation, the model can only predict the turning movement proportions in the short term.

Chen et al. (2012) used the path flow estimator (PFE) technique originally developed to estimate the path flows to derive turning movements in addition to complete link flows. This procedure assumes available traffic volume counts on selected roads and turning movements and flows between some origin-destination pairs. There core component of PFE is a logit-type model in the route choice with independent Gumble distributed errors in travel time perception. A column generation technique is employed to solve the problem and extract turning movement counts. The results of applying the proposed framework on two separate networks indicated that the maximum errors in turning movement estimates could be in excess of %1,000 in some cases.

Ghanim and Shabaan (2018) developed a 3-layer neural network model to estimate the hourly turning movement counts based on all inbound and outbound approach volumes of an intersection. The data of peak hour turning movement counts at 847 intersections in Palm Beach County, Florida, between 2010 and 2014 were obtained for model training and testing. The results indicate an R-squared of 0.87 for the left turn, 0.99 for the through, and 0.90 for the right turn movements in the testing set. Although the results sound promising, the assumption of available approach volumes for each intersection, especially for all inbound and outbound streets, limits this study's real-world application.

Li et al. (2020) presented a partial least square (PLS) based method for short-term prediction of traffic states, including traffic speed, traffic volume, and travel time prediction. The PLS method is a generalization of multiple linear regression, which is robust to collinearity and specifically used in cases where the number of independent variables is more than the number of observations. This technique first reduces the number of attributes to a set of uncorrelated variables and performs least squares regression on these components instead of the original dataset. Therefore, it reduces the problem dimension and computational efforts. The authors of this study applied the PLS method to the turning movement estimation problem of a single intersection covering a span of 23 days. The attributes comprise the number of trajectories, the average number of stops, and the average speed, for each movement. The predictors comprise the mentioned features from the past four hours for all approaches. The study results illustrated an average mean absolute error of 6 vehicles per 15 minutes and an average mean absolute percentage error of 15 percent. Besides, a comparison between the PLS-based method and other prediction models, including ARIMA, KNN, and SVR, illustrated this modeling approach's superiority.

In a more recent study, Mahmoud et al. (2021) predicted the cycle-level turning movement counts at intersections using eXtreme Gradient Boosting (XGBoost), Long

Short-Term Memory (LSTM), and Gated Recurrent Unit (GRU) models. The turning movement counts included the through and left-turn movements five cycles ahead. This research collected one month of turning movement counts from 16 intersections equipped with GRIDSMART sensors along two main corridors in Florida. The attributes used for model development include the turning movement counts in the upstream and downstream intersections, green time for each approach in the target intersection and upstream and downstream intersections, and the traffic signal cycle length in these intersections. The mentioned attributes are compiled from up to 8 cycles before the current cycle to form the input data for training the models. The results of training and testing the models indicated that the XGBoost and GRU models outperformed the LSTM model. Besides, for the best models, the mean absolute error on the testing data for the through movement is almost equal to 5 and for the left-turn movement is almost equal to 1. However, there is no mention of the proportion of the absolute error relative to the traffic counts in each cycle. In terms of prediction in the time horizon, the mean absolute error for through movements increases from 5 to 6 in predicted cycles of 1 to 5 ahead of the current cycle. The limiting assumption in this study is the assumption of availability of turning movement counts in the upstream and downstream intersections of the target intersection, which significantly reduces the applicability of the framework in real-world situations.

In the realm of predicting traffic volumes, there are a vast number of studies that explore time series models in extracting traffic patterns (Hamed et al., 1995; Wild, 1997; Lingras et al., 2000; Boto-Giralda et al., 2010). These studies assume that permanent traffic detectors are installed; therefore, with access to the traffic characteristics in the previous time windows, applying time series models are feasible. However, considering the costs of installing turning movement count detectors, such approaches are impractical in real-world situations.

According to the above description of the previous studies, none of the earlier studies, to the extent of the author’s knowledge, approaches the turning movement behavior from a high-level perspective. In most earlier studies, the turning movement estimation is tackled using the basic models that cannot capture the complex relations between the traffic flow counts of each allowable movement with other traffic flow characteristics. Besides, the effects of introducing emerging data of floating vehicles such as probe vehicle data to the modeling framework are not explored yet. Additionally, the studies that have employed more sophisticated modeling frameworks input attributes such as the turning movement counts of previous time intervals of the target intersection or the current turning movement counts and traffic flow in the adjacent intersections, severely limiting these methodologies' applicability to real-world scenarios. Another gap in the literature is the absence of a cost-benefit analysis based on the input data and the output accuracy of the turning movement count estimates or predictions. From an operator's point of view, the cost-benefit analysis enables decision-making since a huge investment for installing vehicular sensors might not add much value in terms of increasing the model accuracy and reducing the user delay cost and traffic congestion.

This chapter presented a review of traffic volume estimation, turning movement estimation, and prediction studies. In each section of this chapter, the limitations of the previous studies were also presented.

In the first step of this study, we explore the estimation of hourly traffic flow of an exiting freeway main section through an off-ramp. This exploration acts as the building foundation of the much more complex intersection turning movement counts estimation and prediction.

Chapter 3: Methodology

3.1 Overview

This study aims to estimate turning movement at junctions using data-driven approaches and advanced machine learning models. While the study's main contribution is introducing frameworks to address this problem, it is essential to present the underlying ideas behind the models used in the proposed framework. Therefore, this section elaborates on the machine learning models used throughout the study. In addition, this section introduces performance measures used for evaluating the results in the following chapters.

3.2 Multi-Layer Perceptron Model

Advancements in intelligent transportation systems have enabled the deployment of sensors on a large scale with appropriate accuracy and reduced cost for transportation agencies. The sensors installed on the road network generate extensive traffic data with a high time resolution (Zhao et al., 2017). While collecting travel behavior data, these sensors benefit transportation planners to improve the operation of transportation systems to reduce congestion and increase mobility. The emerging extensive traffic data facilities promote the usage of more advanced models to attain more accurate traffic estimations and predictions. Neural Network (NN) models are capable of dealing with highly complex datasets with nonlinear relationships (Karlaftis and Vlahogianni, 2011). The advantages of NN models have encouraged transportation researchers to apply these models in traffic behavior and traffic propagation studies and have generated promising results (Park and Rilett, 1999; Vlahogianni et al., 2004; Huang et al., 2014; Ma et al., 2015; Sekula et al., 2018; Zahedian et al., 2020; Nohekhan et al., 2021).

Multi-Layer Perceptron (MLP) models, as a class of feedforward artificial neural networks (ANN), have great potential in data analysis and forecasting because of using distributed and hierarchical feature representation (Huang et al., 2014). MLP models are potent in working with massive multi-dimensional data and offer generalization and appropriate prediction abilities (Haykin, 1994; Hagan et al., 1997).

An MLP is an interconnected group of neurons, each of which can perform a simple process. When working as a group, these neurons are potent in exhibiting complex behaviors. Nodes are connected elements of MLP. Typically, an MLP has three general layer types: input, hidden, and output layers. The fully connected structure of MLPs used in this study allows for capturing the complicated relationship between variables influencing the turning movement behavior. The output of each neuron is dependent on the outputs of the neurons connected to it in the previous layer based on the forward propagation rule in Equation (1).

$$a_i^{(l)} = f\left(w_i^{(l)} a^{(l-1)} + b_i^{(l)}\right) \tag{1}$$

where

$a_i^{(l)}$ is the output of neuron *i* in layer *l*;

$w_i^{(l)}$ is the weight vector associated with neuron *i* in layer *l*;

$b_i^{(l)}$ is the bias vector between neuron *i* in the layer *l* and all neurons of the layer *l*-1;

$a^{(l-1)}$ is the output vector of all the neurons in layer *l*-1; and

f is the activation function used to account for the nonlinear relationships between the neurons.

In this study, several MLP models are trained with four hidden layers, normalized data, batch normalization, L2 regularization, and random dropout layers for hourly turning movement proportions estimation. Normalizing the input data reduces the scale difference between variables, thus stabilizing the model (Bishop, 1995). Among different input data normalization approaches, this study employs the data standardization method using Equation (2).

$$x_{standardized}^{(i)} = \frac{x^{(i)} - mean\left(x^{(i)}\right)}{standard_{deviation\left(x^{(i)}\right)}} = \frac{x^{(i)} - \frac{1}{m}\sum_{i=1}^{m} x^{(i)}}{\sqrt{\frac{1}{m}\left[x^{(i)} - \frac{1}{m}\sum_{i=1}^{m} x^{(i)}\right]^2}} \qquad (2)$$

where $x^{(i)}$ and $x_{standardized}^{(i)}$ are the initial and standardized vectors of attribute *i* among all observations, and *m* is the number of observations.

Batch normalization is a method similar to data normalization while extending the idea to the inputs of all hidden layers (Ioffe and Szegedy, 2015). This method normalizes the outputs of neurons at each layer using Equation (3).

$$\tilde{z}^{[l](i)} = \gamma^{[l](i)} z_{normalized}^{[l](i)} + \beta^{[l](i)} \quad (3)$$

where $z_{normalized}^{[l](i)}$ is the normalized output of neuron *i* in layer *l* computed using Equation (2), $\gamma^{[l](i)}$ and $\beta^{[l](i)}$ are learnable distribution and $\tilde{z}^{[l](i)}$ is the normalized input to layer *l*+1.

Regularization is a method for penalizing excess estimated weights by incorporating them into the loss function, thereby reducing overfitting (Ng, 2004). The term which will be added to the loss function is shown in Equation (4).

$$\delta = \frac{\lambda}{2m} \sum_{l=1}^{L} \left\| w^{[l]} \right\|_F^2 = \frac{\lambda}{2m} \sum_{l=1}^{L} \sum_{i=1}^{n^{[l-1]}} \sum_{j=1}^{n^{[l]}} \left(w_{ij}^{[l]} \right)^2 \quad (4)$$

where λ is the regularization parameter determined by the modeler, and the rest of the parameters are defined earlier.

The dropout layers improve the generalization (reduce overfitting) of the model by randomly omitting a fraction of the hidden units in hidden layers (Dahl et al., 2013). The Rectified Linear Unit (ReLU) function is the considered activation function of the hidden layers (except for the last hidden layer) because of its several times faster training than other prevalent functions (Krizhevsky et al., 2012). The formulation of the ReLU function is presented in Equation (5).

$$f(x) = \max(0, x) \quad (5)$$

The activation function considered for the last layer is the sigmoid function, as shown in Equation (6).

$$f(x) = \frac{1}{1+e^{-x}} \quad (6)$$

The loss function of the MLP models used in this study is the average of the squared errors between observed and estimated turning movement proportions plus the regularization term, Equation (4), according to the formulation in Equation (7).

$$Loss = \frac{1}{n}\sum_{i=1}^{n}(\hat{y}_i - y_i)^2 + \frac{\lambda}{2m}\sum_{l=1}^{L}\sum_{i=1}^{n^{[l-1]}}\sum_{j=1}^{n^{[l]}}\left(w_{ij}^{[l]}\right)^2 \tag{7}$$

In equation 7,

n is the number of observations;

$\hat{y}_i$ is the estimated turning movement proportion/count for observation i;

y_i is the observed turning movement proportion/count for observation i;

The general structure of the MLP models used in this study is presented in Figure 2. This figure shows the MLP with four hidden and three dropout layers.

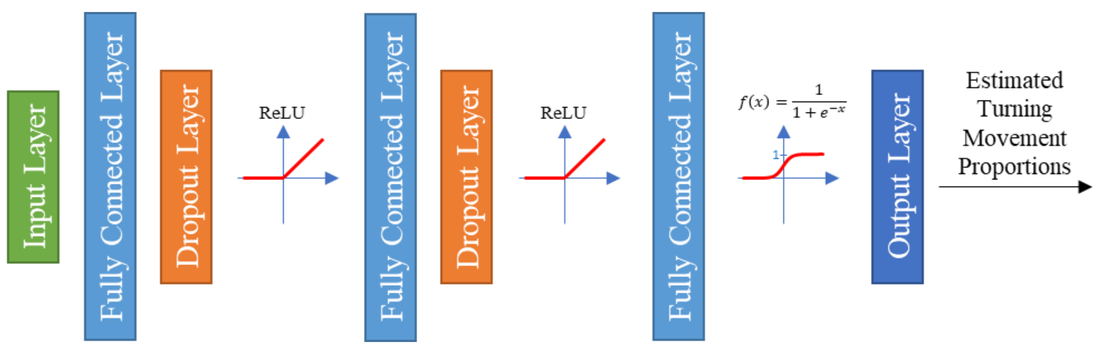

Figure 2. The general structure of the study's MLP models

<u>3.3 Random Forest</u>

The Random Forest (RF) is an ensemble supervised machine learning method. This model can be used for both classification and regression (Han et al., 2011). When used for regression, which is the case in this study, RF uses regression trees.

Regression trees aim to extract patter from data by dividing observations into branches based on their input values. The ultimate goal of branching the data is to minimize the sum of square error (SSE) in each branch. Therefore, the regression tree chooses the variable that splits the data with minimum SSE at each level.

RF model iteratively selects random sets of variables and samples with replacement from the training dataset and uses them to build a forest of regression trees. RF runs the record's input features through all the regression trees and gets the associated values to make estimations for a new record. The final estimation for this new record is the average of the values calculated from all decision trees.

While the idea behind RF is intuitive and simple, this model has proven to provide robust results in many applications. Using multiple regression trees trained on different input features and sample sets makes RF not have the overfitting problem associated with a single regression tree.

3.4 XGBoost Model

XGBoost is the short name for "Extreme Gradient Boosting," an efficient and scalable implementation of gradient boosting framework (Friedman et al., 2000). XGBoost is a cutting-edge application of gradient boosting machines and has proven to push the limits of computing power for boosted trees algorithms. It was developed to improve model performance and computational speed. Boosting is an ensemble technique in which new models are added to adjust the errors made by existing models. The new models are created that predict the residuals of prior models and then added together to make the final prediction. The objective function of the XGBoost algorithm comprises a loss function over the training set and a regularization term penalizing more complex trees to reduce the overfitting:

$$Obj = \sum_i L(y_i, \hat{y}_i) + \sum_k \Omega(f_k) \tag{8}$$

Where $L(y_i, \hat{y}_i)$ can be any convex differentiable loss function and $\Omega(f_k)$. The complexity term is defined as:

$$\Omega(f_k) = \gamma T + \frac{1}{2}\lambda w^2 \tag{9}$$

where T is the number of leaves of the tree f_k and w is the leaf weights. After taking the Taylor expansion and removing the constant terms, the objective function for iteration *m* is as follows:

$$Obj^m = \sum_{j=1}^{T} \left[G_j w_j + \frac{1}{2}\left(H_j + \lambda\right) w_j^2 \right] + \gamma T \tag{10}$$

where G_j and H_j are defined in (11):

$$G_j = \sum_{i \in I_j} \frac{dL\left(y_i, \hat{y}_i{}^{(m-1)}\right)}{d\hat{y}_i{}^{(m-1)}}, H_j = \sum_{i \in I_j} \frac{d^2 L\left(y_i, \hat{y}_i{}^{(m-1)}\right)}{d\left(\hat{y}_i{}^{(m-1)}\right)^2} \tag{11}$$

I_j is the set of training instances in leaf j.

The best leaf weight w_j given the current tree structure will be:

$$w_j = -\frac{G_j}{H_j + \lambda} \tag{12}$$

3.5 Performance Measures

Performance measures enable explaining the results and conclusions. Here, several performance measures are introduced as follows:

Mean Squared Error (MSE):

$$MSE = \frac{1}{n}\sum_{i=1}^{n}(\hat{y}_i - y_i)^2 \tag{13}$$

Mean Absolute Error (MAE):

$$MAE = \frac{1}{n}\sum_{i=1}^{n}|\hat{y}_i - y_i| \tag{14}$$

Mean Absolute Percentage Error (MAPE):

$$MAPE = \left(\frac{1}{n}\sum_{i=1}^{n}\left|\frac{\hat{y}_i - y_i}{y_i}\right|\right) * 100 \tag{15}$$

Coefficient of determination (R^2):

$$R^2 = 1 - \frac{\sum_{i=1}^{n}(y_i - \hat{y}_i)^2}{\sum_{i=1}^{n}(y_i - \bar{y})^2} \tag{16}$$

where $\bar{y}$ is the average of turning movement proportions/counts of all observations, and other parameters are introduced earlier.

In the next chapter, the dataset used for training and testing the models are introduced, followed by presenting the results of evaluating the performance of the models.

Chapter 4: Freeway off-ramp traffic flow estimation

4.1 Overview

The previous chapter introduced the machine learning model structures used in this study. In this chapter, one of the model structures is applied to estimate the freeway turning movement count estimation as proof of concept for the more complex intersection turning movement count estimation problem.

The number of vehicles exiting a freeway through off-ramps is an essential piece of information as it can be used to estimate regional OD demand from a high-level perspective. Freeways and highways serve a significant proportion of traffic, which appropriately represent the regional and countywide traffic patterns, especially in the US, because of its extensive freeway and highway networks. Additionally, observation of traffic flow patterns is more straightforward in freeways and highways because of these infrastructures' uninterrupted traffic flow nature and the number of installed sensors on these types of roads (Nohekhan et al., 2021). For this chapter of the study, which is mainly a proof of concept, the turning movement of vehicles at interchanges is considered.

Nevertheless, the exiting flow from a highway shares various similar characteristics with turning movements at intersections, thus not constraining the application of the proposed methodology. However, the fundamental difference is that in the case of interchanges, the flow that continues moving on the main section of the highway is uninterrupted. The following section describes the data of the interchanges considered as the model's input.

4.2 Input data description

In this study, the model input, called ground truth data, comes from three primary sources: turning movement counts, speed profile, and road characteristics described in the following subsections.

4.2.1 Turning movement counts

The current chapter uses data collected from the Caltrans Performance Measurement System (PeMS) to obtain the turning movement counts. The freeway network of the state of California comprises more than 41,000 directional miles, where more than 18,000 traffic count stations are installed on this network (PeMS, 2019). Traffic conditions are collected every 30 seconds from almost 45,000 individual detectors deployed on the state network (Tian and Pan, 2015). Then, the collected data are aggregated into 5-minutes intervals and uploaded to the website. Figure 3 shows the location of count stations on the network system in California. Each one of the black dots represents a count station, and it is evident that most of the stations are installed in the urban areas of Los Angeles and San Francisco. For training and testing the model,

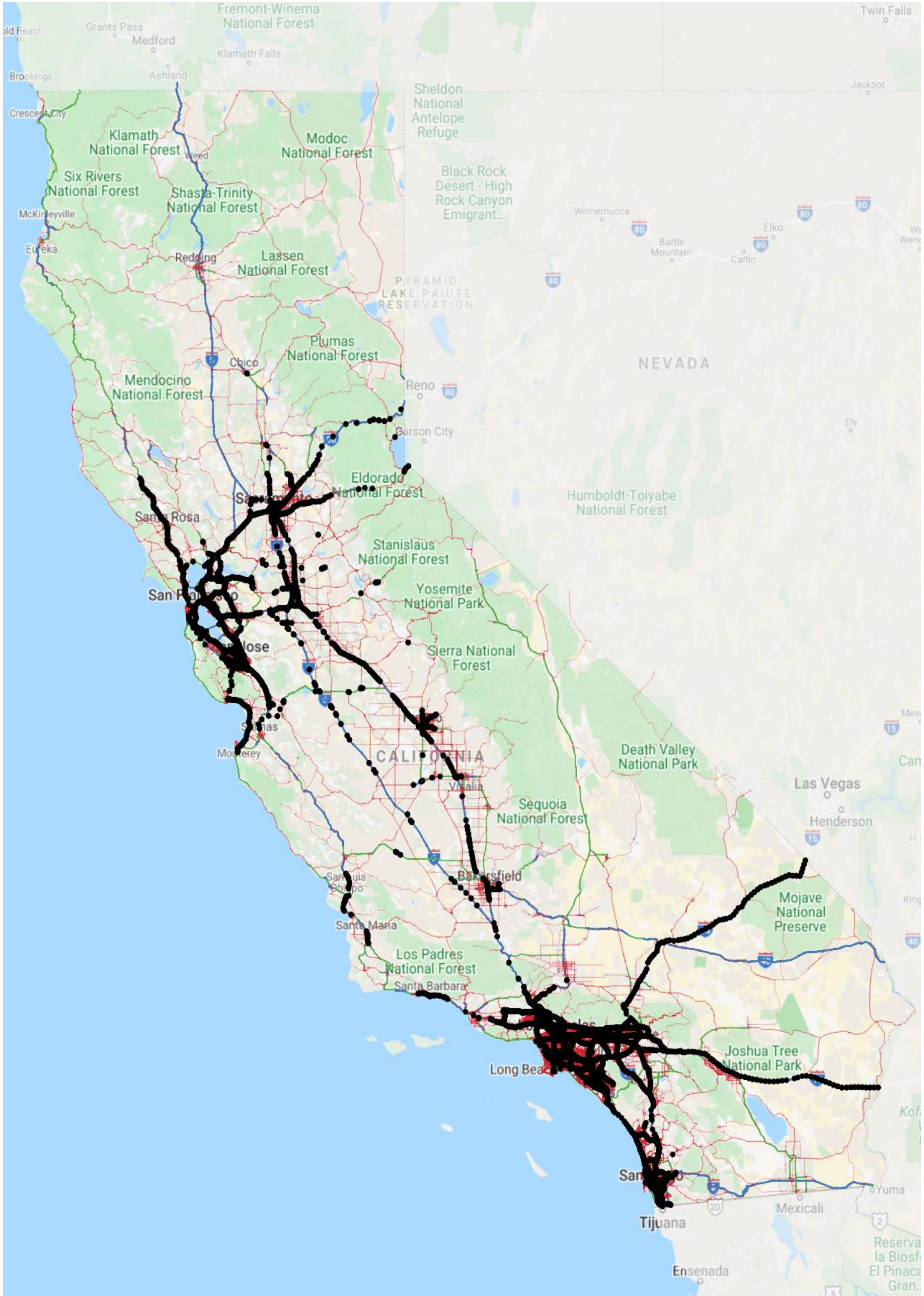

Figure 3. Location of count stations in the road network of California

150 interchanges are selected in the network. Although the number of installed count stations is extensive, they do not accurately record counts. Thus, a sanity check should be performed before feeding the counts to the model. The conservation of flow law is applied to compute the errors in recordings, thus completing the sanity check of the data.

Consider an interchange shown in Figure 4. In this figure, based on the conservation of flow, the sum of ramp and downstream flow must equal the upstream flow. However, due to errors in detection and recording, there will be an error term (ε) as provided in Equation (17).

$$V_{Upstream} = V_{Downstream} + V_{Ramp} + \epsilon \tag{17}$$

The smaller the error, the higher the probability of more accurate detections. In this study, the maximum allowable error is assumed to be $|\epsilon| \leq 0.05V_{Upstream}$ and observations with higher errors are eliminated from the dataset. Thus, after selecting 150 interchanges, a sanity check is performed for each interchange using the entire 2019 hourly volume counts of the PeMS database.

Once the input data is filtered to exclude detections with a higher error rate, the turning movement proportion is computed based on the aggregated hourly volumes using Equation 18.

$$turning\ movement\ proportion = \frac{V_{Ramp}}{V_{Upstream}} \tag{18}$$

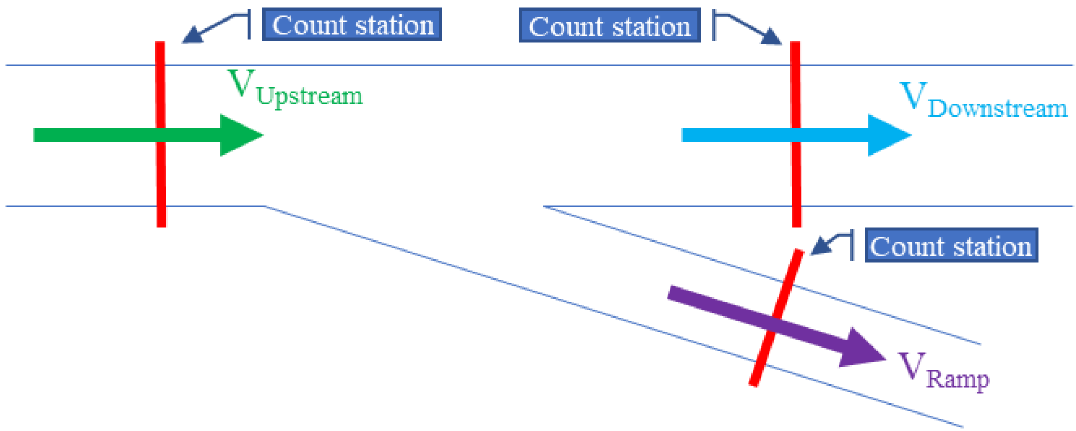

Figure 4. Schematic interchange illustration

4.2.2 Speed profiles

The changes in the speed of a segment are an appropriate indicator of the traffic conditions, and many agencies are utilizing this data to monitor and operate their traffic network. As traffic volumes enter a road at an intersection, they can considerably change the segment's speed. Thus, the information on speed profiles and how they vary with time can significantly benefit the estimation of the traffic volumes and traffic conditions at road segments. Here, speeds at different sections of an interchange are considered to reflect the traffic flow patterns on the highway and the road segments connected to the highway through this interchange. Figure 5 illustrates the approaches and speeds that are the subject of interest. In this interchange, Ramp-1 is the ramp that is under consideration. The speeds that will be considered in the model are as follows:

- S_{RT-D}: downstream speed of the exiting vehicles making a right turn.
- S_{LT-U}: upstream speed of the exiting vehicles making a left turn.
- S_{LT-D}: downstream speed of the exiting vehicles making a left turn.
- S_{RT-U}: upstream speed of the exiting vehicles making a right turn.

These speeds, computed based on GPS data, are obtained from the Regional Integrated Transportation Information System (RITIS, 2020) in an hourly aggregation. Besides

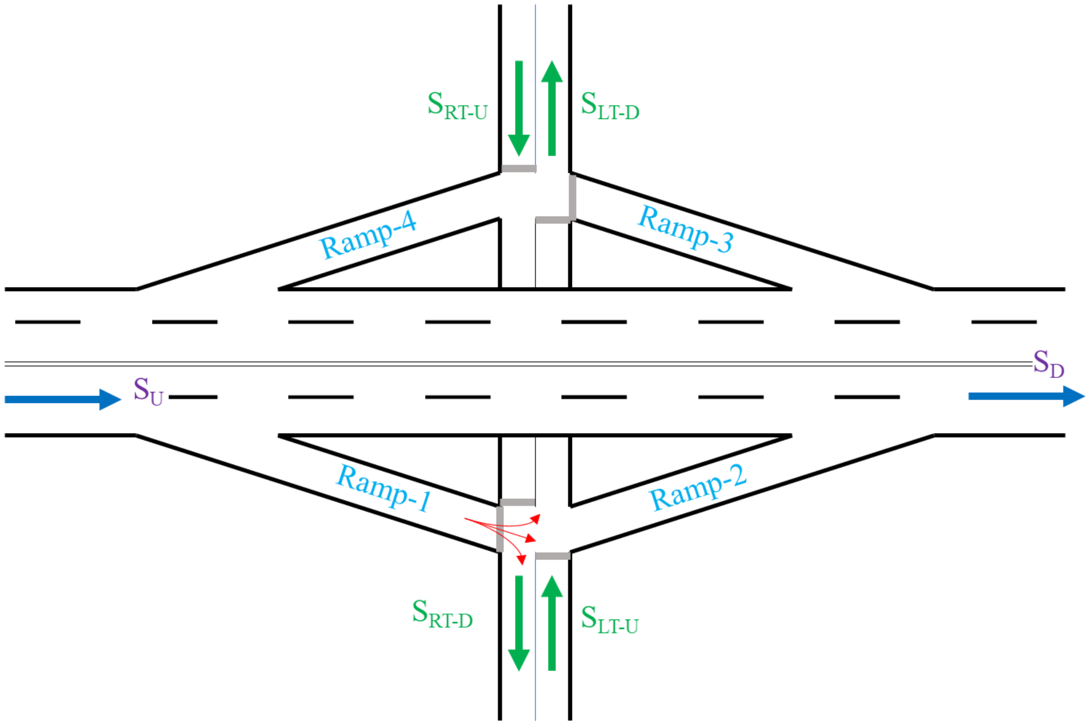

Figure 5. Schematic illustration of the considered speed profiles

average speed, free-flow speed (FFS) is obtained for each of the above approaches. By definition, FFS is the speed at which vehicles can traverse through the road in the absence of any restriction on their movement. The closer the speed in a road segment is to the FFS, the lower the congestion is and vice versa. Thus, this information can be leveraged as a reference for the traffic conditions in each segment.

4.2.2 Other attributes

In addition to volumes and speed characteristics, several other attributes are considered as input. These attributes are presented here:

- Average annual daily traffic (AADT): an essential feature of a road segment reflecting the average road usage in an entire year. This measure is easily accessible information that is calculated every year for different sections of the road network. This study uses the count sensors' records to compute this measure.
- Functional Road Class of the two roads in an interchange which can be one of the following categories:
    - Highways and major intersections
    - Major artery
    - Major road
    - Neighborhood streets
- Number of lanes for the upstream, downstream, ramp, left-turn downstream, left-turn upstream, right turn upstream, and right turn downstream.
- District and county of each interchange
- Month, day of the week, and time of the day
- Route number
- After combining the introduced data sources, the interchanges with less than one-month worth of data in an entire year (1×30×24=720) are omitted from the dataset. This additional filtering is done because those sparse observations for a single interchange bias the dataset, resulting in unreliable turning movement proportion estimates. After cleaning the data, 79 interchanges with a total of 236,552 record rows are obtained. The distribution of these remaining

interchanges is shown in Figure 6, where each black dot represents a remaining interchange. To illustrate how the data is distributed temporally, Figure 7 illustrates the number of observations for each month, week, day, and hour.

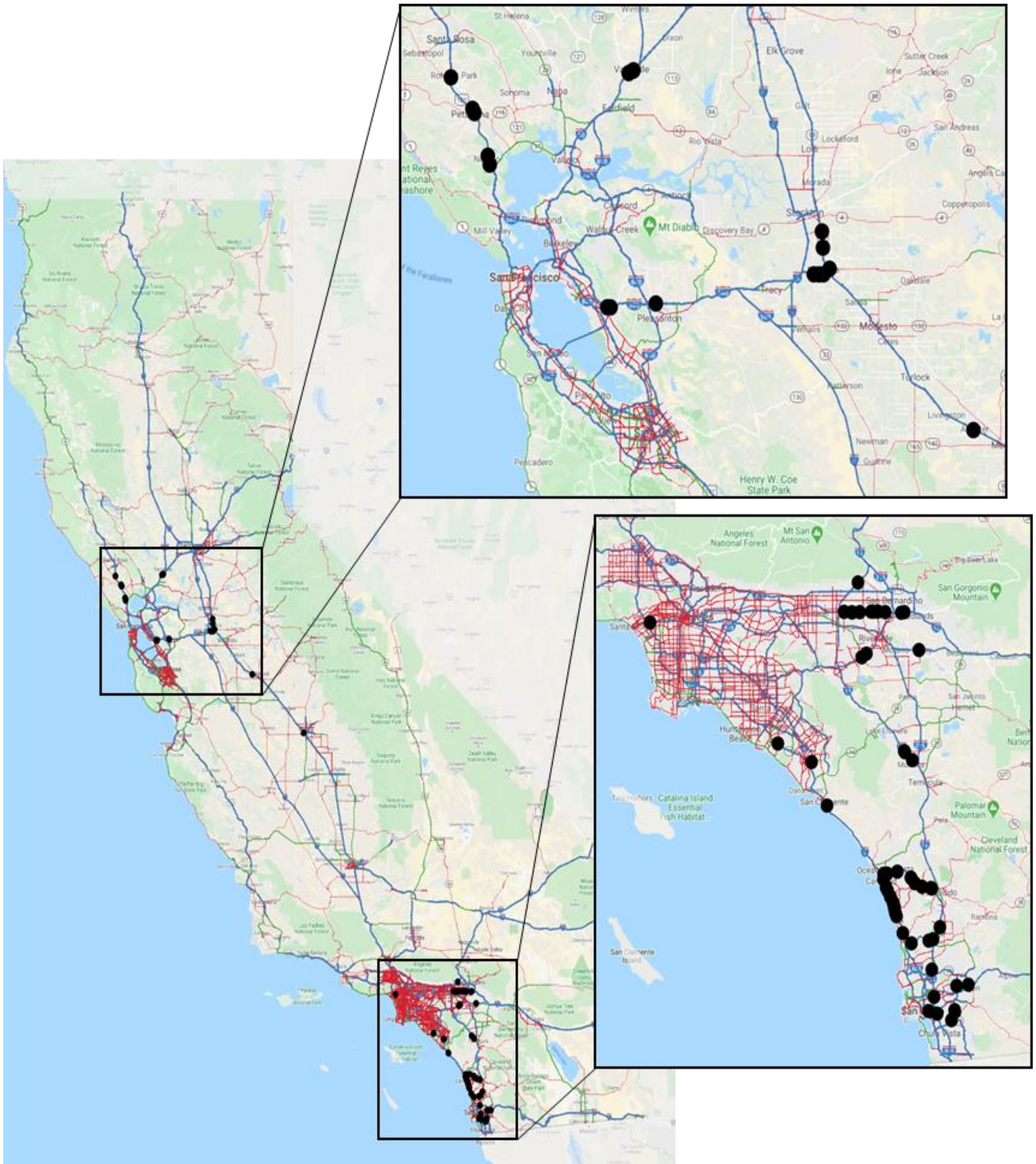

Figure 6. Location of the 79 considered interchanges

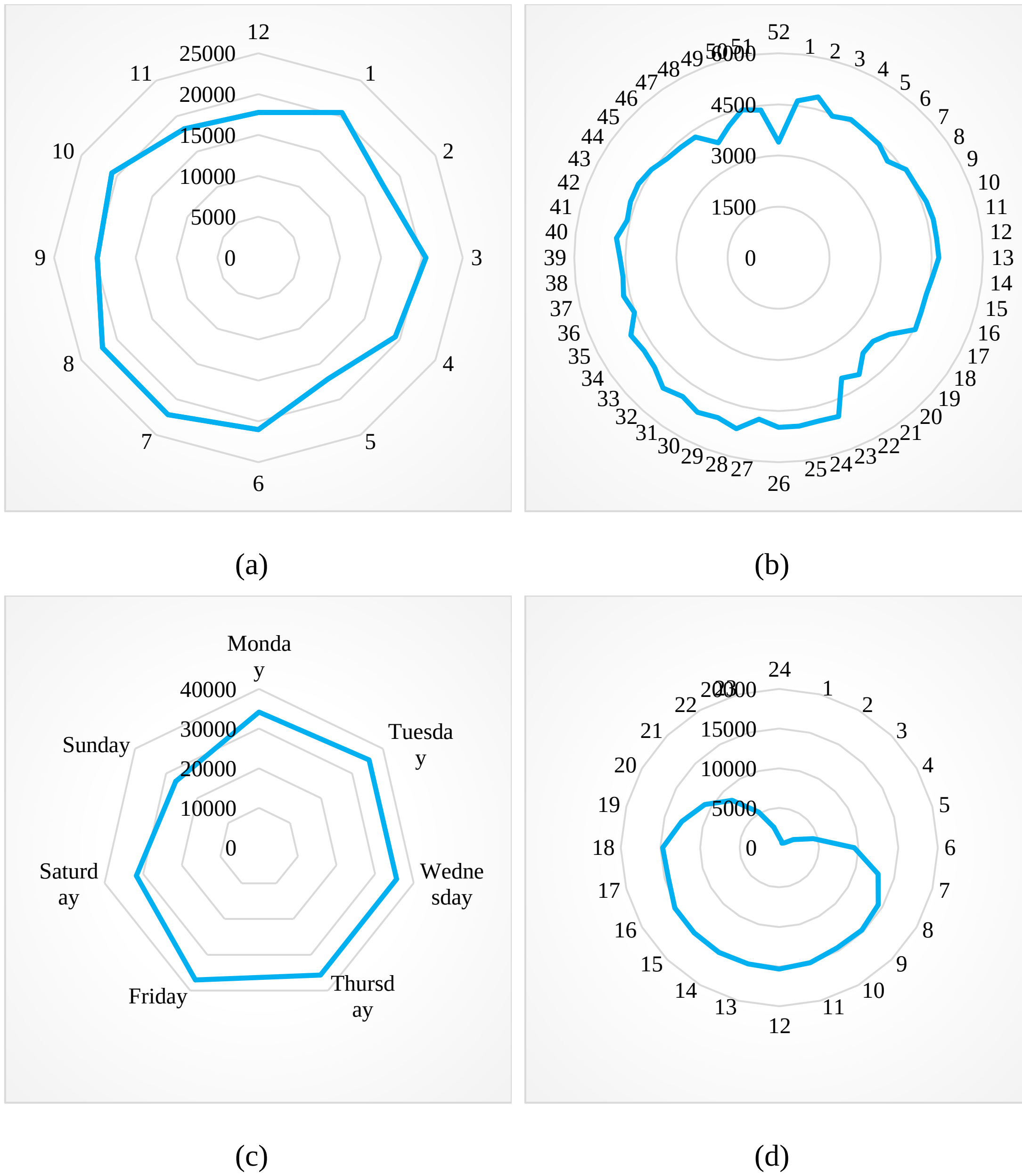

Figure 7. Distribution of the total observations for (a) each month of the year, (b) each week of the year, (c) each day of the week, and (d) each hour of the day.

According to these radar charts, the observations are relatively uniformly distributed except for the hour of the day. The distribution of the number of observations for each interchange is illustrated in Figure 8. This figure shows a considerable amount of variability. Additionally, figure 9 shows the cumulative distribution of the turning movement proportions. According to this figure, turning movement proportions range from 0 to 0.7; however, more than 80 percent of the observations have a turning movement proportion of less than 0.2 and more than 0.05. The input data distributions presented in Figures 7, 8, and 9 mandate multiple random draws of the data for training

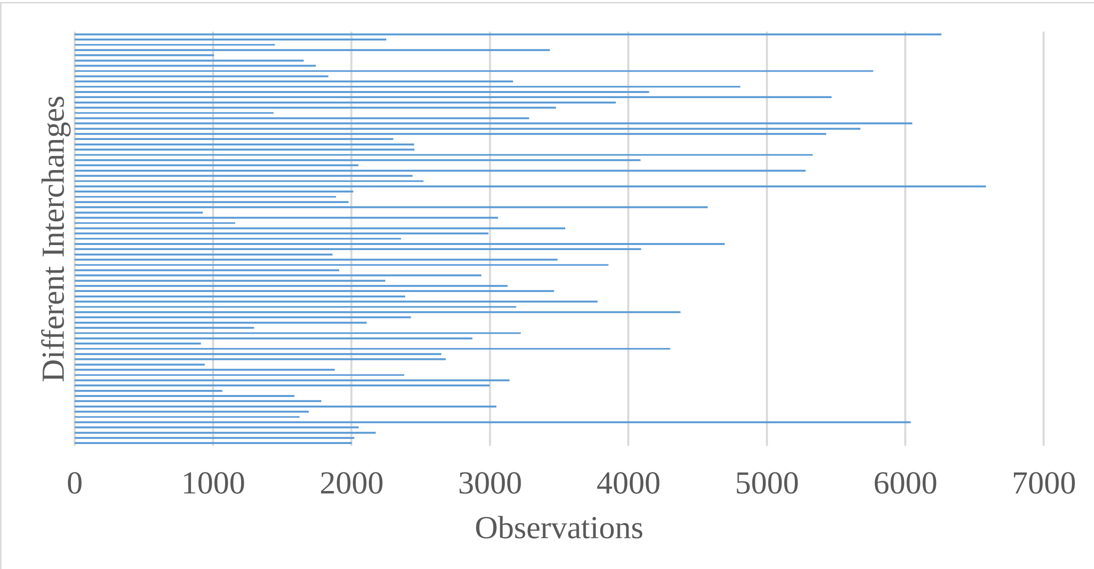

Figure 8. Distribution of observations for interchanges

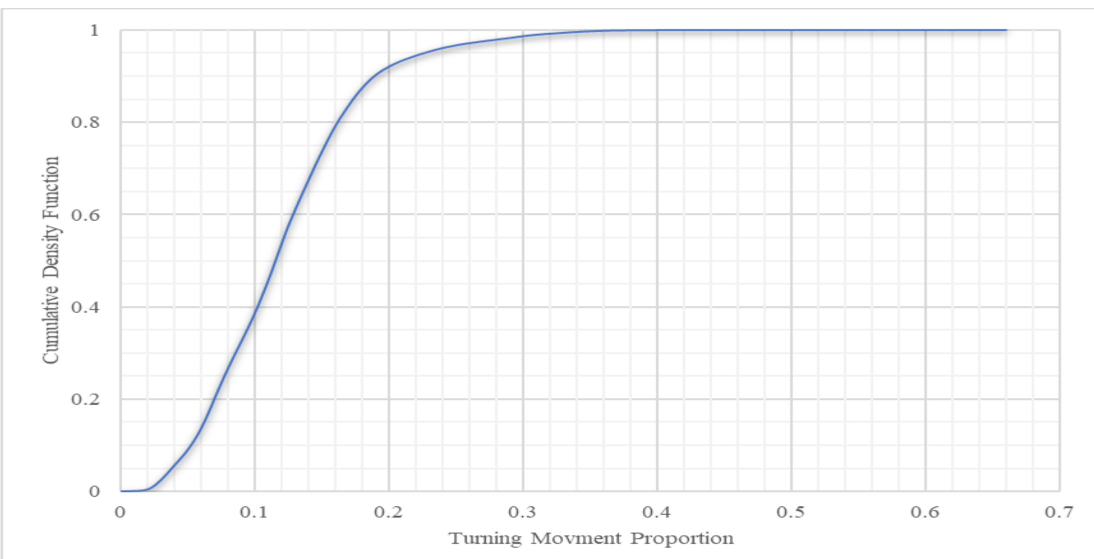

Figure 9. Cumulative distribution of turning movement proportions

and testing to draw conclusions from the results. In the next section, different scenarios for choosing the training data are presented, along with the results of testing the models on validation sets.

4.3 NN model results

In reality, there are a limited number of available sensors compared to the vast road network, which leaves transportation agencies with the problem of deploying detectors on the transportation network. There are two main strategies for installing traffic count sensors for transportation agencies. In the first strategy, to reduce the cost of relocating sensors, detectors are permanently mounted on several interchanges and continuously collect data in those interchanges. This strategy enables having access to the data of a long time duration of traffic conditions and travel behavior, although for a limited number of locations. In the second strategy, to uniformly collect data of all interchanges, sensors are temporarily (e.g., one week) installed on interchanges and relocated to other sites. This strategy enables obtaining data for a large number of locations; however, each site over a short period. The turning movement proportions estimation model can be trained and tested to consider these strategies. Therefore, in this study, a corresponding model is trained and tested for each data collection strategy to estimate each interchange's hourly turning movement proportions. The considered strategies and their final model structures are presented in the following subsections.

4.3.1 Permanent detector installation on a few interchanges

In installing sensors permanently, the model is trained on the data of the interchanges that have detectors collecting data continuously. Given the data of these interchanges, the proportions of turning movements at other interchanges are estimated to evaluate the model's accuracy. As presented previously (refer to Figures 7, 8, and 9), multiple draws of the input data are required to achieve reliable results. In this method, the training set for each random draw is obtained by dividing the data into two sets of training and testing, according to interchange IDs; thus, resulting in two distinct groups of interchanges. For each random draw, 70 interchanges are selected (almost equivalent to 90 percent of the total interchanges in the data) for model training, and the rest is utilized for testing the model. After experimenting with different NN models, the best model structure is chosen according to Figure 10. The results of training and validating the model for 25 training and validation sets drawn randomly from the whole dataset with 253 input variables are shown in Table 2. According to the results of this table, the average error percentage of the model over the validation set is 50% and has relatively high variations, thus illustrating that the model is somewhat unstable. This finding is further repeated based on the R^2, which has a negative minimum showing on some validation sets. This means that the model performs worse than the reported average turning movement proportions for these sets. Comparing each measure between the test and training sets reflects somewhat overfitting. Since the model structure is designed to avoid overfitting (i.e., batch normalization and L2 regularization, and drop-out layers), this should be attributed to the fact that the

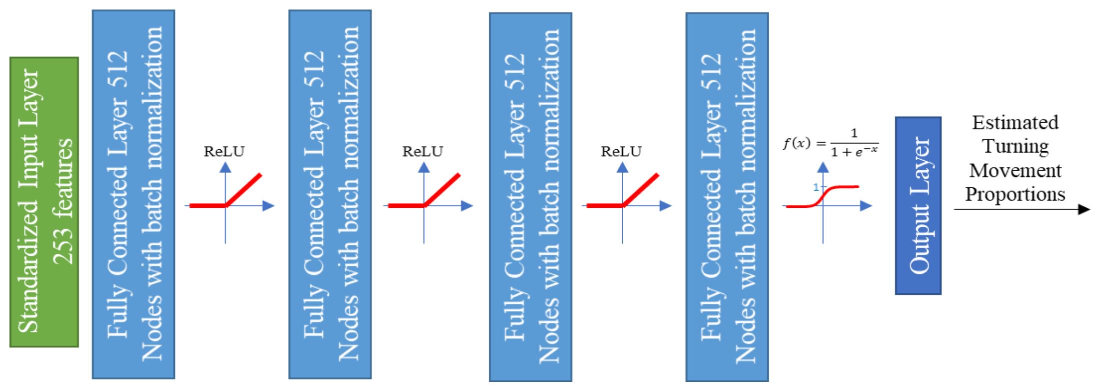

Figure 10. Structure of the NN model for the permanent detector installation

Table 2. Summary statistics of the results of the permanent detector installation model

	Mean	Standard Deviation	Median	Minimum	Maximum
Training MSE	0.0006	0.0000	0.0006	0.0006	0.0006
Validation MSE	0.0027	0.0017	0.0021	0.0008	0.0073
Training MAPE	28.38	2.43	29.34	22.24	30.94
Validation MAPE	51.45	19.48	50.09	25.22	96.98
Training R^2	0.803	0.043	0.815	0.687	0.848
Validation R^2	0.202	0.250	0.233	-0.344	0.575
Training Set Size	213,119	2,922	214,372	206,950	217,392
Runtime (sec.)	1,018	17	1,013	985	1,065

provided data is insufficient to extract the determining factors in turning movement prediction. Figure 11 demonstrates the Box and Whisker plots of MAPE and R^2 measures on the validation sets. This figure confirms the variability of the model performance on different validation sets, thus the relative instability of the model.

4.3.2 Temporary detector installation on all interchanges

In this strategy, for each interchange, one and only one week is selected from the whole dataset and is added to the training dataset. Randomly selecting a week for each interchange in the real world is equivalent to temporarily installing sensors for a single week on each interchange. The best model structure for this method, obtained from experiments, is presented in Figure 12. The summary of the model results of training and testing the temporary detector installation on all interchanges is demonstrated in Table 3. This model is trained with 25 different random training validation sets with 347 input variables. According to the results in this table, this model is relatively stable; however, it does not have an acceptable estimation performance.

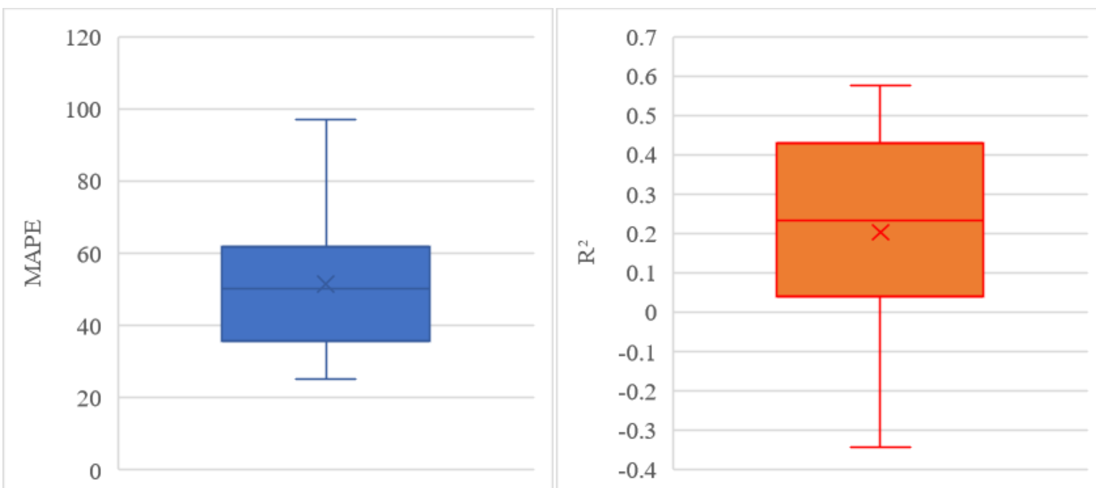

Figure 11. Box and Whisker plots of MAPE and R^2 over the validation sets for the permanent detector installation model

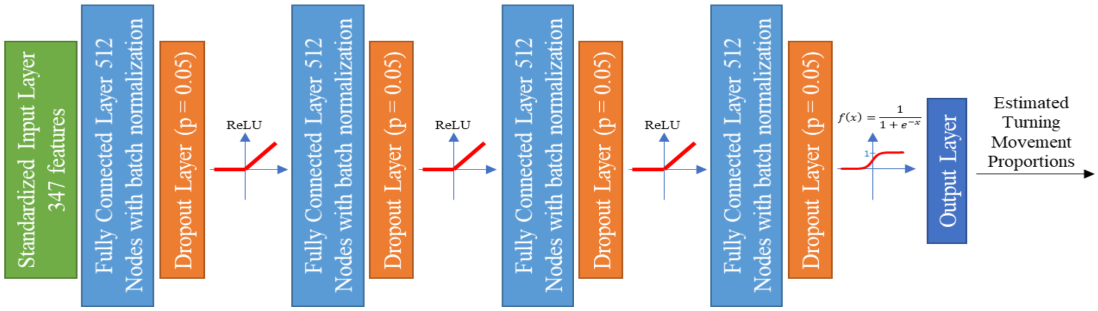

Figure 12. Structures of the NN model for the temporary detector installation method

Table 3. Summary statistics of the results of the temporary detector installation model

	Mean	Standard Deviation	Median	Minimum	Maximum
Training MSE	0.0003	0.0001	0.0003	0.0002	0.0005
Validation MSE	0.0019	0.0004	0.0018	0.0014	0.0034
Training MAPE	18.34	3.99	16.75	13.01	26.90
Validation MAPE	49.12	4.14	49.92	40.44	58.09
Training R^2	0.943	0.021	0.948	0.866	0.969
Validation R^2	0.450	0.115	0.488	0.000	0.578
Training Set Size	3253	212	3253	2770	3697
Runtime (sec.)	2758	1152	2457	1227	4643

Box and Whiskers plot of MAPE and R^2 shown in Figure 13 also provide additional proof for the relative stability of the model. Exploring the reasons for the poor performance of this model illustrates that the number of observations in the training set is too few. The number of observations shows that for each interchange, on average, only 1.7 days' worth of data is included in the training set instead of the ideal seven days of data.

One may argue that the few numbers of observations for each interchange in different weeks are not representative of the real-world situation. In the real world, the number of missing records of each interchange should be minimal when a transportation agency temporarily installs sensors. Therefore, we introduce another to reflect the real-world installation of detectors based on the number of observations in a week. This method is similar to the previous method except in choosing the records incorporated into the training set. Here, the week with the maximum number of observations is incorporated into the training set for each interchange.

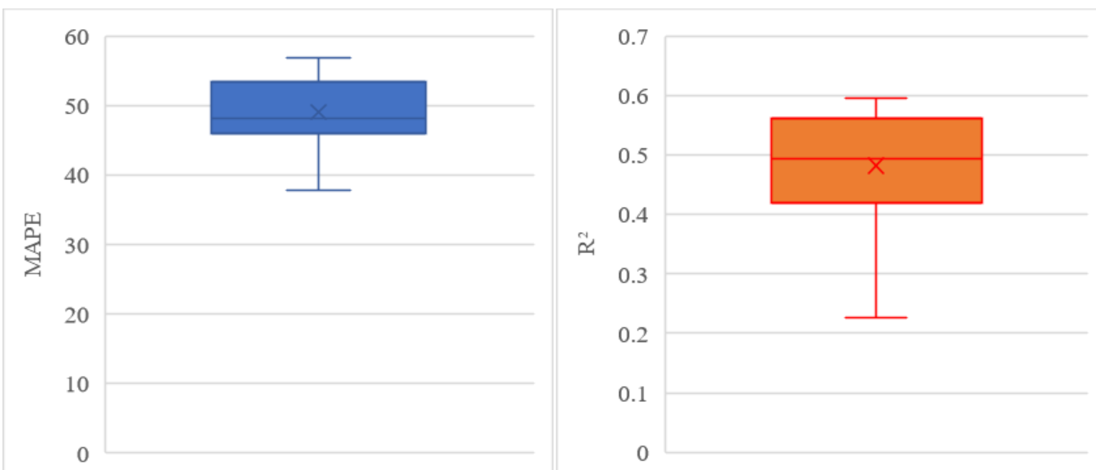

Figure 13. Box and Whisker plots of MAPE and R^2 over the validation sets for the temporary detector installation model

The results of training and testing the same model using this strategy are provided in Table 4. There are 347 input variables in this model. The model is trained 25 times to account for different initial values given to the model. Based on the results in this table, this model has an appropriate performance. The slight variations in the performance measures of this model are due to the initial values given to the model.

Table 4. Summary statistics the results of the temporary detector installation model with maximum observations in a week for each interchange in the training set

	Mean	Standard Deviation	Median	Minimum	Maximum
Training MSE	0.0002	0.0000	0.0002	0.0002	0.0004
Validation MSE	0.0006	0.0001	0.0006	0.0005	0.0008
Training MAPE	12.55	1.25	12.20	11.19	16.91
Validation MAPE	29.80	2.32	29.13	26.48	34.56
Training R^2	0.965	0.010	0.966	0.933	0.979
Validation R^2	0.829	0.022	0.838	0.778	0.853
Training Set Size	7308	0	7308	7308	7308
Runtime (sec.)	2924	1233	2683	1264	5194

4.3 Summary of findings

Chapter 4 presented the results of training models to estimate turning movement proportions at interchanges based on various methods of selecting training datasets and testing corresponding to real-world data collection strategies. The results provide evidence for the possibility of estimating and predicting turning movement proportions at different times and locations using the information on road traffic conditions. The approach taken in this study enables relatively accurate estimation of turning movement proportions with the temporary installation of vehicle detectors on those interchanges. The number of observations that allowed accurate estimation is surprisingly low, which shows the applicability of this method to real-world problems. Thus, this procedure requires a small reliable ground truth data on turning movements of interchanges that are subject to study over a short period. On the other hand, the permanent installation of the detectors' method did not produce acceptable results, which means the spatial relations between the turning movement at different interchanges are not established.

Chapter 5: Data

5.1 Overview

This study proposes a model framework to estimate and predict the 15-minute turning movement traffic volumes using the traffic flow conditions and road characteristics attributes. This chapter presents the data used for training and testing the models. In the first step, the study area is introduced to give an overview of the location of the intersections. Further, the data sources for traffic speed and probe vehicle movements are described, followed by comparing actual turning movement proportions and the probe vehicle dataset proportions. Finally, the turning movement dataset is summarized using distribution figures.

5.2 Study Area

Exploring turning movement traffic volume estimation and prediction requires complex and comprehensive data collection efforts that not all jurisdictions can undergo. Therefore, one of the earliest obstacles this study faces is finding a reliable and comprehensive dataset containing the traffic volumes performing each allowable turning movement at several intersections. In addition to including a considerable duration of data collection with a relatively high resolution of the time unit, the desired ground truth data set should be located where there are access to traffic speed and vehicle probe data movements. One of the very few datasets satisfying the mentioned criteria is the turning movement count repository of the city of Austin in Texas. The data in this repository is collected through the deployed GRIDSMART[1] optical traffic detectors in the selected intersections of Austin. The GRIDSMART sensor is a single-camera system that counts the turning movement traffic volumes using object detection and tracking algorithms based on user-determined regions of interest in the video stream, an example of which is shown in Figure 14.

Figure 14. **Typical GRISMART sensor view**

[1] https://gridsmart.com/

The location of the sensors installed in the network is illustrated in Figure 15.

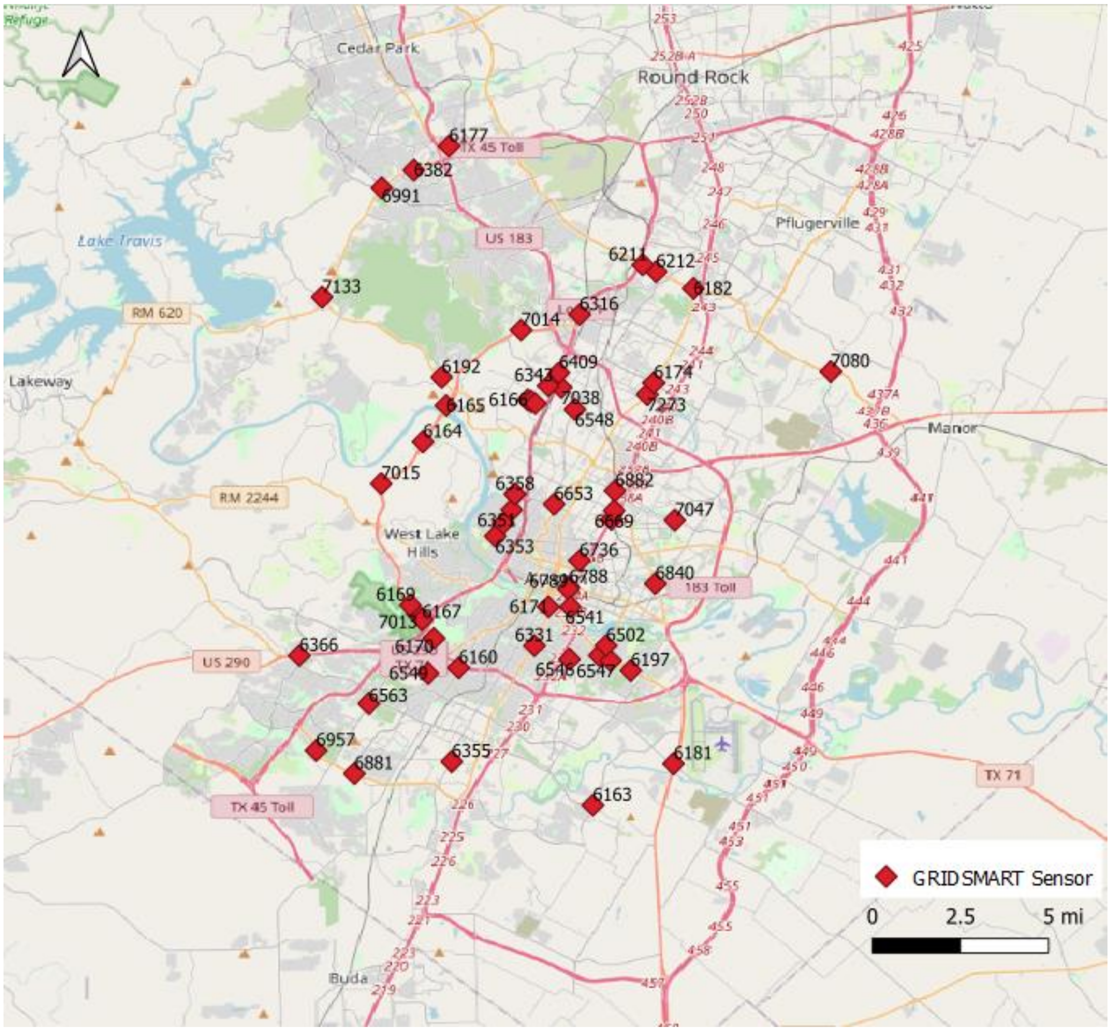

Figure 15. Location of GRIDSMART sensors in Austin, TX

It should be noted that some of these sensors were temporarily installed therefore collecting data for a specific time period. The collected data from the GRIDSMART sensors are continuously uploaded to the City of Austin open data portal[1] and are publicly accessible. Each record row represents the vehicular counts of a specific movement at an intersection in this dataset. The first records in this repository date back to mid-2017. However, the selected date for the analysis in this study is the years 2019 and 2020 since high-resolution speed data is accessible to the author for these years. Besides, for 2020, the INRIX vehicle probe data movements are accessible to the author, which is explored in the current study. The downside of 2020 is the existence of irregular traffic flow characteristics due to the Covid-19 pandemic. The intersections with active sensors during 2019 are illustrated in Figure 16 and 2020 in Figure 17.

5.3 Extraction of speed profiles

The findings of the off-ramp traffic volume estimation model in this study and previous studies have shown the importance of traffic speed on traffic volumes. Although the relations between intersection turning movement counts and traffic speed is much more complicated and somewhat unresolved compared with the case of highway and freeway traffic, the incorporation of the traffic speed attributes into the dataset can benefit the models. Thus, the extraction of traffic speed variables is necessary for the turning movement count estimation framework. In the first step of traffic speed extraction, the

[1] https://data.austintexas.gov/

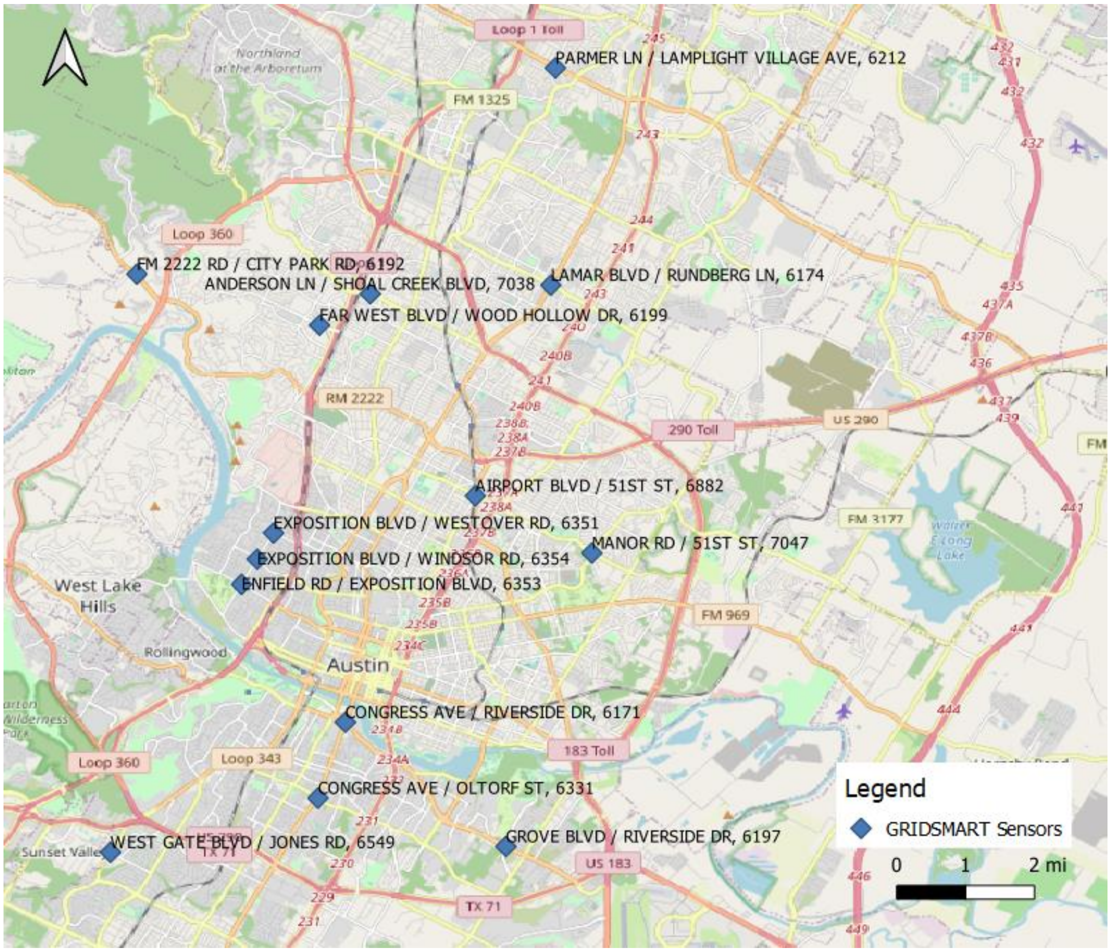

Figure 16. Location of 2019 GRIDSMART sensors in Austin, TX

INRIX XD and TMC segments are manually determined for each of the eight segments of a four-legged intersection and six segments of a T-intersection from the massive data downloader tool of the RITIS dashboard[1]. The advantage of obtaining both XD and TMC segments is that in the case of a missing traffic speed value in the XD-based

[1] https://pda.ritis.org/suite/download/

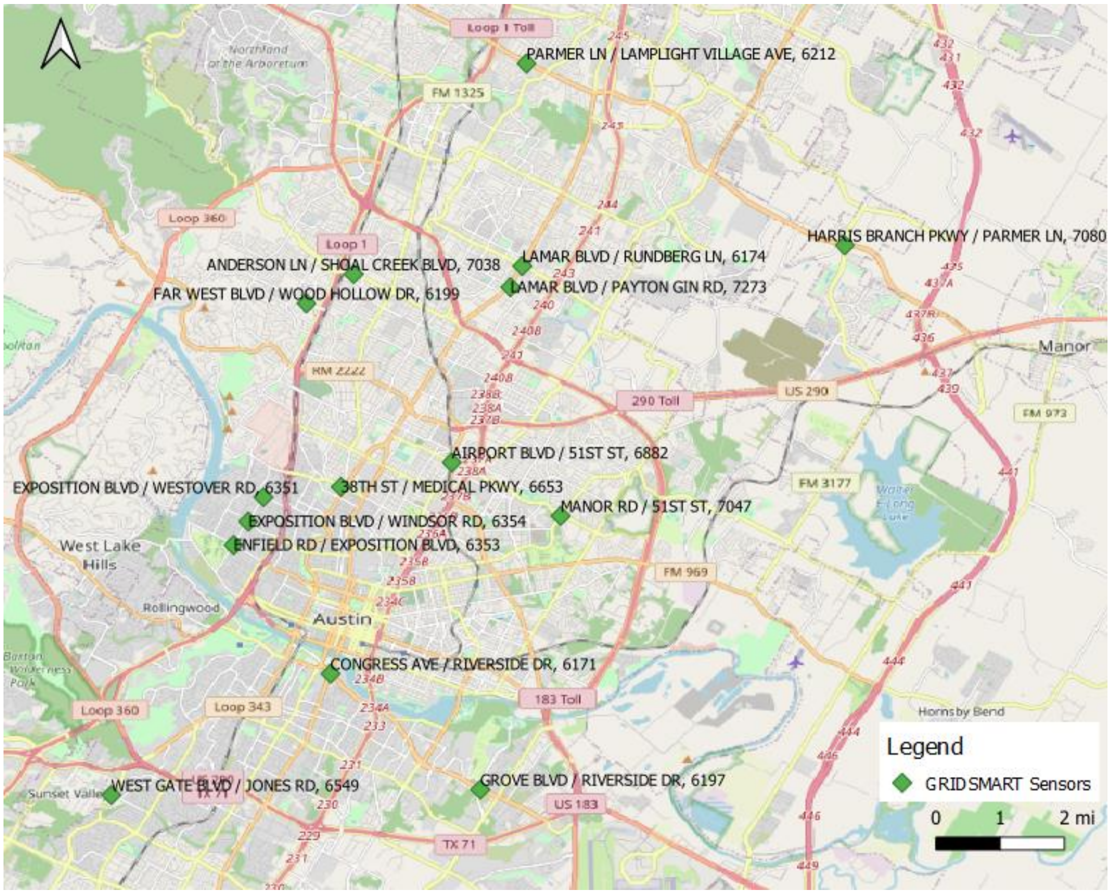

Figure 17. Location of 2020 GRIDSMART sensors in Austin, TX

dataset, the same attribute can be extracted from the TMC-based dataset. The features that are extracted for each mentioned segment are as follows:

- Current speed: The current estimated harmonic mean speed for the roadway segment in miles per hour.
- Average speed: The historical average speed for the roadway segment for that hour of the day and day of the week in miles per hour.
- Reference speed: The calculated "free flow" mean speed for the roadway segment in miles per hour. This attribute is calculated based upon the 66th-percentile point of the observed speeds in that segment for all time periods,

which establishes a reliable proxy for traffic speed at free-flow conditions for that segment.

In the next section, the dataset is summarized and described using different figures to provide a broad overview of the dataset and make the reader more familiar with the data distribution in various locations and times.

5.5 Data descriptive analysis

Different data sources used in the intersection turning movement counts estimation were introduced in the previous sections of the current chapter. This section provides a data description to illustrate the distribution of the observations at different times, different turning movements, etc.

The dataset is constructed as a large table. Each row represents the number of vehicular traffic performing a given specific turning movement during a particular time interval in a determined approach at a given intersection. The duration of each record in the dataset is 15 minutes. The observations selected for model development are from 7 AM to 6 PM. This selection is because these hours typically include the peak traffic volumes; therefore, they are the most important from the perspective of traffic operators and planners. Besides, the dataset's source is from vision-based sensors; thus, the darkness of the environment can negatively affect the detection accuracy, and it is better to avoid using night observations for the present study. With the described configuration of data selection, the total number of observations for a given four-legged intersection with three allowed movement types at each approach, assuming no missing observations, will be 365*12*4*12=210,240 for 2019 and 366*12*4*12=210,816 for 2020.

The first set of figures, Figure 18, represents the distribution of records in 2019 and 2020 based on the month of the year, day of the week, and hour of the day. As it can be seen, according to this figure, the number of record rows in each bin is relatively uniformly distributed except for the number of records in each month. For instance, in the distribution of the number of observations per month in 2020, the months of May to August have distinctly lower records indicating a higher number of missing observations in the database in these months. Additionally, the number of records in each hour illustrates that the start and end hours of the considered durations have lower records in the data, which substantiates that optical traffic detectors can have difficulties detecting vehicles with reduced environment light.

In the next set of figures, Figure 19, traffic counts, turning movement proportions, upstream speed, and the downstream speed for each movement type (i.e., left-turn, right-turn, and through movements) are illustrated as mentioned earlier over 15-minute time intervals. The upstream segment for each specific movement is the entering segment to the intersection, while the downstream segment is the exit segment. The following takeaways can be deduced from Figure 19:

- The intersections with deployed GRIDSMART sensors are generally low-volume intersections with a through movement count that rarely exceeds 960 vehicles per hour, even during peak demand intervals.

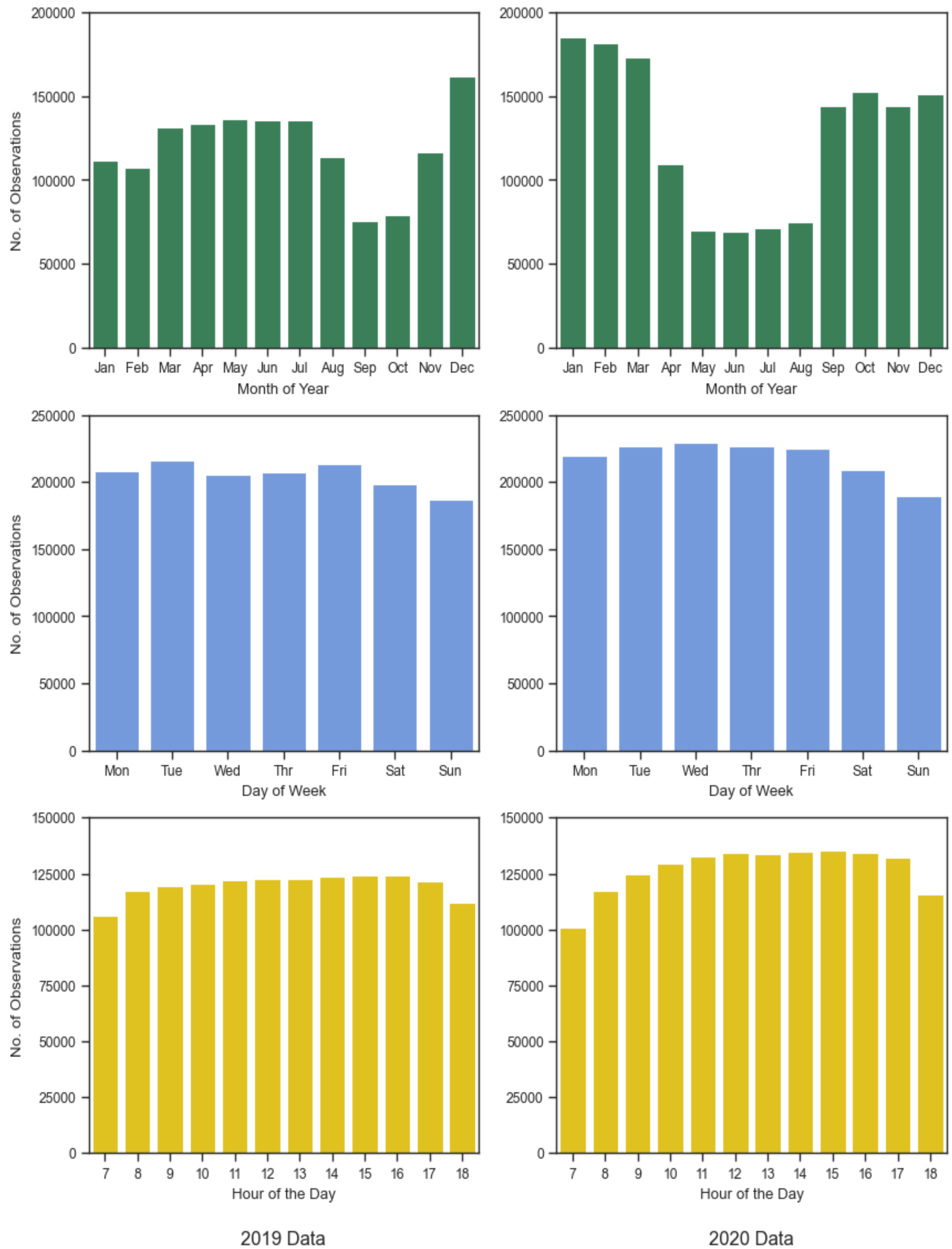

Figure 18. Distribution of the number of observations in month of the year, day of the week, and hour of the day

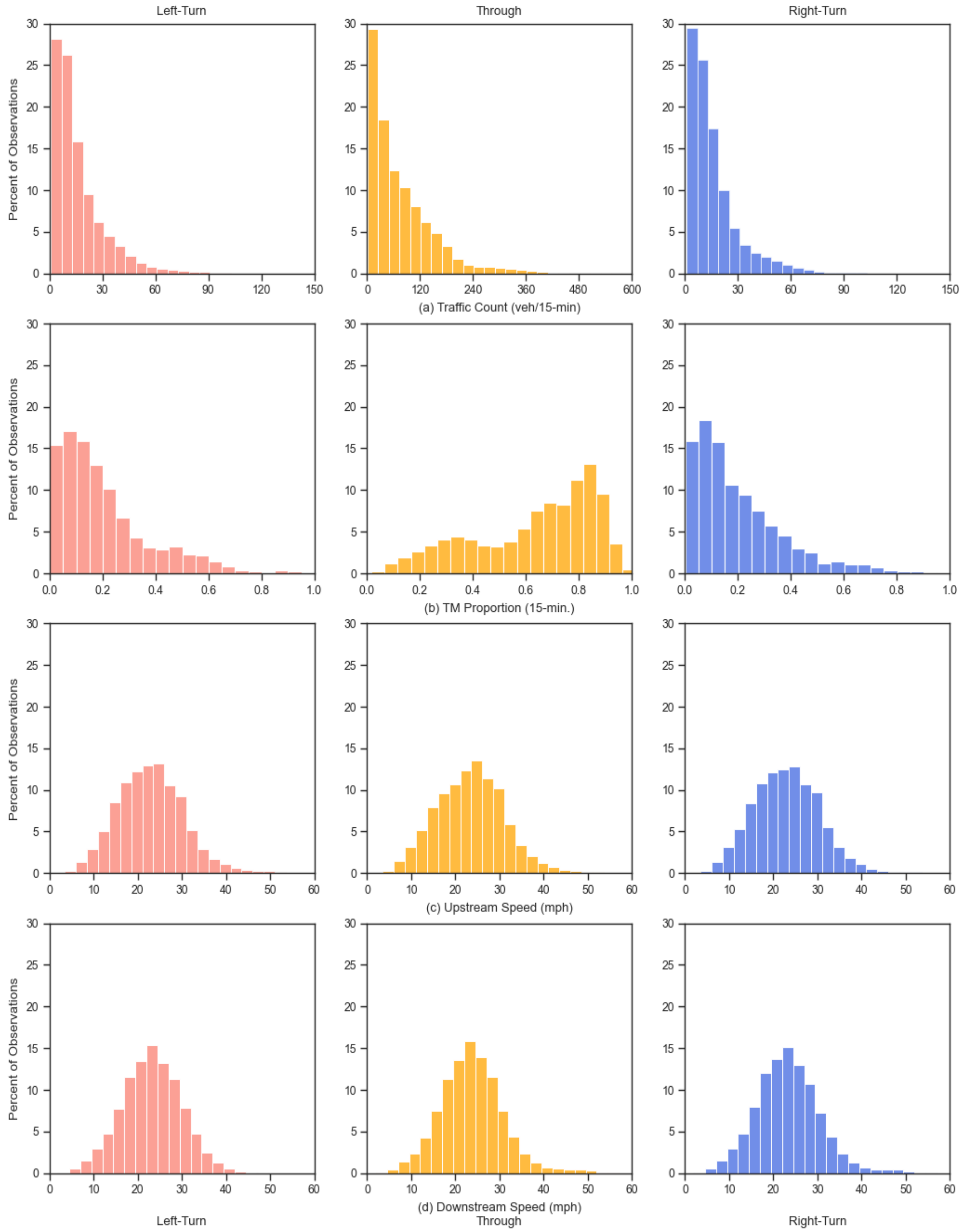

Figure 19. Histogram of (a) Traffic counts (veh./15 min) (b) Turning movement proportions (15 min) (c) Upstream speed (mph) (d) Downstream speed (mph) for all study intersections

- The right- and left-turn movement proportions are typically less than the through movement proportion.
- The speed distribution for each movement's upstream and downstream legs is relatively normally distributed. Most of the observations range from 10 to 40 miles per hour, a reasonable traffic speed for urban arterials. However, the speed variations in the upstream segment are higher than in the downstream, which can be attributed to the impacts of the traffic signal and the arrival time of vehicles relative to the signal configuration.

A summary statistics of the number of observations for each intersection in the 2019 and 2020 datasets are presented separately in Table 5. Note that the maximum possible number of observations is based on counting the number of allowable movements in the selected intersections considering that intersections can be four-legged, T-intersection, or have one-way approaches. The total possible movements in 2019 intersections is 156, and in the 2020 dataset is 168. The maximum number of observations for each specific movement is the multiplication of the number of days in each year (2019, 365 days; 2020, 366 days) by 12 hours (6 AM to 7 PM) by four quarters in each hour. The mean percentage of observations in Table 5 illustrates that the missing record rows in the data are more than 40 percent of the total possible data, which indicates a need for improvement in the GRIDSMART sensors' placement in the intersection, detection and tracking algorithms, maintenance, etc.

Table 5. Summary statistics of the observations

Year	2019	2020
Intersections	15	15
Mean no. of observations	101,716	102,453
Median no. of observations	96,154	109,895
Min. no. of observations	18,915	15,399
Max. no. of observations	194,218	188,831
Total no. of observations	1,525,744	1,536,801
Max. possible no. of observations	156*17,520=2,733,120	168*17,568=2,951,424
Mean percentage of observatios	%55.82	%52.07

5.6 INRIX probe vehicle turning movements

The data of probe vehicle movements can be an appropriate indicator of the general traffic patterns replacing the need for traffic detector deployments to some degree. However, the extracted travel patterns can be biased due to the nature of probe vehicle data since the vehicle probe data employed in this study are provided mainly by commercial vehicles. Commercial vehicles might avoid left-turn movements or have other specific movement patterns that differ from most road users. Therefore, a thorough analysis of the turning movement patterns between the actual traffic and the probe vehicles is necessary. Besides, since the probe vehicle movements are high-priced data rarely available to transportation authorities, MPOs, and researchers, its investigation in turning movement estimation applications is an interesting topic overlooked in the literature.

This study comprehensively fills the gap described by comparing the ground truth and probe vehicle turning movements. The source of probe vehicle data used in the present study is INRIX, a well-known transportation data provider. This data is for the year 2020 and aggregated over 15-minute time intervals.

A comparison between the turning movement proportions of the actual traffic and the probe vehicle data for each specific movement is illustrated in Figure 20. The proportions are computed using Equation 19.

$$turning\ movement\ proportion\ for\ movemnt\ \mathrm{i} = \frac{V_i}{V_{Approach}} \tag{19}$$

where V_i is the traffic volume of movement "i," and $V_{Approach}$ is the total traffic volume in the corresponding approach.

As can be seen in Figure 20, there are significant differences between the turning movement proportions of the ground-truth and INRIX probe vehicle datasets. The concentration of observations in the probe vehicle turning movement data is in the proportions equal to zero or one, indicating that the number of probe vehicles in each quarter of an hour is too small to capture the actual turning movement proportions. One solution for this problem is to explore the turning movement proportions with higher levels of aggregation in time. Figures 21 and 22 illustrate the comparison of

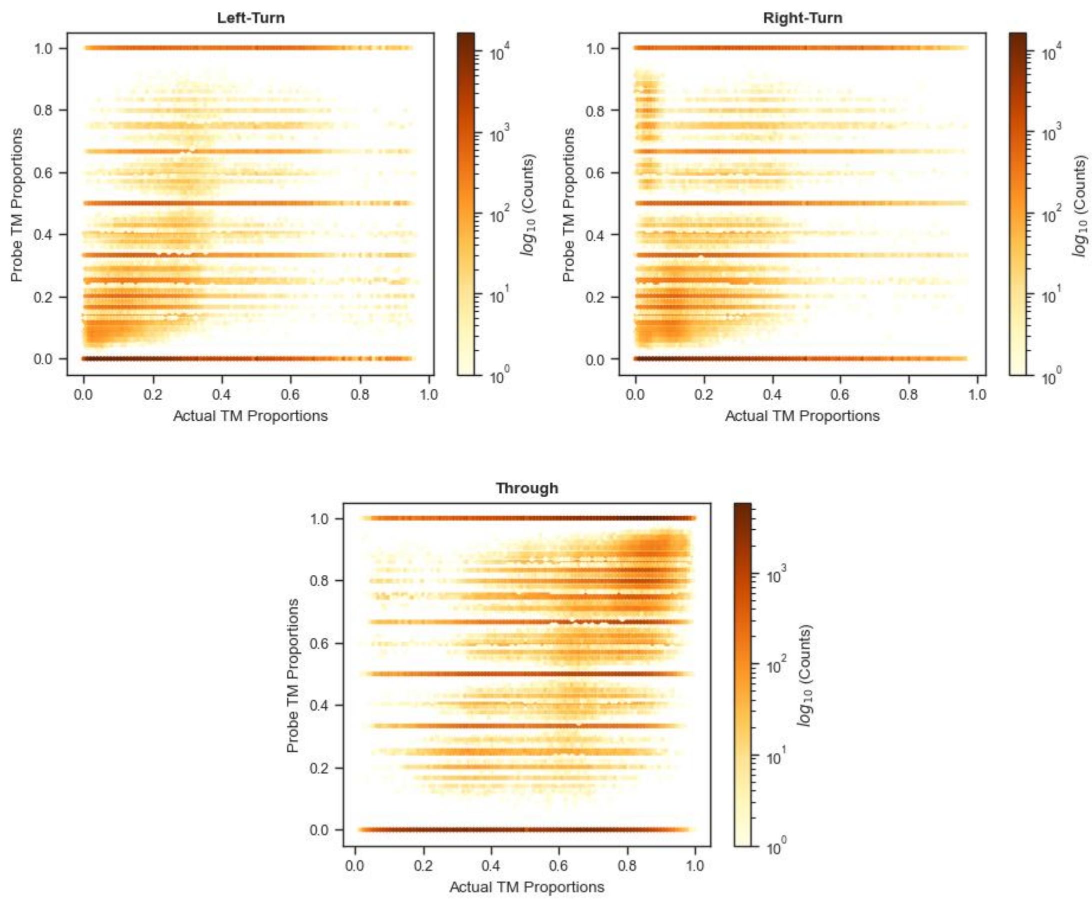

Figure 20. Comparison between turning movement proportions of the actual traffic vs. probe vehicle datasets in each quarter of an hour

turning movement proportions every 30 minutes as well as every 60 minutes. According to these figures, although some error reduction levels are achieved, the differences are still very high. Since another possible cause for this issue can be the lack of INRIX probe vehicles at some time intervals and in some locations, the distributions of turning movement proportion differences are plotted for each level of probe vehicle volume in the upstream approach in Figure 23. As it is evident in this figure, there are extreme differences between the actual turning movement proportions and INRIX turning movement proportions. For instance, even in the highest volume of

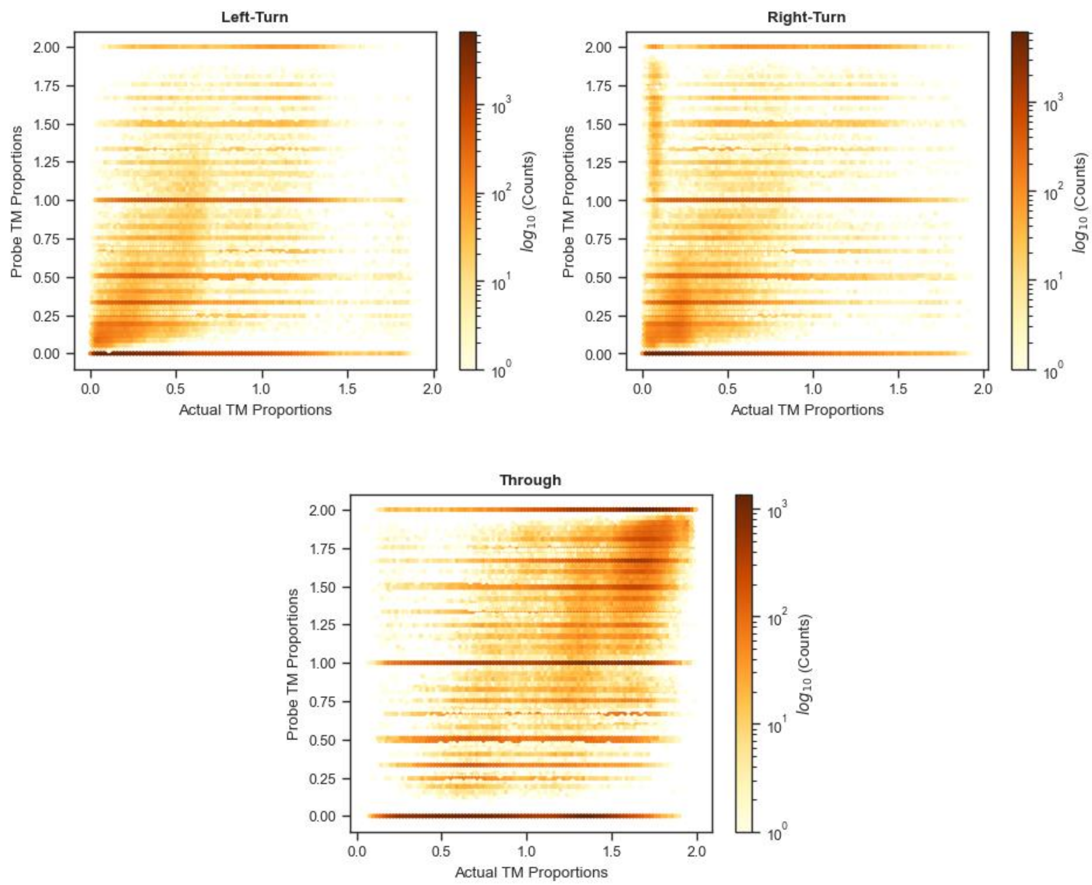

Figure 21. Comparison between turning movement proportions of the actual traffic vs. probe vehicle datasets in each half of an hour

upstream probe vehicles, differences in turning movement can be as high as 0.5. Besides, the probe vehicle volumes of more than 20 vehicles per 15 minutes are only observed in 0.26 percent of the entire dataset. Therefore, the turning movement proportions of the INRIX probe vehicle are not a suitable representative of the actual turning movement counts.

This chapter described different data pieces that built up the turning movement estimation investigation database. From each dataset in 2019 and 2020, 15 intersections with the GRIDSMART optical sensors are selected. The temporal distribution of the

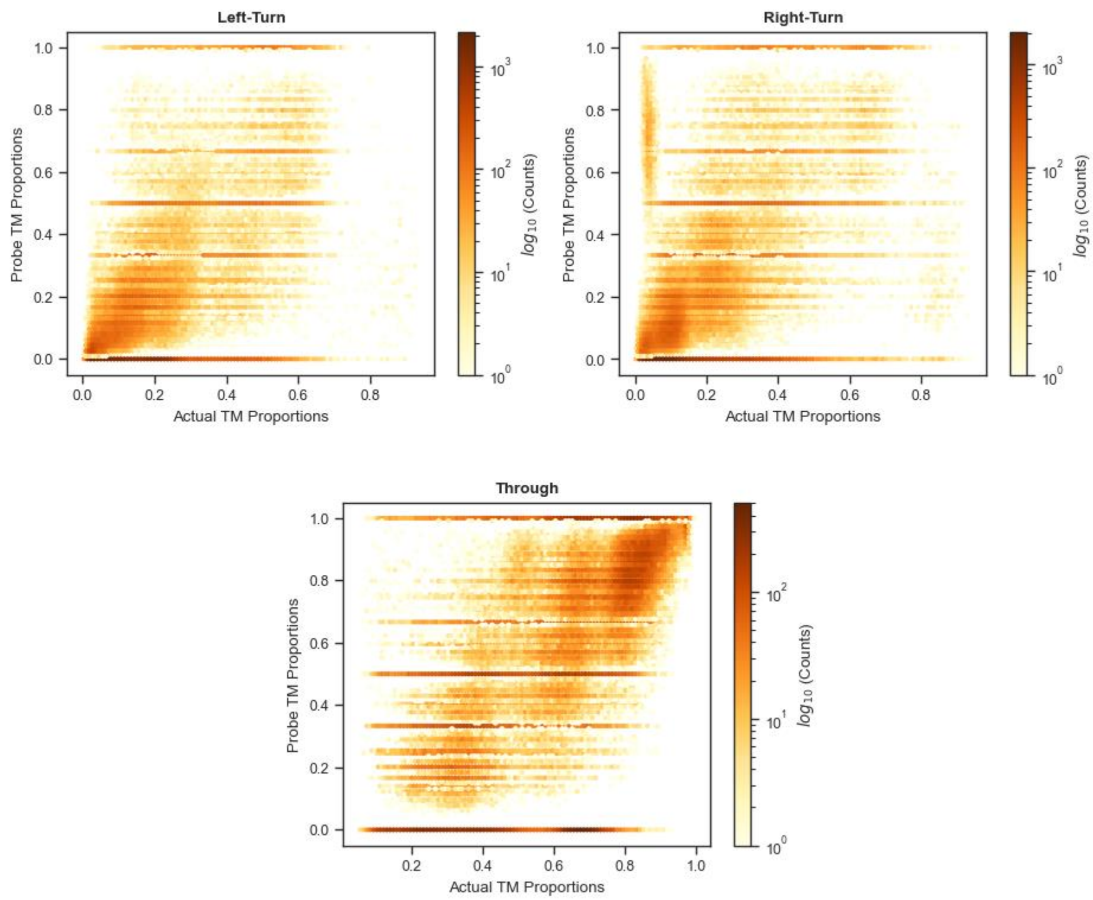

Figure 22. Comparison between turning movement proportions of the actual traffic vs. probe vehicle datasets in each hour

observations illustrated a relatively uniform number of observations at each hour and day of the week and to lesser degrees in the month of the year. The distribution of traffic volume for each turning movement illustrated that the intersections were located in low to mid traffic volume areas. Comparing the INRIX probe vehicle data and the GRIDSMART data as the ground truth revealed significant differences between the two datasets. In the next chapter, the turning movement count estimation framework is presented along with experiments to investigate the prediction accuracy resulting from each configuration.

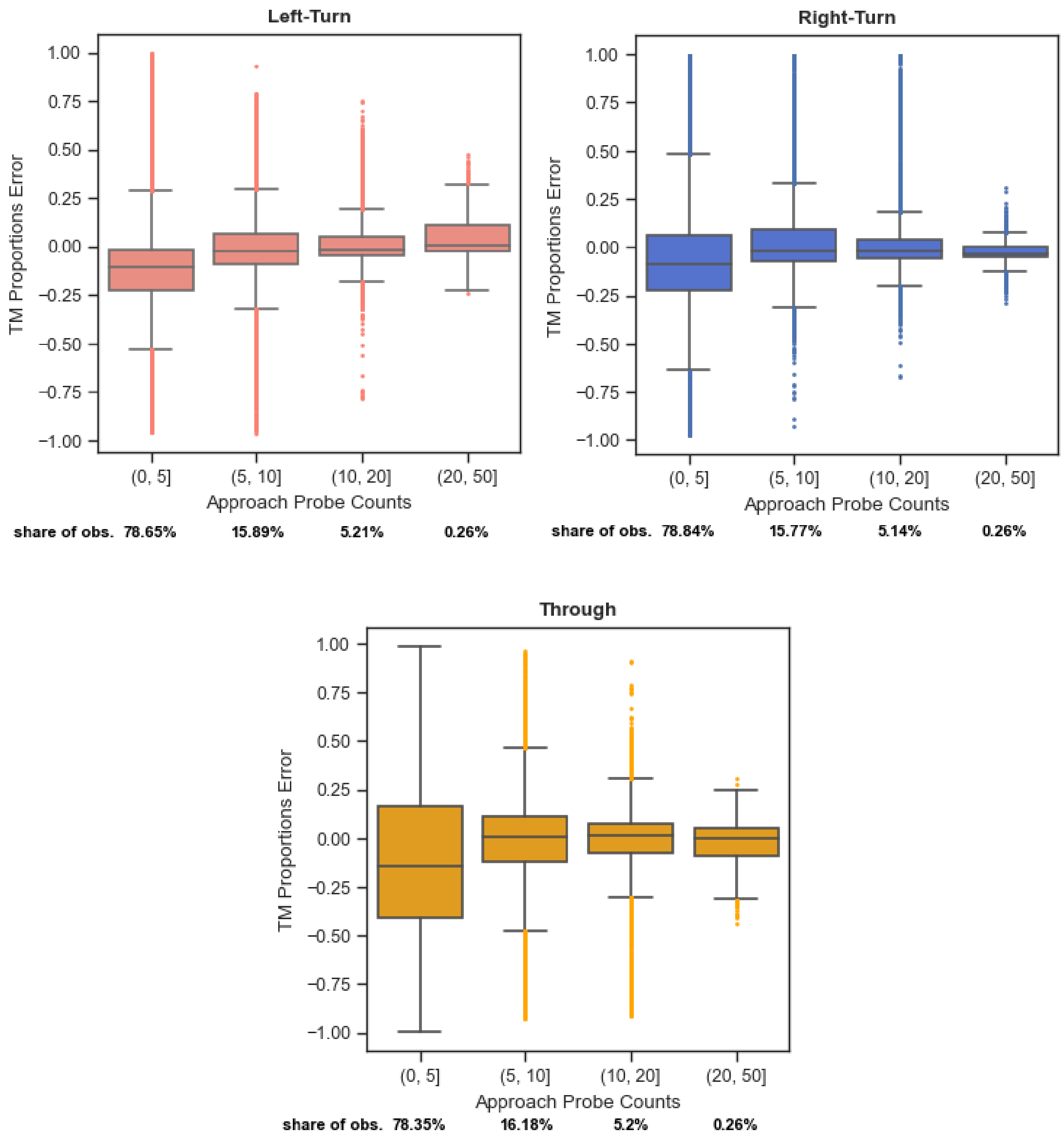

Figure 23. Differences between turning movement proportions of the actual traffic vs. INRIX probe vehicle dataset in each quarter of an hour based on upstream probe vehicle volume

Chapter 6: Intersection Turning Movement Count Estimation

6.1 Overview

This chapter presents the results of the experiments with the turning movement count estimation and prediction models. In the first part, the results of testing different model structures are evaluated. This part is followed by an investigation of the input variables in the model, data collection durations, and the prediction performance of the proposed framework.

6.2 Model structure investigation

The estimation and prediction of turning movement counts require a model capable of capturing the complex relations between different variables and the vehicular volume of each specific turning movement. Therefore, in this study, three advanced machine learning algorithms are applied to the dataset to estimate the turning movement counts in a given time interval. These machine learning algorithms are Random Forest, XGBoost, and Multi-Layer Perceptron. Since a description of each of these models is presented in earlier chapters, in this section, the details of selecting the training, validation, and test sets are described, along with a comparison of performance measures for the models. The dataset used for developing the models is the 2019 intersection turning movement counts data. Since each turning movement is composed of two legs of the intersection (one is entering the intersection and one is exiting the intersection), the characteristics of both of these legs are incorporated as input variables into the model. The following example clearly illustrates the definition of upstream and downstream for each movement. In Figure 23, the specific movement of the Eastbound-Left Turn is illustrated. As it can be seen, the upstream segment for this movement is the eastbound entering leg to the intersection, and the downstream is the northbound exiting leg from the intersection. A similar definition can be introduced for the set of upstream and downstream segments of each of the 12 possible turning movements of a four-leg intersection.

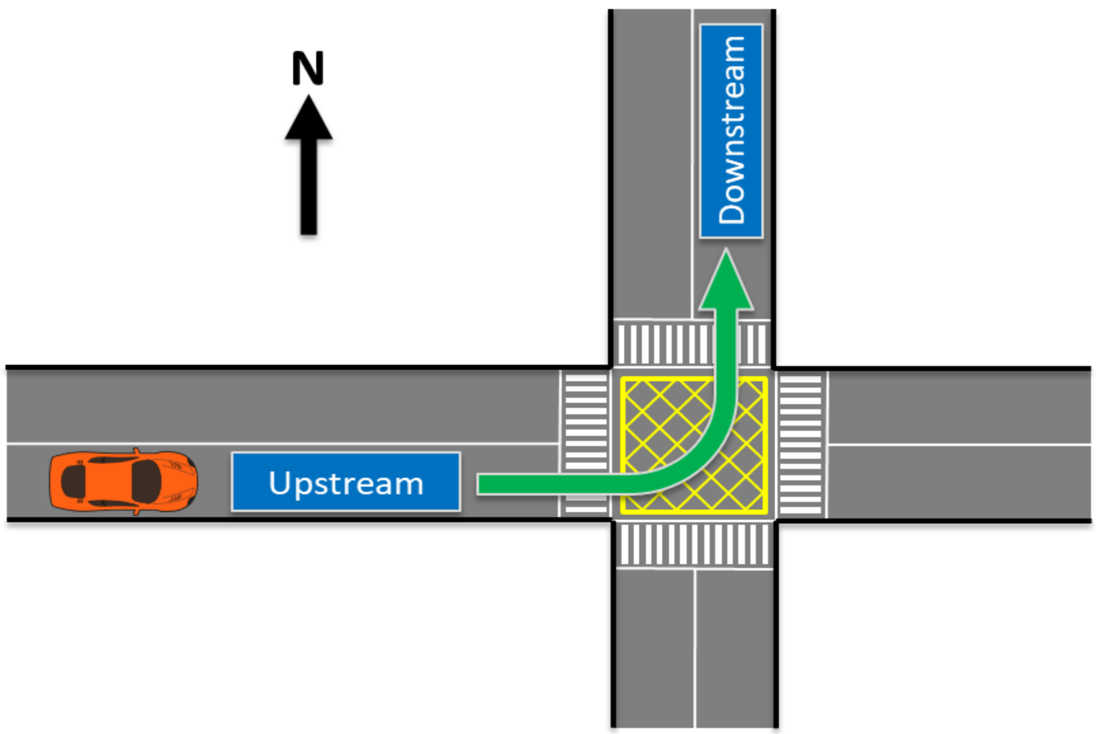

Figure 24. Illustration of upstream and downstream for a specific turning movement

With the description of the upstream and downstream segments for each movement, the input variables for the model can be the following:

- Traffic speed and average traffic speed of the upstream and downstream segments
- Approach volume of the upstream and downstream segments
- Annual average daily traffic (AADT) of the upstream and downstream segments
- Number of lanes of the upstream and downstream segments
- Exclusive lane configuration
- Movement type (Through, Left Turn, or Right Turn)
- Movement direction (NB, SB, EB, or WB)
- Time of the day
- Day of the week (Monday, Tuesday, …, Sunday)

It is assumed that one week of data is acquired for model training for each intersection. A model is trained using its own training set data for each intersection. The test set is drawn randomly without replacement 25 times to account for the randomness in the data collection start date. The validation set used to determine the best hyperparameters for each model is chosen to be the next week of the training set. The test set, which is the base for comparing the models, is the entire observations for the target intersection minus the training and validation sets. The described procedure is performed for each one of the models yielding 3 (model structures) * (15 intersections) * 25 (test sets) = 1,125 models. Since machine learning models benefit from a larger training set size and a fine-tuning for the MLP model can be performed to tailor the model for each target intersection, an MLP model with fine-tuning is explored in addition to the RF, XGBoost, and MLP models. This model, called MLP-FT, combines the training sets of all 15 intersections in training a single model. Later, all of the model layers are fixed, except the last layer, which is trained on the training set of each specific intersection. The procedure for determining the training, validation, and testing sets is the same as in other models. Therefore in total, we end up with 1,500 models for estimating turning movement counts in every 15 minutes. The performance measures of R^2, MAPE, and MAE are computed for each model structure to compare the performance of each model structure in turning movement count estimation. The distribution of R^2 for the four model structures is presented in Figure 25. As it is shown in this figure, the median of R^2 for the MLP-FT model is the highest and for the XGBoost and MLP-FT are almost

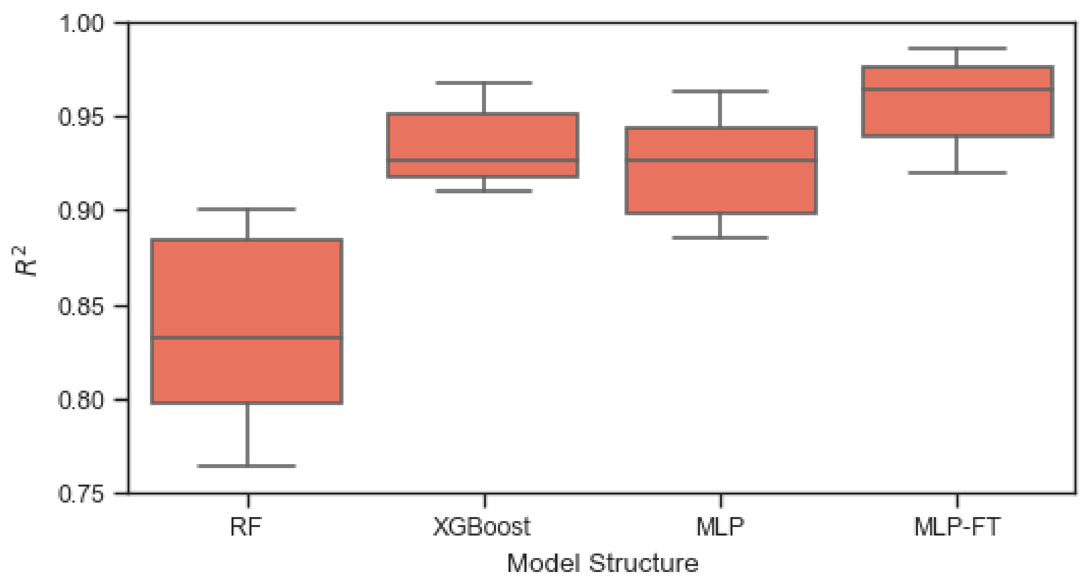

Figure 25. Distribution of TM count estimation R^2 for different model structures

equal. However, the variations in the R^2 for the XGBoost and MLP-FT models are less than that of the MLP model. The Random Forest model has the lowest R^2 with the highest variations presenting a poor performance relative to other model structures. The average absolute percentage of errors in the turning movement count estimates are presented in Figure 26 for the four models. This figure illustrates that the MLP-FT outperforms other model structures significantly. The median MAPE for the MLP-FT is almost equal to %5, with variations in the range of 4 to 10 percent. A comparison between the MLP and XGBoost illustrates that the median MAPE for the MLP model is lower; however, the variations of MAPE for this model are much more than that of the XGBoost model.

The RF model in the MAPE measure, similar to the R^2, is shown to be the least accurate model for turning movement estimation applications. A different picture of the

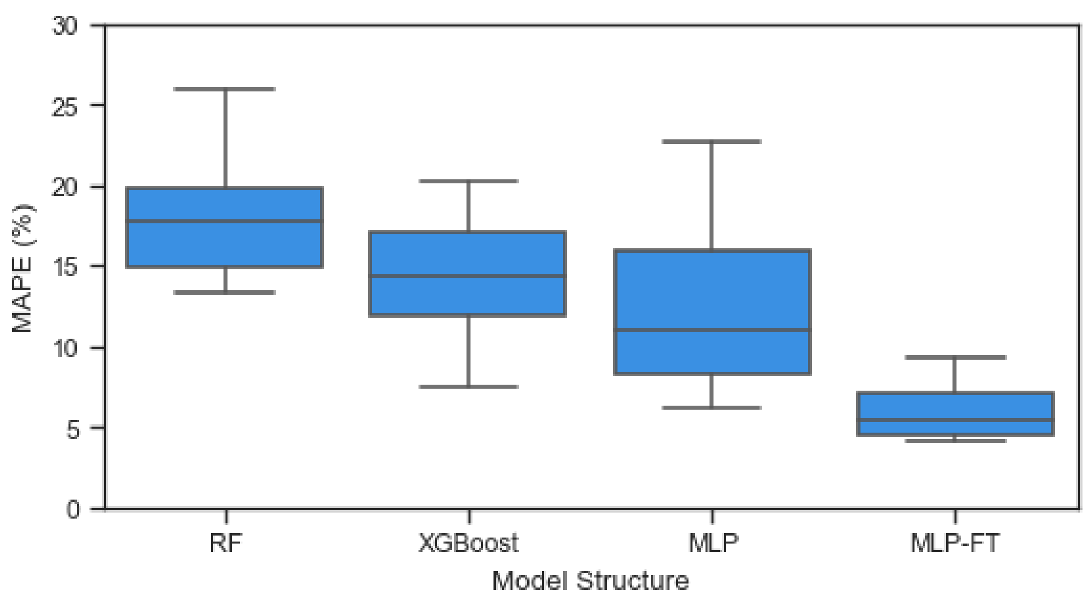

Figure 26. Distribution of TM count estimation MAPE for different model structures

performance of each model is obtained by computing the errors in terms of the difference between the actual and estimated number of vehicles in each specific turning movement and each time interval. The MAE is the measure that demonstrates that picture. The distribution of the MAE for each model is presented in Figure 27. According to this figure, the MLP-FT is superior to other models, with a median MAE of less than three vehicles every 15 minutes. In comparison between the XGBoost and MLP models, it is clear that although the XGBoost model has a higher median MAE and higher variations in the MAE measure, it is inferior to the MLP model based on this measure. Similar to the previous measures, the Random Forest model has the highest error, with a median of above seven vehicles per 15 minutes.

The summary statistics of the performance measures are provided in Table 6. The key takeaway of the model comparisons is that the MLP-FT model is the best structure for

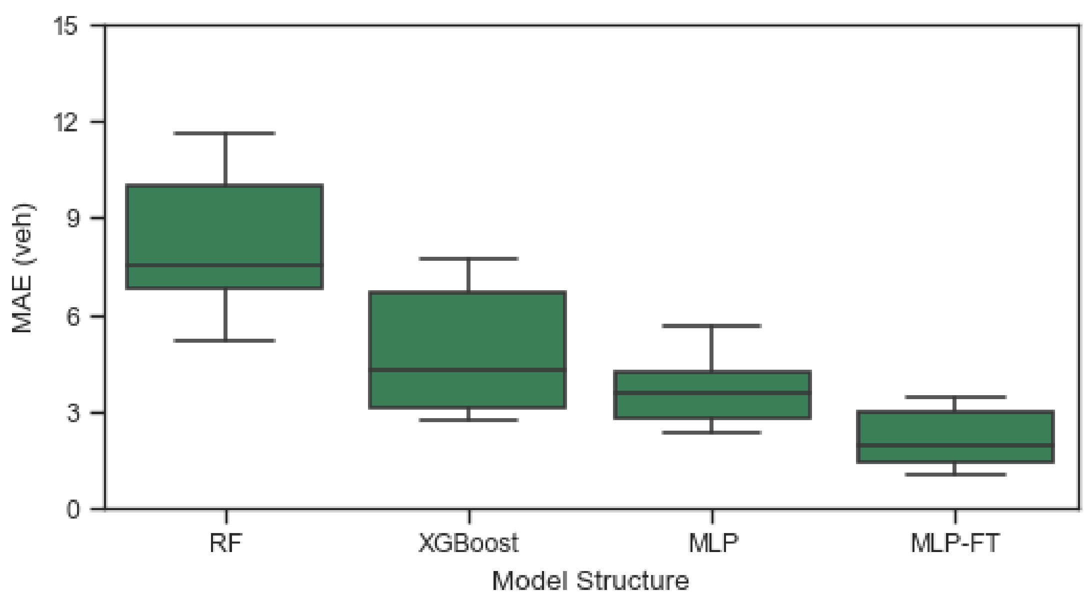

Figure 27. Distribution of TM count estimation MAE for different model structures

estimating the turning movement counts. This finding illustrates the benefits of training the MLP model with a larger dataset and fine-tuning the trained model to each intersection.

An important point that needs to be emphasized here is that the approach traffic volume input is helping the models significantly. However, the approach traffic volumes might not be an input readily available in all jurisdictions requiring huge investments for collecting. Therefore, a more plausible assumption and closer to real-world conditions

Table 6. Summary statistics of different model structures' performance

Measure	Model	RF	XGBoost	MLP	MLP-FT
R^2	Mean	0.84	0.93	0.92	0.96
	Min	0.76	0.91	0.89	0.92
	Median	0.83	0.93	0.93	0.96
	Max	0.90	0.97	0.96	0.99
MAPE (%)	Mean	17.90	13.96	12.72	6.12
	Min	13.39	7.49	6.25	4.20
	Median	17.79	14.43	11.01	5.48
	Max	25.92	20.31	22.74	9.30
MAE (veh/15min)	Mean	8.16	4.90	3.71	2.18
	Min	5.21	2.75	2.32	1.03
	Median	7.55	4.26	3.56	1.96
	Max	11.59	7.71	5.67	3.42

is assuming that the traffic volume on some but not all of the approaches are available and exploring methods to take advantage of the traffic volumes in these approaches. The following section explores the effects of training the turning movement count estimation models without the approach traffic volume inputs to make the modeling framework realistic. More importantly, a framework is presented to utilize the available approach traffic volumes to improve the model performance.

6.3 Approach traffic volume input

Different models were trained on the data in the previous section, assuming that the upstream and downstream traffic volumes are available as inputs. The traffic volumes on these segments can be obtained through the installation of continuous count traffic sensors on these segments, as illustrated in Figure 28 as an example where loop

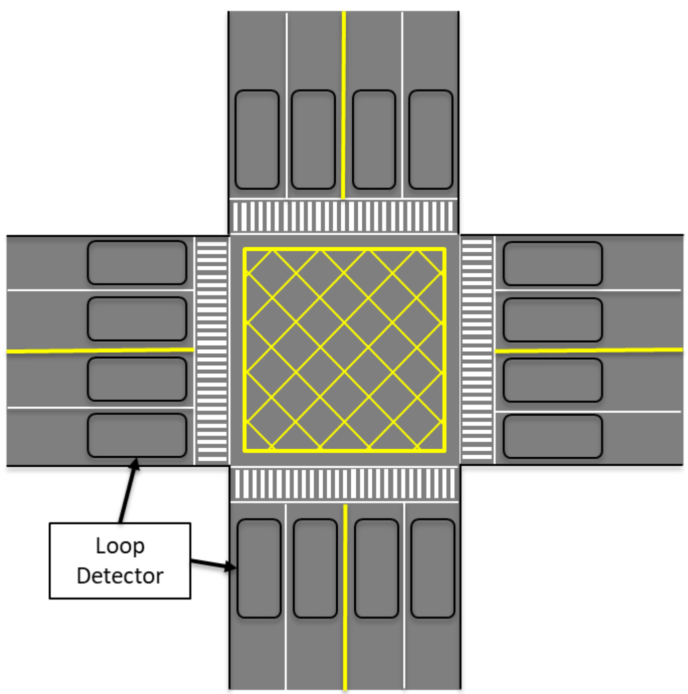

Figure 28. Example configurations of loop detectors to collect approach traffic counts

detectors are installed on all entering and exiting segments of the target intersection. Another possible method is summing up the traffic volume of segments entering the target segment. However, due to these sensors' installation and maintenance costs, the traffic count sensors' configuration rarely allows for the extraction of upstream and downstream traffic volume counts.

In this study, we propose a modeling framework in which, as the first step utilizing the available traffic volume counts, a volume estimation model is trained to generate estimates of traffic volumes at each intersection approach.

In the second step, the inputs of the volume estimation model are combined with the approach traffic counts and fed to the turning movement estimation model. One of the advantages of the proposed framework is that the data of traffic counts with any given level of availability are used to improve the model performance. Another advantage is that, unlike previous studies, which use a complete set of inputs for training the turning movement estimation model, the proposed framework can generate estimates for the missing attributes making it applicable to real-world turning movement count estimation.

The flowchart of the proposed framework is presented in Figure 29, where on the left side is the volume estimation module, and on the right side is the turning movement count estimation module. The segment-level attributes and temporal features are used to train a volume estimation model for all of the approaches of the study intersections. Further, the model generates traffic volume estimates for the approaches of each intersection. These generated traffic counts are replaced with the actual volumes

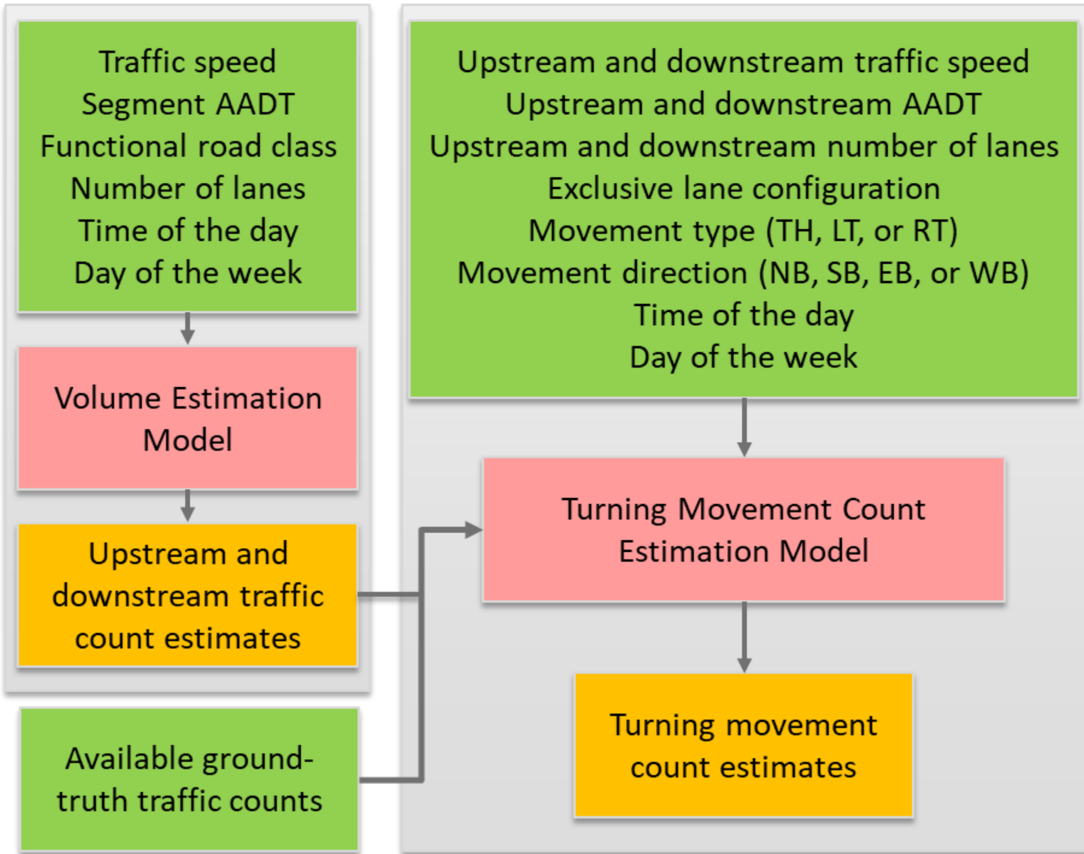

Figure 29. Proposed framework for TM count estimation with incomplete approach traffic volumes

wherever the ground-truth data exists and is accessible. The obtained traffic counts are used in addition to movement-specific and temporal features to train the turning movement count estimation model, the output of which is the estimation of traffic counts for each specific movement during 15 minutes.

Since different numbers of traffic count sensors might exist in a given road network, a sensitivity analysis is performed to investigate the impacts of varying approach traffic count availability levels. These levels of data availability are summarized in Table 7, wherein in the final row, a “Base” scenario is added, which is the turning movement estimation model without any approach traffic volumes to illustrate the improvements of the turning movement count estimates with this input feature.

Table 7. Summary of the traffic volume ground-truth data availability scenarios

<table>
<tr><th>Scenario name</th><th>percent of segments with continuous traffic count sensors</th><th colspan="3">volume estimation model ground truth</th></tr>
<tr><td>0/8</td><td>0</td><td rowspan="9">one week of turning movement count ground-truth</td><td rowspan="9">+</td><td rowspan="9">traffic volume of segments with continuous traffic count sensors</td></tr>
<tr><td>1/8</td><td>12.5</td></tr>
<tr><td>2/8</td><td>25.0</td></tr>
<tr><td>3/8</td><td>37.5</td></tr>
<tr><td>4/8</td><td>50.0</td></tr>
<tr><td>5/8</td><td>62.5</td></tr>
<tr><td>6/8</td><td>75.0</td></tr>
<tr><td>7/8</td><td>87.5</td></tr>
<tr><td>8/8</td><td>100</td></tr>
<tr><td>Base</td><td colspan="4">No volume estimation module</td></tr>
</table>

Each percentage of intersection segments with traffic count sensors training sets are 25 times randomly drawn, similar to the previous section's experiments. Based on the model structure analysis results, the MLP-FT model structure was selected for this experiment since it showed the highest performance. The three following figures present the distribution of performance measures for the turning movement count estimates using the proposed framework. In Figure 30, the distribution of R^2 for each introduced scenario is illustrated. As it can be seen, the addition of the volume estimation module improves the turning movement estimation model performance significantly. Besides, for this study's target intersections, incorporating ground-truth volumes after a certain point is not improving the performance by a large margin. Therefore, for this study, the reasonable proportion of segments in which traffic count sensor installation is beneficial is up to 25 or 37.5 percent of the entire segments. Note that the "8/8" scenario is similar to the MLP-FT model in the previous section.

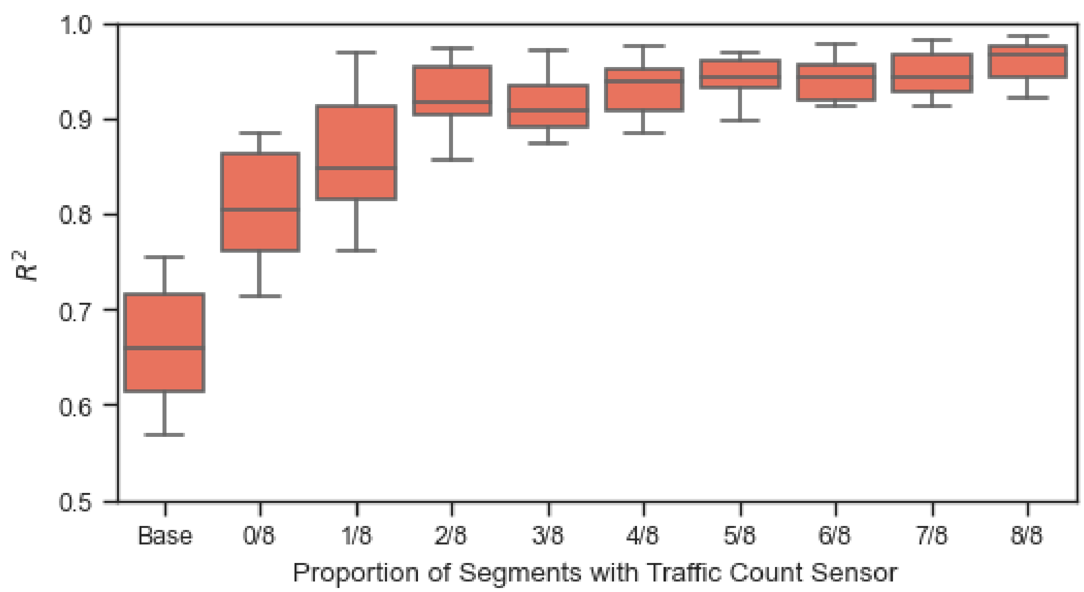

Figure 30. Distribution of TM count estimation R^2 for volume data availability scenarios

The distribution of MAPE for the introduced scenarios is presented in Figure 31. The conclusions that can be drawn from the distribution of MAPE are similar to those from the R^2 distribution. However, in this case, the optimum proportion of segments with traffic volume sensors is around 37.5 percent, where the median MAPE is approximately 15 percent.

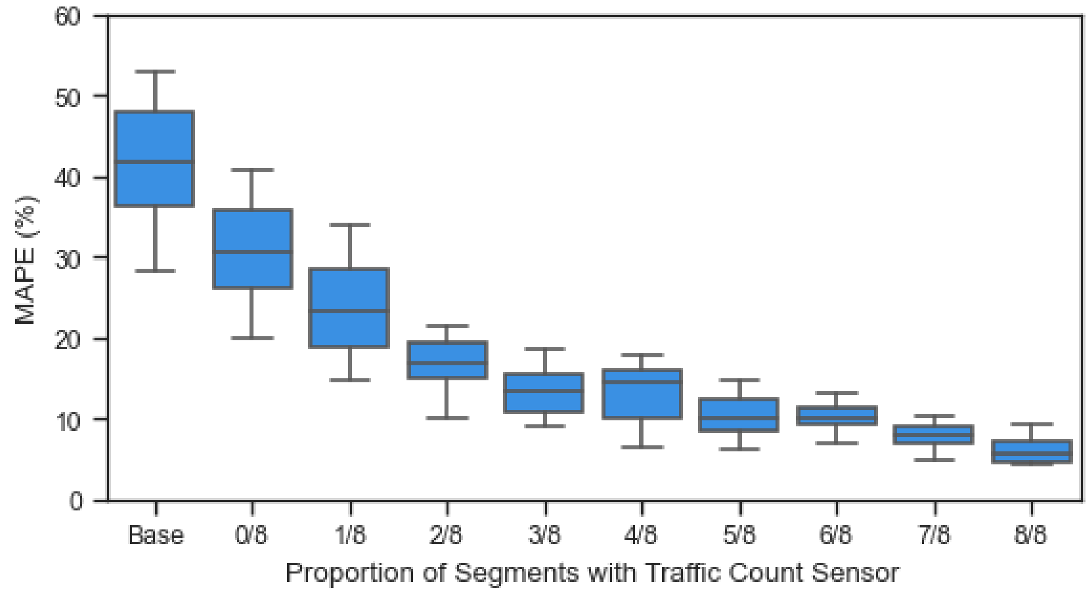

Figure 31**. Distribution of TM count estimation MAPE for volume data avaialibility scenarios**

Figure 32 presents the distribution of MAE for the turning movement count estimation using the proposed framework. The takeaway of the MAE distribution is that the median MAE is continuously reducing with around nine vehicles per 15 minutes for the scenario without any installed continuous traffic count sensors down to almost equal to 2 for the installation of continuous count sensors on all segments. According to this figure, the optimum proportion of intersection approaches with continuous count sensors is around 50 percent. The summary statistics of model performance measures are presented in Table 8.

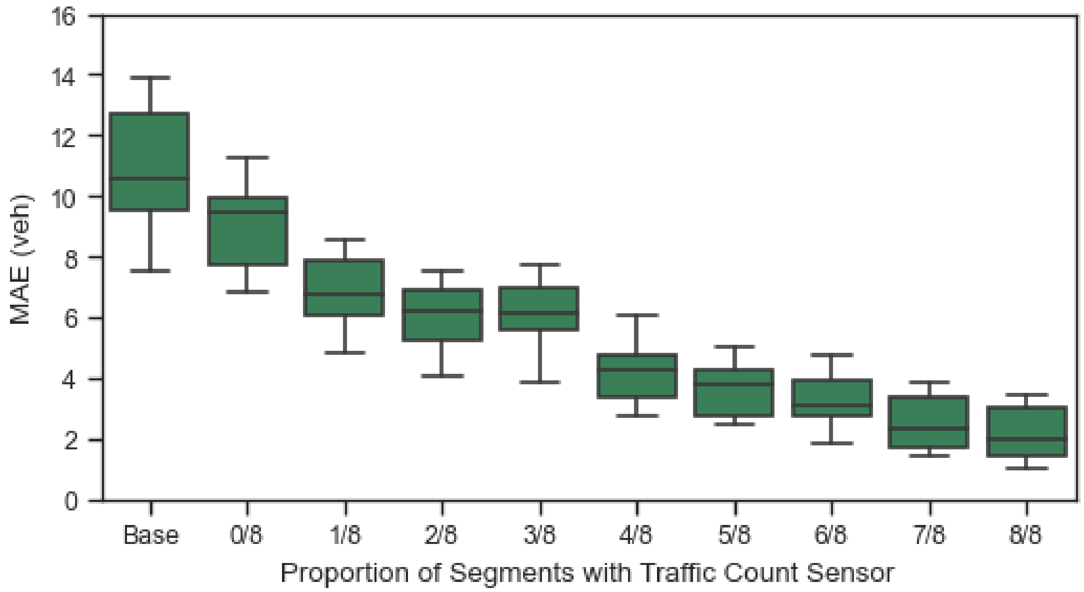

Figure 32. Distribution of TM count estimation MAE for different volume data availability scenarios

The conclusion from the results of this section is that the incorporation of approach volume counts or their estimates from a volume estimation module into the turning movement estimation model has significant advantages for the model performance. Even at low penetration rates of continuous traffic count sensors, the turning movement counts can be more accurate with the volume estimation module. Additionally, it can be deduced that the installation of continuous traffic count sensors has a diminishing marginal benefit to the model, and this benefit does not significantly increase after a certain point. As mentioned for the models trained so far, the assumption is that one week of turning movement count data is available. In the next section, a sensitivity analysis on the size of turning movement count ground-truth is performed.

Table 8. Summary statistics of traffic volume availability scenarios' model performance

Measure	Scenario	Base	0/8	1/8	2/8	3/8	4/8	5/8	6/8	7/8	8/8
R^2	Mean	0.66	0.80	0.86	0.92	0.91	0.93	0.94	0.94	0.95	0.96
	Min	0.57	0.71	0.76	0.86	0.87	0.88	0.90	0.91	0.91	0.92
	Median	0.66	0.81	0.85	0.92	0.91	0.94	0.94	0.94	0.94	0.97
	Max	0.75	0.88	0.97	0.97	0.97	0.98	0.97	0.98	0.98	0.99
MAPE (%)	Mean	41.66	30.74	23.79	16.53	13.41	13.22	10.34	10.23	7.91	6.12
	Min	28.17	19.81	14.74	10.02	9.00	6.46	6.14	7.01	4.74	4.20
	Median	41.82	30.52	23.16	16.68	13.49	14.30	10.05	10.07	8.04	5.48
	Max	52.86	40.58	33.90	21.49	18.57	17.72	14.67	13.05	10.37	9.30
MAE (veh / 15min)	Mean	10.74	9.09	6.79	6.02	6.10	4.22	3.67	3.28	2.49	2.18
	Min	7.50	6.82	4.84	4.02	3.83	2.70	2.46	1.85	1.39	1.03
	Median	10.58	9.43	6.73	6.17	6.11	4.28	3.76	3.11	2.35	1.96
	Max	13.87	11.28	8.58	7.49	7.73	6.04	5.04	4.73	3.84	3.42

6.4 Turning movement ground-truth data size

Although the turning movement count estimation models trained in the previous sections use one week of ground-truth data for each specific turning movement, the data collection costs can be very high, especially for the turning movement traffic count. Therefore, a sensitivity analysis is beneficial to investigate the model performance given different sizes of the ground-truth data enabling transportation authorities to do a cost-benefit analysis depending on their budget level and desired accuracy. Undoubtedly, the decision-makers of the system would rather avoid data collection expenditures in case there is a limited gain in the turning movement estimation accuracy beyond a certain level of data collection. The results of training the MLP-FT model on different levels of ground-truth data are presented here. It is assumed that 25 percent of the segments have traffic volume sensors installed and provide traffic count data. The distribution of R^2 for the different number of days of data availability of turning movement counts is presented in Figure 33.

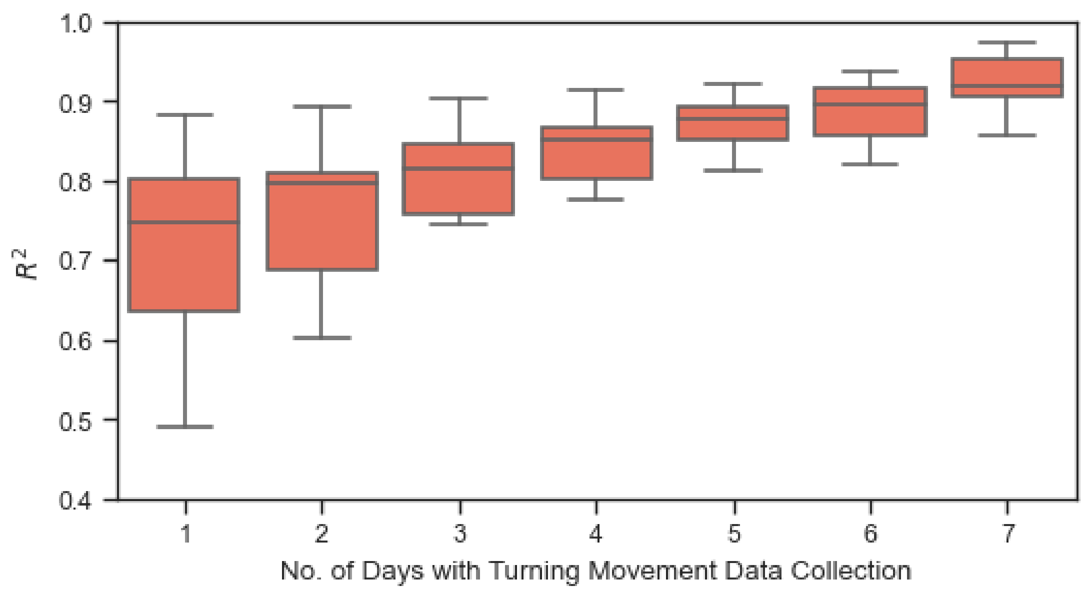

Figure 33. Distribution of TM count estimation R^2 based on ground-truth data availability scenarios

Expectedly, the accuracy of the model estimates decreases with a reduction in ground-truth data collection. However, the reduction in accuracy is much more when the data collection duration is less than three or four days in a year. The distribution of MAPE for each turning movement count data collection duration is presented in Figure 34. As can be seen, the duration of data collection has a considerable impact on the model accuracy, and with four days of data collection, the errors can reach as high as 90 percent. Therefore, according to the MAPE measure and for the intersections of the present study, a minimum of five data collection days are required to produce meaningful estimates. In Figure 35, the distribution of MAE for the same experiment is presented. Based on this Figure, no clear point can be selected as the minimum data collection duration. The summary statistics of the performance measures for these models are presented in Table 9.

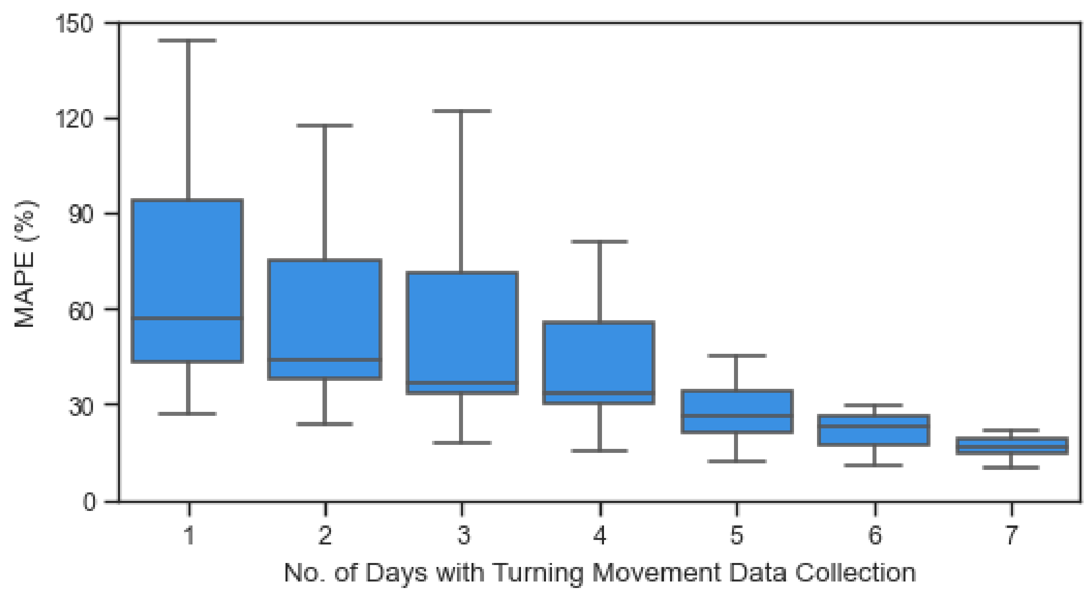

Figure 34. Distribution of TM count estimation MAPE based on ground-truth data availability scenarios

The takeaway of this experiment is that the model accuracy is highly affected by the turning movement count data collection duration. Therefore, depending on the desired accuracy for each specific application and considering the costs, the duration of data collection should be determined.

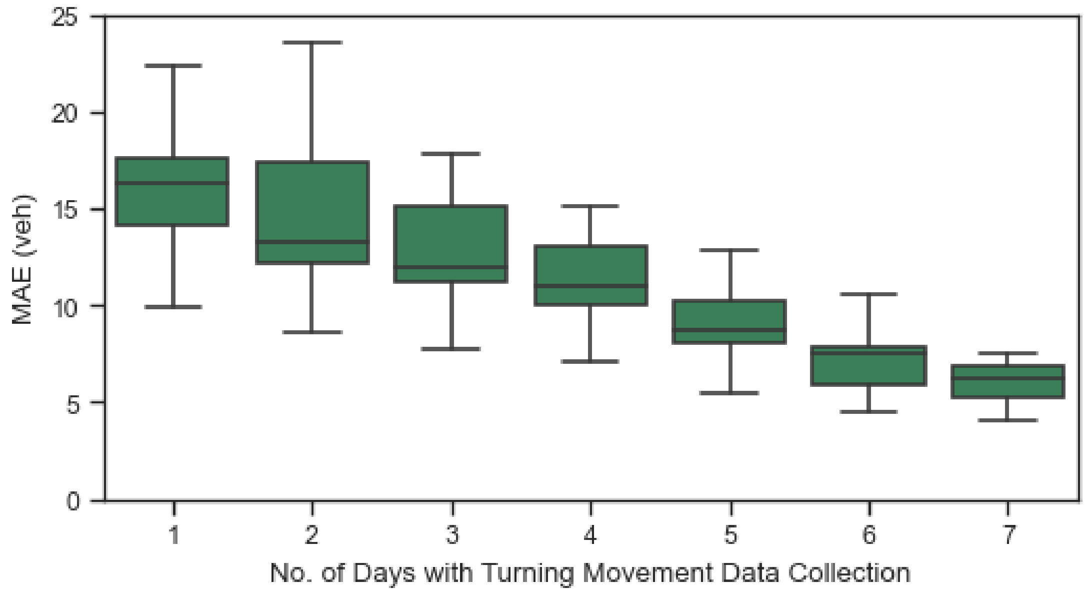

Figure 35. Distribution of TM count estimation MAE based on ground-truth data availability scenarios

According to the experiments in this chapter, it can be concluded that:

1. MLP-FT model is superior to Random Forest, XGBoost, and MLP without fine-tuning in turning movement count estimation.
2. The incorporation of approach traffic volume counts into the model significantly improves the model accuracy. In the absence of complete traffic count data for the approaches, a volume estimation model is beneficial in estimating the traffic volumes for segments without a traffic sensor or missing data points.

3. The increase in turning movement count data collection duration is reflected in the model accuracy to a great extent. The investment in collecting this data can pay back in the applications of the developed model.

Table 9. Summary statistics of ground-truth data availability scenarios' model performance

Measure	Scenario	1	2	3	4	5	6	7
R^2	Mean	0.67	0.74	0.78	0.82	0.85	0.89	0.92
	Min	0.39	0.51	0.62	0.70	0.79	0.82	0.86
	Median	0.75	0.80	0.81	0.85	0.88	0.90	0.92
	Max	0.88	0.89	0.90	0.91	0.92	0.94	0.97
MAPE (%)	Mean	68.62	54.94	51.71	46.47	27.50	21.64	16.53
	Min	26.97	23.74	17.72	15.07	12.00	11.00	10.02
	Median	56.88	43.93	36.70	33.54	26.00	23.12	16.68
	Max	144.12	117.22	121.70	92.69	45.00	29.61	21.49
MAE (veh / 15min)	Mean	17.21	15.79	13.56	11.84	9.39	7.22	6.02
	Min	9.94	8.56	7.77	7.05	5.45	4.47	4.02
	Median	16.31	13.30	11.92	11.03	8.66	7.49	6.17
	Max	22.88	25.24	21.03	17.45	13.51	10.56	7.49

Building upon the findings of the current chapter, multiple applications can be put forward from the proposed framework. In the next chapter, two of the applications are illustrated with examples to provide a clear view of the framework's real-world uses.

Chapter 7: Application of the Proposed Framework

7.1 Overview

In the previous chapter, through the design and implementation of different experiments, the model performance is investigated under different conditions of model structure, approach traffic volume inputs, and turning movement data collection duration. The findings of the previous chapter indicate that the MLP-FT model is the superior model structure using the framework presented in Figure 29, which is essentially a traffic volume estimation model, the outputs of which are fed as inputs to the turning movement estimation model. Therefore, it is time to apply the proposed framework to solving real-world problems. This chapter explores the implementation of the proposed framework in two applications. First, the framework is employed to predict the turning movement traffic counts in various time horizons, and second is using the predictions to design traffic signal cycles according to the predicted traffic counts. In the following sections, these applications are investigated in detail.

7.2 Prediction of Turning Movement Traffic Counts

There are numerous benefits to predicting the turning movement counts at intersections ahead of time ranging from real-time designing and modification of traffic signal timing and scheme to traffic operation and congestion mitigation measures in advance. Therefore, one of the advantages of a robust and accurate turning movement estimation framework is the ability to make predictions. Although there are various advanced time-series methods in the literature, the implication in the real-world application of these approaches is that turning movement count detectors are permanently installed at the intersection. Taking into account the costs of deployment and maintenance of such systems, the present study explores the prediction of turning movement counts with short-time data collection using the proposed turning movement estimation framework.

In the previous chapter, each data point includes various attributes such as traffic speed, time of the day, etc., along with the traffic counts of that specific turning movement during 15 minutes. For the prediction purpose, the same attributes at, say t=ta, are fed to the model to predict the turning movement counts at t=ta+h, where "h" is the time horizon. Since, for this approach, the model requires data at times ta and ta+h, the number of observations that can be used for model development reduces. The prediction horizons considered here are 15, 30, 45, and 60 minutes ahead. Therefore, given the current attributes such as speed, the model generates turning movement count predictions for the next 15, 30, 45, and 60 minutes. Table 10 illustrates the definitions of prediction models more clearly.

The prediction model structure is MLP-FT assuming approach traffic sensors on 25 percent of the intersection segments and seven days of turning movement traffic count data collection for each intersection. The data collection days and the segments with continuous traffic count sensors are drawn randomly 25 times for each intersection. In applying the proposed framework for prediction purposes, the approach traffic volume estimation model generates traffic volumes for segments without traffic counts, followed by a turning movement count prediction model. Figure 36 illustrates the distribution of turning movement count prediction models R^2 for different time horizons. In this figure, the plot for the prediction horizon equal to zero stands for the model used to estimate the turning movement (h=0). According to this figure, while the prediction of turning movement counts in the next 15-minutes interval and for some applications up to the next 30 minutes are acceptable, predictions farther than that have a very low R^2.

Table 10. Configuration of prediction models in time

<table>
<tr><th>Prediction horizon</th><th>Model type</th><th>Input features</th><th>Output</th></tr>
<tr><td>h=0</td><td>TM count estimation</td><td rowspan="5">Average between t=a-15 to t=a</td><td>TM counts during t=a-15 to t=a</td></tr>
<tr><td>h=15</td><td rowspan="4">TM count prediction</td><td>TM counts during t=a to t=a+15</td></tr>
<tr><td>h=30</td><td>TM counts during t=a+15 to t=a+30</td></tr>
<tr><td>h=45</td><td>TM counts during t=a+30 to t=a+45</td></tr>
<tr><td>h=60</td><td>TM counts during t=a+45 to t=a+60</td></tr>
</table>

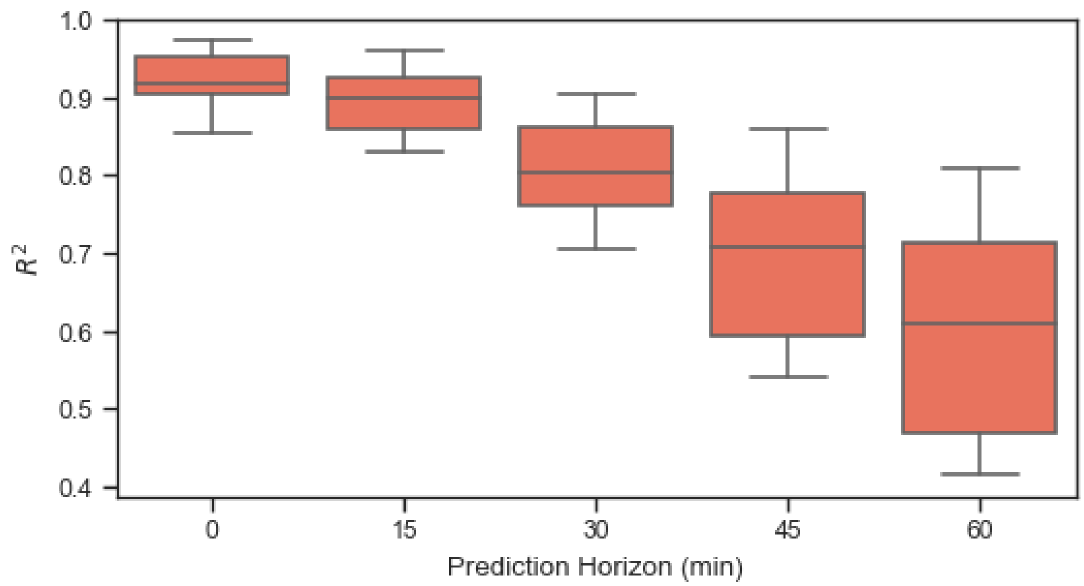

Figure 36. Distribution of TM count prediction models R^2

The comparison of MAPE for turning movement count predictions for different horizons is presented in Figure 37. According to this figure, the model is capable of producing turning movement count predictions for 30 minutes from the current time with a median MAPE of less than 25 percent. Besides, the model's accuracy in the 15 minutes prediction is comparable with the estimation at the present time.

The distribution of MAE for these models is presented in Figure 38, which illustrates that predictions for the 15-minutes time interval starting from the next 45 minutes have a median of fewer than nine vehicles in every 15 minutes. The summary statistics of the prediction models' performance measures are illustrated in Table 11.

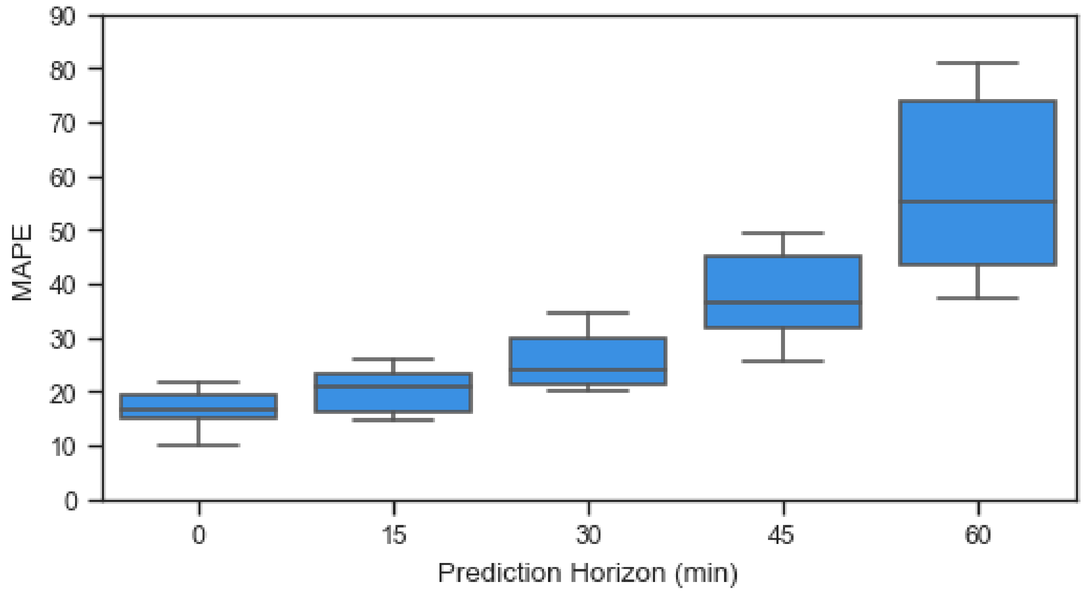

Figure 37. Distribution of TM count prediction models MAPE

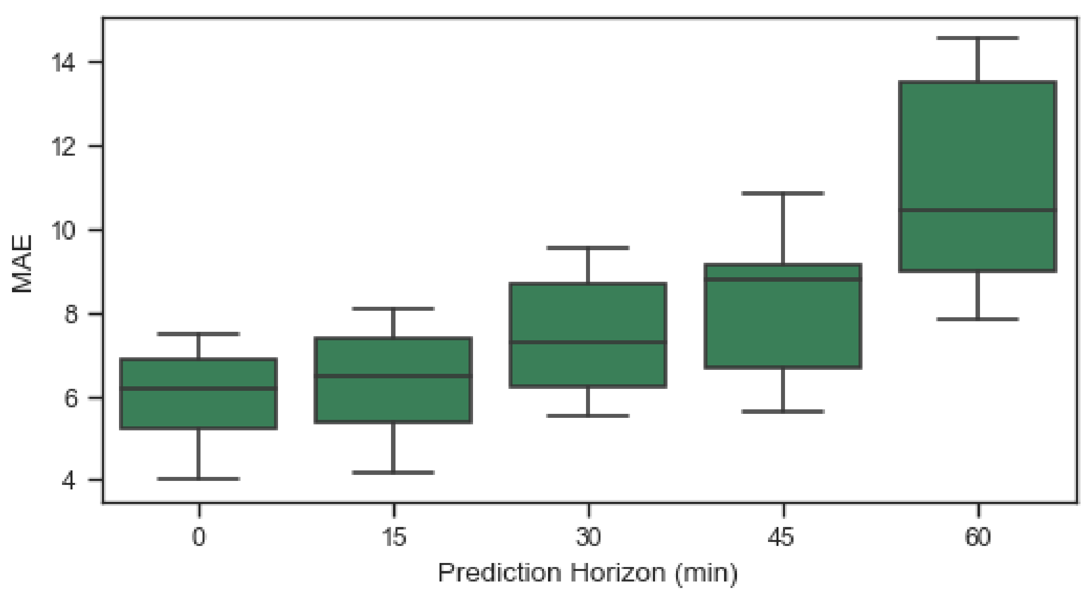

Figure 38. Distribution of TM count prediction models MAE

Table 11. Summary statistics of the prediction models performance measures

Measure	Prediction horizon	h=0	h=15	h=30	h=45	h=60
R^2	Mean	0.92	0.89	0.81	0.70	0.60
	Min	0.86	0.83	0.70	0.54	0.42
	Median	0.92	0.90	0.80	0.71	0.61
	Max	0.97	0.96	0.90	0.86	0.81
MAPE (%)	Mean	16.53	20.48	25.76	37.31	56.70
	Min	10.02	14.54	20.13	25.65	37.33
	Median	16.68	21.00	24.00	36.59	55.00
	Max	21.49	26.00	34.36	49.25	81.00
MAE (veh / 15min)	Mean	6.02	6.32	7.38	8.17	11.07
	Min	4.02	4.18	5.51	5.64	7.81
	Median	6.17	6.46	7.30	8.77	10.42
	Max	7.49	8.11	9.53	10.84	14.57

According to the above figures illustrating the prediction performance of the proposed framework, it can be concluded that the model can be used to predict turning movement counts for the next 15 minutes, given the current traffic conditions. Additionally, the 15-minute time interval 30 minutes ahead of the current time is somewhat acceptable.

Evaluation of the model performance in prediction during the peak and off-peak hours can provide more insight into the applicability of the proposed framework. Therefore, a more disaggregate illustration of model performance in 15 minutes predictions is presented here in Figures 39-41. The considered time intervals are AM-Peak (7 AM-9 AM), Off-Peak (9 AM-3 PM), and PM-Peak (3 PM-6 PM). According to these figures, the model's predictions are more accurate during peak periods for the R^2 and MAPE. On the contrary, the MAE is lower during off-peak times due to lower traffic volumes during those times.

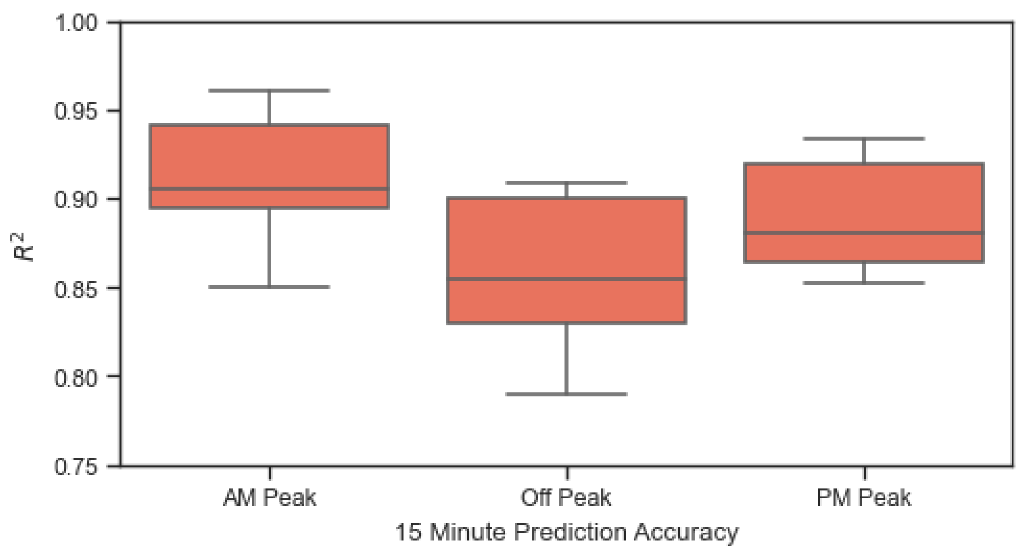

Figure 39. Distribution of R^2 in 15 minutes predictions of TM counts at different times of the day

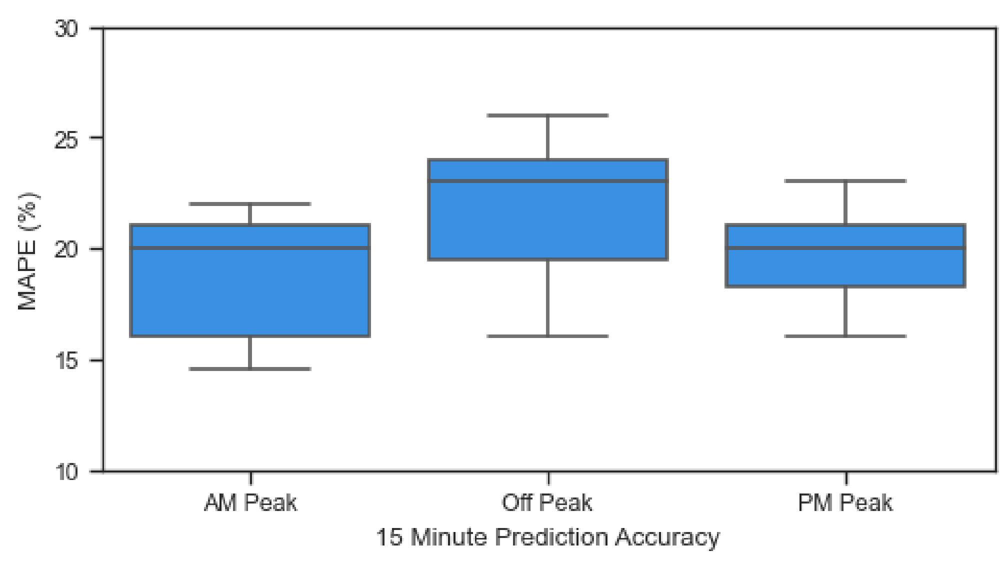

Figure 40. Distribution of MAPE in 15 minutes predictions of TM counts at different times of the day

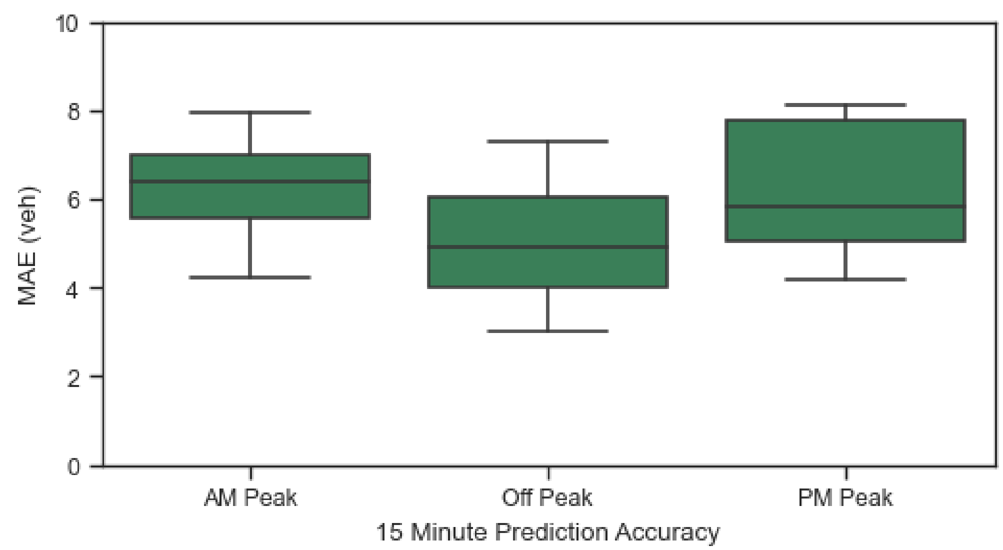

Figure 41. Distribution of MAE in 15 minutes predictions of TM counts at different times of the day

7.3 Traffic signal design

The proposed framework in the present study can generate turning movement count predictions that can be used to design and modify the signal timing in target intersections. The traffic signal plans and timings can be fine-tuned in advance depending on the predicted turning movement counts in this application. This application is illustrated in one of the study intersections and compared with a situation in which a pre-timed traffic signal is designed without using a prediction model.

The study intersection is located at the junction of North Lamar Boulevard and East Rundberg Lane, Austin, TX. The schematic lane configuration of the intersection is presented in Figure 42. According to this figure, all left-turn movements have exclusive lanes, but the right-turns have shared lanes except for the west-bound direction.

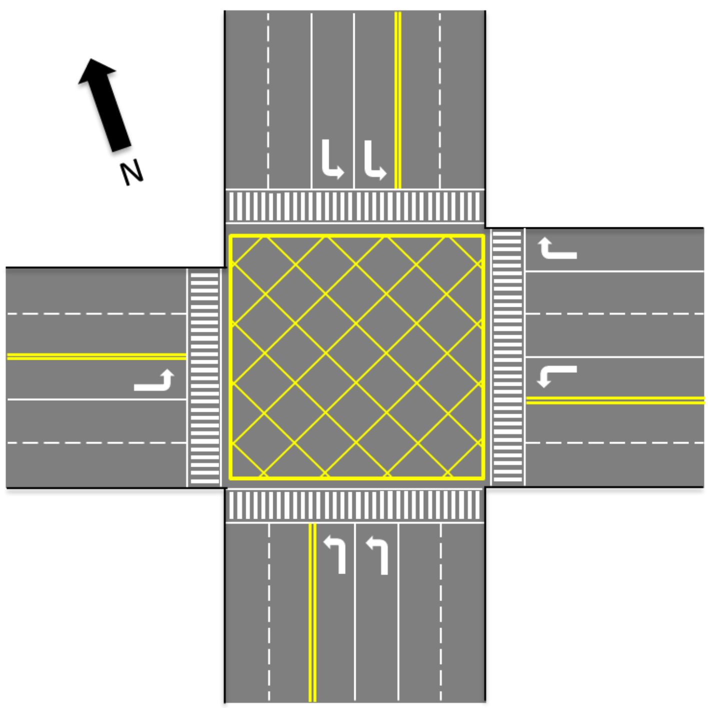

Figure 42. Schematic configuration of the study intersection

In the absence of the proposed framework, a one-day data collection is usually performed to design the traffic signal timing. A more accurate signal timing design might be achieved if the data collection duration is increased. The analysis of this section assumes that there are different scenarios of data collection durations ranging from one day to seven days. Corresponding to each of the collected data, a pre-timed signal timing can be designed. Additionally, each scenario's collected turning movement count data can be used to develop prediction models and design traffic signal timings according to the turning movement counts at each 15-minutes. According to the described configuration, there are 14 scenarios in total, as summarized in Table 12. Based on the signal timings designed in each scenario, the annual user delay in terms of time and monetary values for the target intersection can be computed and compared.

The signal timing design for the first scenario, which is one day of turning movement data collection and a pre-timed signal design for the entire year, is described here. The data collection day is selected randomly. The timing of the signal is performed according to the HCM (2010) and Roess et al. (2004). The considered phase diagram for this intersection is presented in Figure 43, which illustrates a four-phase traffic signal timing.

Table 12. Summary of signal timing scenarios

Scenario	TM count data collection duration	Signal timing
1	1	Pre-timed
2	1	Desinged based on TM count predictions
3	2	Pre-timed
4	2	Desinged based on TM count predictions
5	3	Pre-timed
6	3	Desinged based on TM count predictions
7	4	Pre-timed
8	4	Desinged based on TM count predictions
9	5	Pre-timed
10	5	Desinged based on TM count predictions
11	6	Pre-timed
12	6	Desinged based on TM count predictions
13	7	Pre-timed
14	7	Desinged based on TM count predictions

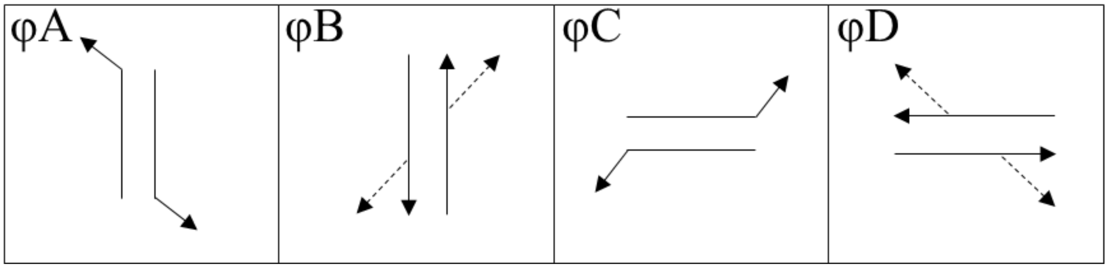

Figure 43. Phase diagrams of the selected intersection

The following parameters are assumed in designing the signal timing according to Roess et al. (2004):

$t = driver\ reaction\ time = \ 1.0\ s$

$S_{85} = 85th\ percentile\ speed\ of\ approaching\ vehicles = 35 + 5 = 40mph$

$a = acceleration\ rate\ of\ vehicles = 10.0\frac{ft^2}{s}$

$G = grade\ of\ approach = 0.0\ \%$

$W = distance\ from\ the\ departures\ STOP\ line\ to\ the\ far\ side\ of\ the$

$\quad farthest\ conflicting\ traffic\ lane = 100\ feet$

$L = length\ of\ a\ standard\ vehicle = 20\ feet$

$S_{15} = 15th\ percentile\ speed\ of\ approaching\ vehicles = 35 - 5 = 30mph$

$l_1 = start - up\ lost\ time = 2.0\ s/phase$

$e = motorist\ use\ of\ yellow\ and\ all - red = 2.0\ s/phase$

We determine the lost time per cycle in the first step, assuming a four-phase signal timing. The length of the yellow or change interval is calculated as:

$$y = t + \frac{1.47S_{85}}{2a + (64.4 * 0.01G)} = 1 + \frac{1.47 * 40}{2 * 10 + (64.4 * 0.01 * 0)} \cong 3.9\ s \tag{20}$$

The length of the all-red, considering no pedestrian activity in the intersection, is calculated as:

$$y = \frac{W + L}{1.47S_{15}} = \frac{100 + 20}{1.47 * 30} \cong 2.7\ s \tag{21}$$

Therefore, the total lost time per cycle is computed as:

$$L = 4(l_1 + l_2) = 4(3.9 + 2.7) \cong 26.4\ s \tag{22}$$

In the next step, we determine the critical-lane volumes and their summation, which are summarized in Table 13.

Using the numbers in Table 12, we can compute the cycle length as follows:

$$Cycle\ Length = \frac{L}{1 - (\frac{V_c}{\frac{3600}{2} * {}^{v}/_{c}})} = \frac{26.4}{1 - (\frac{1234.3}{\frac{3600}{2} * 0.9})} \cong 110.88s \tag{23}$$

Therefore, the cycle length is assumed to be 115 seconds, and the green split will be:

$$g_1 = (C - L)\left(\frac{V_1}{V_c}\right) = (115 - 26.4)\left(\frac{172.2}{1234.3}\right) = 12.4\ s \tag{24}$$

$$g_2 = (C - L)\left(\frac{V_2}{V_c}\right) = (115 - 26.4)\left(\frac{610.5}{1234.3}\right) = 43.8\ s \tag{25}$$

$$g_3 = (C - L)\left(\frac{V_3}{V_c}\right) = (115 - 26.4)\left(\frac{201.6}{1234.3}\right) = 14.5\ s \tag{26}$$

$$g_4 = (C - L)\left(\frac{V_4}{V_c}\right) = (115 - 26.4)\left(\frac{250.0}{1234.3}\right) = 17.9\ s \tag{27}$$

Table 13. Computation of through vehicle equivalent volumes for signal timing

Movement	Critical Lane Volume (tvu/h/ln)
NB-LT SB-LT	172.2
NB-TH NB-RT SB-TH SB-RT	610.5
EB-LT WB-LT	201.6
EB-TH EB-RT WB-TH WB-RT	250.0
Total critical lane volumes (V_C)	172.2+610.5+201.6+250.0=1234.3

The above computations led to a pre-timed signal timing that can be used for the entire year. This signal timing does not require any modeling framework to predict the turning movement counts; however, it will not reflect the changes in traffic volumes and demand into signal timing. Corresponding to each without prediction model scenario, 25 different randomly drawn days for data collection are selected to account for the randomness in the data collection, for each of which a set of traffic signal timings are obtained. For the scenarios with prediction model, first using the available ground truth, a prediction model is trained. The turning movement count predictions generated by the model are used to design a signal timing for every 15 minutes. Same as the scenarios without a prediction model, the data collection days are selected 25 times randomly for these scenarios to account for the randomness. Therefore, in total, there are 7*25=135 turning movement prediction models. The user delay is computed using a simulation framework in the next step.

The computation of user delay is approached from a high-level perspective since a microscopic analysis, while hugely increasing the complexity and computation times, does not add much to the findings since there are significant uncertainties and randomness in the nature of the problem, such as vehicle arrival distribution, traffic conditions, pedestrian activity, changes in predictions due to signal timings, etc. In the simulation adopted in the present study, the maximum number of vehicles that can pass the intersection for each approach is computed as the critical volume of each lane group. Further, any demand for each specific movement higher than the critical volume should wait in the queue for the next cycle or cycles until they can pass the intersection.

It is assumed that the vehicle arrivals are uniformly distributed in each 15-minutes. A stationary observer can approximate the delay as follows:

$$D_t^i = d_{1,t}^i + d_{2,t}^i = \frac{1}{2}\left(q_{t-1}^i + q_t^i\right)(15) + \frac{1}{2}\left(V_t^i\right)\left(\frac{C_t - g_t^i}{60}\right) \tag{28}$$

and,

$$q_t^i = \max\left(q_{t-1}^i + \left(V_t^i - V_t^{i,c}\right), 0\right) \tag{29}$$

where:

D_t^i, is the total delay experienced by vehicles of lane group *i*, at time interval *t*;

$d_{1,t}^i$, is the delay experienced by vehicles of lane group *i*, at time interval *t* due to queue;

$d_{2,t}^i$, is the delay experienced by vehicles of lane group *i*, at time interval *t* due to arrival time relative to signal state;

q_t^i, is the queue length in number of vehicles for lane group *i*, at the end of time interval *t*;

V_t^i is the traffic volume of lane group *i*, at time interval *t*;

$V_t^{i,c}$, is the critical traffic volume of lane group *i*, at time interval *t*, which is used for signal timing;

C_t, is the cycle length (in seconds) at time interval *t*, and

g_t^i is the green time (in seconds) of lane group *i*, at time interval *t*.

The user delays in hours per year for each scenario are computed based on different data collection days, using the above-described method for each lane group and each time interval. The distribution of the user delay is presented in Figure 44. As it can be seen, the increase in the duration of data collection does not significantly reduce the user delay without a prediction model. Besides, even with a few days of data collection combined with the proposed turning movement count prediction framework, the user delay is reduced to less than half of the scenarios without prediction models. The cost of user delay is computed based on an average value of time for the users, which is found to be equal to 19 dollars per hour in recent studies (Goldszmidt et al., 2020). The multiplication of the value of time and the annual user delay yields the user delay cost in a year, as presented in Figure 45. As it can be seen, the median user delay cost of more than 8 million dollars can be reduced to around 3 million dollars resulting in about 60 percent time and cost savings.

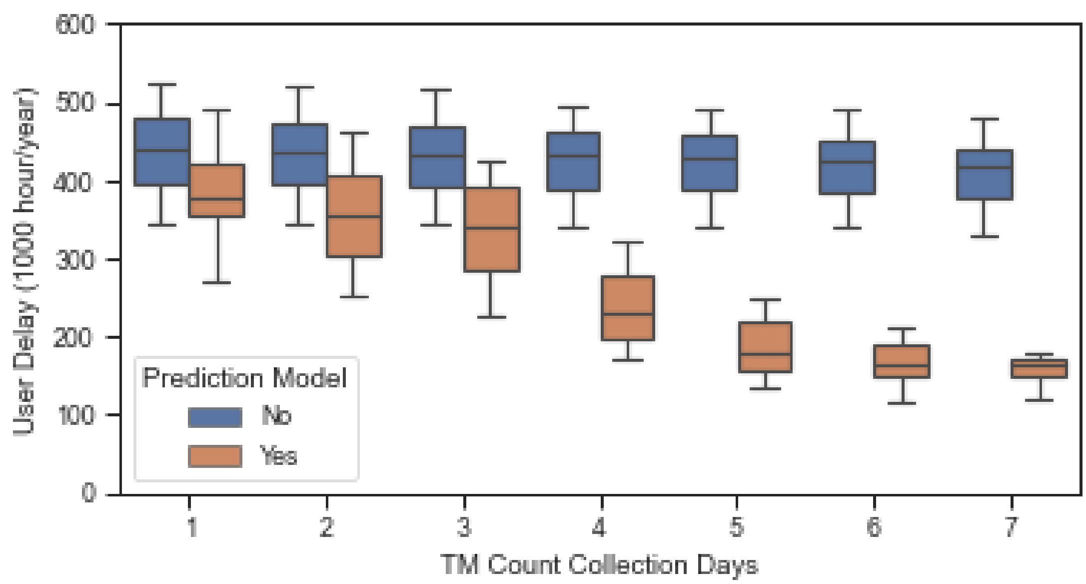

Figure 44. Distribution of annual user delay for the target intersection

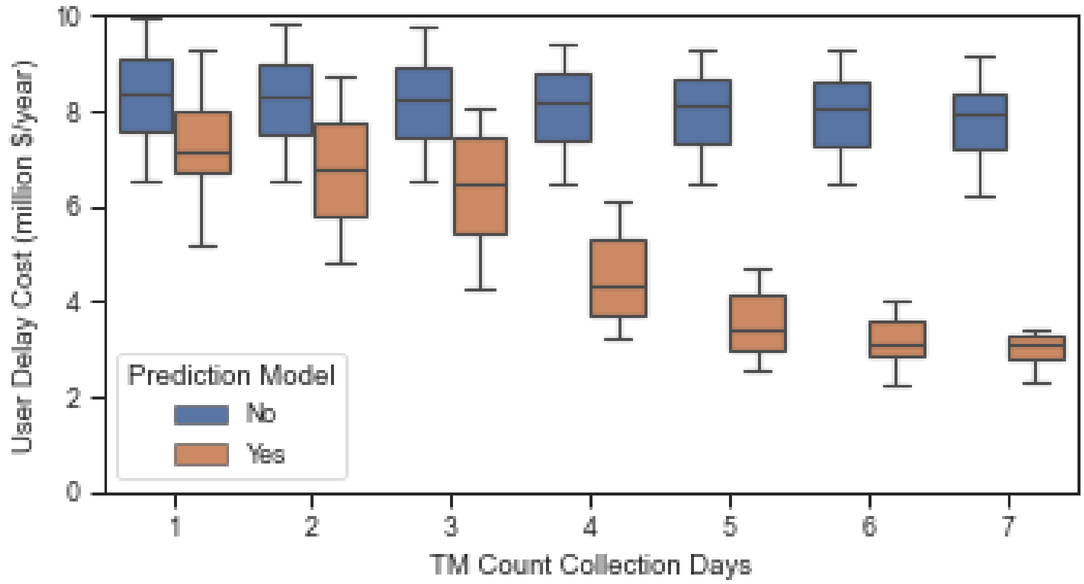

Figure 45. Distribution of annual user delay cost for the target intersection

It should be noted that the computations in this section assume that no feedback is given to the prediction model based on the queue length and traffic speed. In a real-world implementation, this feedback can improve the signal timing and reduce user delays in excess of the presented numbers. Therefore, the actual user delay reductions can be much more since signal failures comprise the balk part of the user delay. In the next section, a brief cost-benefit analysis is presented to compare the data collection costs against the time and money savings of using the proposed framework for turning movement count prediction and design of traffic signal phasing and timing based on the predicted demand.

7.4 Cost-Benefit Analysis

To perform a cost-benefit analysis, the cost of one day of turning movement count data collection is extracted from the FHWA guidance for roadway safety data to support the highway safety improvement program (Lefler et al., 2011). In this report, based on the costs given by 12 data collection vendors, a cost of 720 dollars per intersection (2010 US dollars) is obtained. Assuming around 2 percent of the national inflation rate leads us to a rough estimation of approximately 1,000 dollars per intersection each day. Due to the post-pandemic situations, one may assume that the costs have increased, especially labor costs, in which case still the data collection cost per day should be less than 3,000 dollars. Considering that we used the data of 15 intersections for the present study with at most seven days of data collection leads us to 15*7*3,000=315,000 dollars for the data collection. According to another FHWA report (Mimbela and Klein, 2007), the purchase costs of inductive loops for collecting traffic count data are between 500 and 800 dollars (1999 US dollars). Another study (Sobie, 2016) states that the ten-year costs of a loop detector purchase, installation, and maintenance are around 20,000 dollars, translating into 2,000 dollars each year. Compared with the turning movement count data collection costs, these numbers are not significant, and considering the inflation can be around 3,000 dollars. If the data for all 15 intersections are collected, the total costs will be 315,000+15*3,000=360,000 dollars per year. Although this number is significant for transportation agencies, particularly smaller jurisdictions, comparing it with the savings in user delay costs makes this investment rational. The amount of 5 million dollars of savings per year for one intersection is a considerable number that justifies the costs in data collection. Assuming that the other intersections' savings are approximately equal to the mentioned intersection's savings, the total savings add up to around 45 million dollars per year. This saving illustrates itself to the users in reduced travel times, higher travel time reliability, less traffic congestion, etc.

The study findings are summarized in the next chapter, and the study's conclusions are presented. Finally, suggestions for improving the present research in future works are described.

Chapter 8: Conclusions and Future Work

8.1 Research Summary and Contributions

This study presented data-driven approaches to estimate and predict turning movement counts at junctions of roads. Turning movement counts are essential data needed for various intersection analyses. However, it is costly to collect this data directly. The traditional approach for obtaining this data is counting vehicles manually for a short time at intersections. This limited data is then used for all the required analyses. With the recent advancements in technology and video processing tools, manual data collection can be replaced with optical vehicle detectors. However, the downside of these sensors is that their deployment on a large scale is highly costly. Therefore, a framework that provides turning movement estimations with acceptable accuracy is of great importance for intersections analysis. However, the number of studies in this area is limited due to the complexity of turning movements in their nature and the lack of ground truth data. To fill this gap, the current research introduced frameworks that leverage other traffic data, such as probe speed data and advanced machine learning methods. Additionally, this study investigated the input ground truth turning movement data's impact on the proposed frameworks to illustrate its application in practice.

The first part of this study focused on turning movement estimation at interchanges by developing models to estimate the proportion of vehicles that exit freeways using off-ramps and investigating temporary and permanent data collection strategies at target interchanges. For these purposes, various fully connected feedforward multi-layer NN models were trained. The ground truth data used in interchanges' analysis is from the PeMS website, a repository for volume count records, among other traffic flow measures of California's road network. The main inputs to the NN models are road features and probe speed data at all segments whose traffic conditions affect the target interchanges.

The results of this part revealed that the introduced framework could achieve acceptable accuracy in estimating off-ramps vehicle proportions when ground truth data is collected at all intersections, even for a short duration as low as approximately two days. Additionally, the results indicated that continuous data collection at some interchanges doesn't help estimate count proportions at locations without ground truth data.

The second part of the study investigated the estimation and prediction of turning movement counts at intersections during each 15 minutes interval. The ground-truth data of turning movement counts were extracted from the GRIDSMART optical sensors installed on selected intersections in Austin, TX. The data of turning movement counts for 15 intersections in 2019 and 15 intersections in 2020 were used for analysis. Since 2019 was in pre-pandemic conditions, the traffic patterns were not affected by the lockdowns and other disease spread prevention measures. The 2020 data of turning movement counts were also used since the 2020 INRIX vehicle probe data was provided to the author. The opportunity to compare this data and the ground-truth turning movement proportions led us to extract the 2020 actual turning movement counts in addition to the 2019 data. The comparison of turning movement proportions between the actual turning movements and the INRIX data illustrated significant differences between the two datasets. Therefore, it is concluded that the INRIX turning movement data is not an appropriate indicator of the actual traffic patterns in this application.

Following the investigation of INRIX probe vehicle turning movements, machine learning models' estimation of turning movement counts was explored. The attributes that were used for turning movement count estimation models were the traffic speed of the upstream and downstream of each movement, day of the week, time of the day, movement-specific characteristics, and the approach volume for each specific movement. In this investigation, several experiments were designed to obtain a more detailed understanding of the estimation of turning movement counts. The experiments and the findings of each experiment are as follows:

Evaluation of different model structures: The turning movement count estimation models were trained for each intersection separately. The machine learning models for this experiment were random forest, XGBoost, multi-layer perceptron (MLP), and an MLP with fine-tuning (MLP-FT), which uses the data of all intersections to train the general model followed by fine-tuning the last layer for each specific intersection. The models were trained on 25 randomly drawn ground truths, each including seven days of data collection. The results of this experiment revealed that the MLP-FT outperforms other models in all measures with a median R^2 of 0.96, median MAPE of %5.48, and median MAE of 1.96 vehicles in every 15 minutes.

Investigation of approach traffic volume input: In the previous experiment, it was assumed that the approach traffic volumes for each intersection were available. This assumption is limiting the findings since it requires traffic detectors on all entering and exiting legs of an intersection. The described situation rarely is faced in real-world problems. Therefore, this study proposed a framework to use the available traffic count data to develop a traffic volume estimation model to generate the traffic volumes for intersection legs without a detector. Using this method, the need for traffic detectors on all approaches is relaxed. The experiments on the proportion of intersection legs with traffic detectors indicated that deploying detectors on a quarter of all intersection legs is almost sufficient to obtain accurate turning movement count estimates. The obtained performance measures for the model with traffic detectors on 25 percent of approaches are 0.92 for median R^2, %16.68 for median MAPE, and 6.17 vehicles per 15 minutes for median MAE.

Turning movement ground-truth data size: An essential factor from the perspective of transportation agencies and authorities is the data collection duration required to obtain accurate turning movement count estimates. A set of experiments were designed in this study to evaluate the estimation accuracy depending on the duration of data collection ranging from one day per year to seven days per year. The findings of this analysis revealed that while five days of data collection per year is not significantly different from seven days, in some applications, even four days per year can be sufficient. The performance measures for the five days of data collection are equal to 0.88 median R^2, %23.12 median MAPE, and 8.66 vehicles per 15 minutes median MAE.

Based on the findings of the above-described experiments, it was concluded that the best combination in terms of costs and model performance is the MLP-FT model with traffic detector sensors deployed on 25 percent of intersection segments and a five-day per year turning movement count data collection for each intersection.

Following the experiments with the turning movement count estimation framework, two applications among possible uses of the proposed framework were presented. In the first application, the prediction of turning movement counts was explored, which illustrated that the model could generate relatively accurate predictions 15 minutes and 30 minutes ahead of time. The performance measures for predicting turning movement counts 15 minutes ahead illustrated a median R^2 of 0.90, median MAPE of %21, and median MAE of 6.46 vehicles per 15 minutes.

In the second application, the predictions in 15 minutes ahead were utilized to design the traffic signal timing in one of the study intersections. This investigation was performed with different durations of data collection. The signal timings and the resulting user delays were compared with a situation where the collected ground truth is used to design pre-timed signal timings. The comparisons illustrated that employing the presented framework can reduce the user delay to approximately 1/3 of the pre-timed signal design. For instance, with seven days of turning movement count data collection, the median user delay with using the proposed framework approximately equals 170 thousand hours per year, while without using the framework, it is around 420 thousand hours. It should also be noted that in the implementation of the proposed framework, the traffic conditions in response to the designed signal timing can feedback the framework to update the predictions and re-design the signal timing or more accurately design the signal for subsequent intervals, which can even reduce user delay in excess of the computed values. The following cost-benefit analysis of the signal timing illustrated that even seven days of data collection costs are negligible relative to the user delay costs savings. Therefore, the transportation authorities can find methods to divert a proportion of the user delay cost savings into their own budget and use it for deploying the proposed framework and traffic sensors.

8.2 Potential Future Research

Several aspects of this study can be expanded in future works to investigate various components of turning movement counts estimation. The following is a list of recommended directions for future research:

1. This study provided a descriptive analysis to investigate the quality of probe vehicles turning movement proportions. Based on the findings of this analysis, probe data proportions accuracy is highly dependent on the number of probe vehicle counts. The data available for this research did not have an acceptable quality to be considered for further analysis. However, given the ongoing improvement in commercial probe data’s penetration rate, the effect of such data, when added as an input to the turning movement counts estimation model, can be a direction to build upon these study’s findings.

2. One other possible direction for future work is to expand the study's framework to estimate OD patterns by exploring the effect of adding this study's estimated turning movements to the OD pattern estimation approaches. An iterative framework can be developed, given the availability of vehicles' trajectory data (from probe vehicles or location-based services (LBS)). From a high-level view, this framework can calculate OD patterns based on the sample trajectories and modify them using estimated turning movement counts to estimate actual OD patterns.
3. The lack of continuous ground truth turning movement counts on consecutive intersections prevented this study from considering the spatial relation between turning movement counts in a network of intersections. Given a dataset without such limitations is available, investigating the impact of adding spatial relationships (Zahedian, 2021) to the turning movement estimation models can be an interesting topic for future research. Additionally, advanced graph-based machine learning models such as graph neural network models can be used to expand the current study's framework to incorporate spatial correlations in a network of intersections.
4. The findings of this study indicated that the turning movement counts estimations accuracy significantly improves if approach volumes data is added to the model. Additionally, we showed that approach volumes could be estimated if there are sensors deployed in limited locations to collect approach volume ground truth data. Developing a model that optimizes the locations of

such sensors concerning the final turning movement estimation accuracy is another area to advance the current study's proposed frameworks.

5. One other parameter whose impact on the turning movement estimation framework was presented in this study was the duration for which ground truth turning movement data is collected at each specific intersection. Given the high cost of such data collection, a scheduling framework can be developed in future research to optimize the duration and orientation of data collection over a network of intersections.
6. In this study, due to the costs of turning movement count detector installation, the considered strategy of detector deployment is a temporary installation. With moving toward the large-scale deployment of advanced traffic detectors and a connected environment, the system operator can access real-time data of turning movement counts. In such a situation, one of the fascinating future research directions is to predict the turning movement counts using time-series models capable of capturing the patterns of traffic volumes.

Bibliography

"Caltrans, Performance Measurement System (PeMS)," 2019. [Online]. Available: http://pems.dot.ca.gov

Alibabai, H., and Mahmassani, H.S., 2008. Dynamic origin-destination demand estimation using turning movement counts. *Transportation research record*, *2085*(1), pp. 39-48.

Ashok, K., and Ben-Akiva, M.E., 2000. Alternative approaches for real-time estimation and prediction of time-dependent origin–destination flows. *Transportation Science*, *34*(1), pp. 21-36.

Ashok, K., and Ben-Akiva, M.E., 2002. Estimation and prediction of time-dependent origin-destination flows with a stochastic mapping to path flows and link flows. *Transportation Science*, *36*(2), pp. 184-198.

Bell, M.G., 1984. Log-linear models for the estimation of origin-destination matrices from traffic counts: an approximation. In *Proc. 9th Int. Symp. on Transpn. and Traffic Theory*, pp. 451-470.

Bell, M.G., 1991. The real time estimation of origin-destination flows in the presence of platoon dispersion. *Transportation Research Part B: Methodological*, *25*(2-3), pp. 115-125.

Bell, M.G., 1991a. The estimation of origin-destination matrices by constrained generalised least squares. *Transportation Research Part B: Methodological*, *25*(1), pp. 13-22.

Bishop, C.M., 1995. *Neural networks for pattern recognition*. Oxford university press.

Boto-Giralda, D., Díaz-Pernas, F.J., González-Ortega, D., Díez-Higuera, J.F., Antón-Rodríguez, M., Martínez-Zarzuela, M. and Torre-Díez, I., 2010. Wavelet-based denoising for traffic volume time series forecasting with self-organizing neural networks. *Computer-Aided Civil and Infrastructure Engineering, 25*(7), pp.530-545.

Chang, G.L., and Tao, X., 1998. Estimation of time-dependent turning fractions at signalized intersections. *Transportation Research Record*, *1644*(1), pp. 142-149.

Chen, A., Chootinan, P., Ryu, S., Lee, M., and Recker, W., 2012. An intersection turning movement estimation procedure based on path flow estimator. *Journal of Advanced Transportation*, *46*(2), pp. 161-176.

Chen, C., Skabardonis, A., and Varaiya, P., 2004. Systematic identification of freeway bottlenecks. *Transportation Research Record*, *1867*(1), pp. 46-52.

Cheng, X., Zhang, R., Zhou, J., and Xu, W., 2018, July. Deeptransport: Learning spatial-temporal dependency for traffic condition forecasting. In *2018 International Joint Conference on Neural Networks (IJCNN)* (pp. 1-8). IEEE.

Cremer, M., and Keller, H., 1987. A new class of dynamic methods for the identification of origin-destination flows. *Transportation Research Part B: Methodological*, *21*(2), pp. 117-132.

Cui, Z., Henrickson, K., Ke, R., and Wang, Y., 2019. Traffic graph convolutional recurrent neural network: A deep learning framework for network-scale traffic learning and forecasting. *IEEE Transactions on Intelligent Transportation Systems*, *21*(11), pp. 4883-4894.

Dahl, G.E., Sainath, T.N., and Hinton, G.E., 2013, May. Improving deep neural networks for LVCSR using rectified linear units and dropout. In *2013 IEEE international conference on acoustics, speech and signal processing* (pp. 8609-8613). IEEE.

Davis, G.A., 1993. Estimating freeway demand patterns and impact of uncertainty on ramp controls. *Journal of Transportation Engineering*, *119*(4), pp. 489-503.

Davis, G.A., and Lan, C.J., 1995. Estimating intersection turning movement proportions from less-than-complete sets of traffic counts. *Transportation research record*, *1510*, pp. 53-59.

Downs, A., 1962. The law of peak-hour expressway congestion. *Traffic Quarterly*, *16*(3).

Ferguson, E., 2018. *Travel demand management and public policy*. Routledge.

Foy, M.D., Benekohal, R.F., and Goldberg, D.E., 1992. Signal timing determination using genetic algorithms. *Transportation Research Record*, (1365), p. 108.

Friedman, J., Hastie, T., and Tibshirani, R., 2000. Additive logistic regression: a statistical view of boosting (with discussion and a rejoinder by the authors). *The annals of statistics*, *28*(2), pp. 337-407.

Gentili, M., and Mirchandani, P.B., 2011. Survey of models to locate sensors to estimate traffic flows. *Transportation Research Record*, *2243*(1), pp. 108-116.

Ghanim, M.S., and Shaaban, K., 2018. Estimating turning movements at signalized intersections using artificial neural networks. *IEEE Transactions on Intelligent Transportation Systems*, *20*(5), pp. 1828-1836.

Ghods, A.H., and Fu, L., 2014. Real-time estimation of turning movement counts at signalized intersections using signal phase information. *Transportation Research Part C: Emerging Technologies*, *47*, pp. 128-138.

Gholami, A., Tian, Z., and Andalibian, R., 2016. Innovative detector layout for automated traffic turning volume counting. *Journal of Advanced Transportation*, *50*(8), pp. 1958-1971.

Goldszmidt, A., List, J.A., Metcalfe, R.D., Muir, I., Smith, V.K., and Wang, J., 2020. *The Value of Time in the United States: Estimates from Nationwide Natural Field Experiments* (No. w28208). National Bureau of Economic Research.

Guo, K., Hu, Y., Qian, Z., Liu, H., Zhang, K., Sun, Y., Gao, J., and Yin, B., 2020. Optimized graph convolution recurrent neural network for traffic prediction. *IEEE Transactions on Intelligent Transportation Systems*, *22*(2), pp. 1138-1149.

Hagan, M.T., Demuth, H.B., and Beale, M., 1997. *Neural network design*. PWS Publishing Co.

Hamed, M.M., Al-Masaeid, H.R. and Said, Z.M.B., 1995. Short-term prediction of traffic volume in urban arterials. *Journal of Transportation Engineering*, *121*(3), pp.249-254.

Han, J., Pei, J., and Kamber, M., 2011. *Data mining: concepts and techniques*. Elsevier.

Hauer, E., Pagitsas, E., and Shin, B.T., 1980. Estimation of turning flows from automatic counts. *Transportation Research Record*, *795*, pp. 1-7.

Haykin, S., 1994. Neural networks: A comprehensive foundation, prentice hall ptr. *Upper Saddle River, NJ, USA*.

Hu, S.R., and Liou, H.T., 2012, November. Estimation of time-dependent intersection turning proportions for urban signal controls. In *2012 12th International Conference on ITS Telecommunications*, pp. 124-128. IEEE.

Huang, W., Song, G., Hong, H., and Xie, K., 2014. Deep architecture for traffic flow prediction: deep belief networks with multitask learning. *IEEE Transactions on Intelligent Transportation Systems*, *15*(5), pp. 2191-2201.

Hurdle, V.F., Hauser, E., Cremer, M., and Keller, H., 1983. Dynamic identification of flows from traffic counts at complex intersections. In *Proceedings of the Eighth International Symposium on Transportation and Traffic Theory, Toronto, Canada, June 24-26, 1981*.

Ioffe, S., and Szegedy, C., 2015, June. Batch normalization: Accelerating deep network training by reducing internal covariate shift. In *International conference on machine learning*, pp. 448-456. PMLR.

Jeffreys, M., and Nonman, M., 1970. On finding realistic turning flows at road junctions. *Traffic Engineering & Control*, *18* (Analytic).

Jiao, P., Lu, H., and Yang, L., 2005, September. Real-time estimation of turning movement proportions based on genetic algorithm. In *Proceedings. 2005 IEEE Intelligent Transportation Systems,* pp. 96-101. IEEE.

Jiao, P., Sun, T., and Du, L., 2014. A Bayesian combined model for time-dependent turning movement proportions estimation at intersections. *Mathematical Problems in Engineering*, *2014*.

Karlaftis, M.G., and Vlahogianni, E.I., 2011. Statistical methods versus neural networks in transportation research: Differences, similarities and some insights. *Transportation Research Part C: Emerging Technologies*, *19*(3), pp. 387-399.

Katriniok, A., Kleibaum, P., and Joševski, M., 2017. Distributed model predictive control for intersection automation using a parallelized optimization approach. *IFAC-PapersOnLine*, *50*(1), pp. 5940-5946.

Kessaci, A., Farges, J.L., and Henry, J.J., 1990. On line estimation of turning movements and saturation flows in PRODYN. In *Control, Computers, Communications in Transportation*, pp. 191-197. Pergamon.

Krizhevsky, A., Sutskever, I., and Hinton, G.E., 2012. Imagenet classification with deep convolutional neural networks. *Advances in neural information processing systems*, *25*.

Lan, C.J., and Davis, G.A., 1997. Empirical assessment of a Markovian traffic flow model. *Transportation research record*, *1591*(1), pp. 31-37.

Lan, C.J., and Davis, G.A., 1999. Real-time estimation of turning movement proportions from partial counts on urban networks. *Transportation Research Part C: Emerging Technologies*, *7*(5), pp. 305-327.

Lefler, N., Fiedler, R., McGee, H., Pollack, R., and Miller, J., 2011. *Background report guidance for roadway safety data to support the highway safety improvement program* (No. FHWA-SA-11-39). The United States. Federal Highway Administration. Office of Safety.

Li, W., Wang, J., Fan, R., Zhang, Y., Guo, Q., Siddique, C., and Ban, X.J., 2020. Short-term traffic state prediction from latent structures: Accuracy vs. efficiency. *Transportation Research Part C: Emerging Technologies*, *111*, pp. 72-90.

Li, Y., Yu, R., Shahabi, C., and Liu, Y., 2017. Diffusion convolutional recurrent neural network: Data-driven traffic forecasting. *arXiv preprint arXiv:1707.01926*.

Lingras, P., Sharma, S.C., Osborne, P. and Kalyar, I., 2000. Traffic volume time-series analysis according to the type of road use. *Computer-Aided Civil and Infrastructure Engineering*, *15*(5), pp.365-373.

Ma, X., Dai, Z., He, Z., Ma, J., Wang, Y., and Wang, Y., 2017. Learning traffic as images: a deep convolutional neural network for large-scale transportation network speed prediction. *Sensors*, *17*(4), p. 818.

Ma, X., Tao, Z., Wang, Y., Yu, H., and Wang, Y., 2015. Long short-term memory neural network for traffic speed prediction using remote microwave sensor data. *Transportation Research Part C: Emerging Technologies*, *54*, pp. 187-197.

Mahmoud, N., Abdel-Aty, M., Cai, Q., and Yuan, J., 2021. Predicting cycle-level traffic movements at signalized intersections using machine learning models. *Transportation research part C: emerging technologies*, *124*, p. 102930.

Manual, H.C., 2010. HCM2010. *Transportation Research Board, National Research Council, Washington, DC, 1207*.

Michalopoulos, P.G., O'Connor, J., and Novoa, S.M., 1978. Estimation of left-turn saturation flows. *Transportation Research Record*, *667*, pp. 35-41.

Mimbela, L.E.Y., and Klein, L.A., 2007. Summary of vehicle detection and surveillance technologies used in intelligent transportation systems.

Mountain, L.J., and Westwell, P.M., 1983. The accuracy of estimation of turning flows from automatic counts. *Traffic Engineering & Control*, *24*(HS-034 323).

Ng, A.Y., 2004, July. Feature selection, L 1 vs. L 2 regularization, and rotational invariance. In *Proceedings of the twenty-first international conference on Machine learning* (p. 78).

Nihan, N.L., and Davis, G.A., 1987. Recursive estimation of origin-destination matrices from input/output counts. *Transportation Research Part B: Methodological*, *21*(2), pp. 149-163.

Nihan, N.L., and Davis, G.A., 1989. Application of prediction-error minimization and maximum likelihood to estimate intersection OD matrices from traffic counts. *Transportation Science*, *23*(2), pp. 77-90.

Nohekhan, A., Zahedian, S., and Haghani, A., 2021. A deep learning model for off-ramp hourly traffic volume estimation. *Transportation Research Record*, *2675*(7), pp. 350-362.

Okutani, I., 1987. The Kalman filtering approaches in some transportation and traffic problems. *Transportation and traffic theory*.

Ory, D.T., and Mokhtarian, P.L., 2005. When is getting there half the fun? Modeling the liking for travel. *Transportation Research Part A: Policy and Practice*, *39*(2-3), pp. 97-123.

Park, D., and Rilett, L.R., 1999. Forecasting freeway link travel times with a multilayer feedforward neural network. *Computer-Aided Civil and Infrastructure Engineering*, *14*(5), pp. 357-367.

RITIS (2020), 'The regional integrated transportation information system (RITIS),' http://www.cattlab.umd.edu/?portfolio=ritis. Accessed: 2020-01-14.

Roess, R.P., Prassas, E.S., and McShane, W.R., 2004. *Traffic engineering*. Pearson/Prentice Hall.

Santiago-Chaparro, K.R., Chitturi, M., Bill, A., and Noyce, D.A., 2016. Automated turning movement counts for shared lanes: leveraging vehicle detection data. *Transportation Research Record*, *2558*(1), pp. 30-40.

Schrank, D., Eisele, B. and Lomax, T., 2019. Urban mobility report 2019.

Sekuła, P., Marković, N., Vander Laan, Z., and Sadabadi, K.F., 2018. Estimating historical hourly traffic volumes via machine learning and vehicle probe data: A Maryland case study. *Transportation Research Part C: Emerging Technologies*, *97*, pp. 147-158.

Shatnawi, I., Yi, P., and Khliefat, I., 2018. Automated intersection delay estimation using the input–output principle and turning movement data. *International Journal of Transportation Science and Technology*, *7*(2), pp. 137-150.

Shoup, G., Remias, S.M., Hainen, A.M., Grimmer, G., and Davis, A.D., 2013. Characterizing Reliability of Manual Intersection Turning Movement Counts Using Modern Data Collection Technology.

Sobie, C.E., 2016. *Life cycle cost analysis of vehicle detection technologies and their impact on adaptive traffic control systems* (Doctoral dissertation, Northern Arizona University).

Tian, Y., and Pan, L., 2015, December. Predicting short-term traffic flow by long short-term memory recurrent neural network. In *2015 IEEE international conference on smart city/SocialCom/SustainCom (SmartCity)*, pp. 153-158. IEEE.

Van Zuylen, H.J., 1979. The estimation of turning flows on a junction. *Traffic Engineering & Control*, *20*(11).

Vlahogianni, E.I., Golias, J.C., and Karlaftis, M.G., 2004. Short-term traffic forecasting: Overview of objectives and methods. *Transport Reviews*, *24*(5), pp. 533-557.

Wild, D., 1997. Short-term forecasting based on a transformation and classification of traffic volume time series. *International Journal of Forecasting*, *13*(1), pp. 63-72.

Wu, Y., and Tan, H., 2016. Short-term traffic flow forecasting with spatial-temporal correlation in a hybrid deep learning framework. *arXiv preprint arXiv:1612.01022*.

Xiao, F., Qian, Z.S., and Zhang, H.M., 2013. Managing bottleneck congestion with tradable credits. *Transportation Research Part B: Methodological*, *56*, pp. 1-14.

Xu, K., Yi, P., Shao, C., and Mao, J., 2013. Development and testing of an automatic turning movement identification system at signalized intersections. *Journal of Transportation Technologies*, *3*(04), p. 241.

Zahedian, S., 2021. *Introducing a Graph-Based Neural Network for Networkwide Traffic Volume Estimation* (Doctoral dissertation, University of Maryland, College Park).

Zahedian, S., Sekuła, P., Nohekhan, A., and Vander Laan, Z., 2020. Estimating hourly traffic volumes using artificial neural network with additional inputs from automatic traffic recorders. *Transportation Research Record*, *2674*(3), pp. 272-282.

Zhao, Z., Chen, W., Wu, X., Chen, P.C., and Liu, J., 2017. LSTM network: a deep learning approach for short-term traffic forecast. *IET Intelligent Transport Systems*, *11*(2), pp. 68-75.